Abstract

SPATIAL MODELING OF THE RISK OF MOSQUITO-BORNE DISEASE TRANSMISSION, CHESAPEAKE, VIRGINIA

by Haley Leanna Cleckner

May 2010

Director: Dr. Tom Allen

Major Department: Geography

The increase in mosquito populations following extreme weather events poses a major threat to humans because of mosquitoes' ability to carry disease-causing pathogens. In areas with reservoirs of disease, mosquito abundance information can help to identify the areas at higher risk of disease transmission. Using a Geographic Information System (GIS), mosquito abundance is predicted across the City of Chesapeake, Virginia. The mosquito abundance model uses mosquito light trap counts, habitat suitability, and dynamic environmental variables to predict the abundance of the species *Culiseta melanura,* as well as the combined abundance of the ephemeral species, *Aedes vexans* and *Psorophora columbiae,* for the year 2003. The predicted mosquito abundance values are compared to vulnerable population indices to determine the spatial distribution of risk of disease transmission. The goal of this project is to create a portable, reproducible model that could be embedded in a decision support system to aid in detecting areas at high risk of mosquito-borne disease transmission.

SPATIAL MODELING OF THE RISK OF MOSQUITO-BORNE DISEASE TRANSMISSION, CHESAPEAKE, VIRGINIA

A Thesis

Presented to

The Faculty of the Department of Geography

East Carolina University

In Partial Fulfillment

of the Requirements for the Degree

Masters of Geography

By

Haley L. Cleckner

May 2010

SPATIAL MODELING OF THE RISK OF MOSQUITO-BORNE DISEASE TRANSMISSION, CHESAPEAKE, VIRGINIA

By

Haley Leanna Cleckner

APPROVED BY:

DIRECTOR OF THESIS:_____
Thomas R. Allen, PhD

COMMITTEE MEMBER:_____
Thomas W. Crawford, PhD

COMMITTEE MEMBER:_____
Ronald L. Mitchelson, PhD

COMMITTEE MEMBER:_____
Alice L. Anderson, PhD

CHAIR OF THE DEPARTMENT OF GEOGRAPHY:_____
Burrell Montz, PhD

DEAN OF THE GRADUATE SCHOOL:_____
Paul J. Gemperline, PhD

ACKNOWLEDGEMENTS

I would like to acknowledge several people who have helped me throughout my thesis work. I would first like to express my gratitude to my advisor, Dr. Tom Allen, who guided me through the research project and has encouraged me to reach my full potential as a student and researcher. I also extend thanks to the other professors on my committee for their help and support during this study. I would like to acknowledge my friends and colleagues for their support throughout my graduate work. I thank the Chesapeake GIS Department as well as the Chesapeake Mosquito Control Commission who have provided valuable data for this project, particularly Gene Payne (Director). Most importantly, I would like to thank my family for their support and guidance throughout my undergraduate and graduate career.

TABLE OF CONTENTS

LIST OF FIGURES vi

LIST OF TABLES viii

CHAPTER 1: INTRODUCTION 1

Vector-borne Diseases and Public Health 1

GIS and Public Health 2

Mosquito Species and Disease 3

Predicting the Risk of Vector-borne Disease Transmission 4

CHAPTER 2: LITERATURE REVIEW 6

Overview 6

Climate and Vector-borne Diseases 6

Surveillance and Control 9

Methods Used to Research Vector-borne Diseases 11

GIS and Public Health 13

Assessing Vector-borne Diseases using GIS Technology 14

Synthesis of Literature 18

CHAPTER 3: DATA AND METHODS 19

Overview 19

Study Area 20

Habitat Suitability Index (HSI) 23

Dependent Variables 23

Independent Variables 26

Linear Regression Models 38
Mosquito Abundance Models 42
Independent Variables 43
Predicting Monthly Mosquito Abundance 51
Predicting Human Risk of Mosquito-borne Disease Transmission 56
Dasymetric Mapping of the Vulnerable Population 56
Predicting the Risk of Mosquito-Borne Disease Transmission 63
CHAPTER 4: RESULTS 65
Habitat Suitability Index (HSI) 65
Weighted Influence of Independent Variables on Mosquitoes (WSC) 67
Mosquito Abundance 69
Ephemeral Species Abundance 69
C. melanura Abundance 73
Model Results vs. Interpolated Surfaces 77
Human Vulnerability 78
Risk of Mosquito-Borne Disease Transmission 81
Risk of Disease Infection from the Ephemeral Species 81
Risk of Disease Infection from *C. melanura* 82
CHAPTER 5: DISCUSSION AND CONCLUSIONS 84
Mosquito Abundance Patterns 84
Risk of Disease Transmission 86
Study Limitations 87
Model Validation 89

Significance of Research 93

REFERENCES 96

APPENDIX A: 2003 C. MELANURA TRAP DATA 102

APPENDIX B: 2003 EPHEMERAL SPECIES TRAP DATA 104

LIST OF FIGURES

1. Overview of the steps involved in predicting the risk of disease transmission across Chesapeake 20

2. Map of Cheapeake, Virginia 22

3. Light trap locations throughout Chesapeake in 2003 24

4. Interpolated surfaces of the normalized monthly trap counts for the ephemeral species 25

5. Interpolated surfaces of the normalized monthly trap counts for *C. melanura* 26

6. Tasseled-Cap Indices 32

7. Percent hydric composition of the soil 33

8. Soil drainage potential 34

9. Soil runoff potential 35

10. Water Table Depth 36

11. Available water holding capacity of the soil 37

12. HSI model for the ephemeral species (a) and *C. melanura* (b) 41

13. HSI results for ephemeral species group and *C. melanura* 42

14. Slope surface of the DEM 44

15. Flow accumulation surface 45

16. Topographic soil moisture index (TMI) surface 46

17. Monthly average air temperature grid (AWAT) 48

18. Monthly average rainfall 50

19. Product of average monthly temperature and average monthly precipitation 50

20. Abundance model for *C. melanura* 54

21. The weighted influence of the independent variables (WSC) on ephemeral species abundance (a) and *C. melanura* (b)..... 55

22. The population less than 5 years of age (a), population greater than 50 years of age (b), and the sum of children and elderly population overlaid with vulnerable location points (c) 60

23. Vulnerable population by block group 61

24. Reclassified land cover types used as the ancillary units in dasymetric map 62

25. Spatial overlay of the vulnerable population and land cover..... 63

26. Spatial overlay used to predict the risk of disease transmission for June, 2003..... 64

27. Monthly abundance of the ephemeral species 71

28. Trap sites overlaid onto the monthly abundance maps for the ephemeral species 72

29. Trap sites overlaid onto the monthly abundance maps of the ephemeral species with areas of correlation highlighted..... 73

30. Monthly abundance of *C. melanura* 75

31. Trap sites overlaid onto the monthly abundance maps of *C. melanura*..... 76

32. Trap sites overlaid onto the monthly abundance maps of *C. melanura* with areas of correlation highlighted..... 77

33. Dasymetric map of the population that is most vulnerable to mosquito-borne diseases..... 80

34. Risk of disease transmission from the ephemeral mosquito species 82

35. Risk of disease transmission from *C. melanura* 83

36. Cases of WNV in birds, chickens, and horses across Chesapeake in 2003..... 91

37. Cases of EEE in birds, chickens, and horses across Chesapeake in 2003 92

LIST OF TABLES

1. Independent variables considered for HSI linear regression models 28
2. Soil attributes used as independent variables in HSI regression models 29
3. Independent variables chosen to be used in HSI regression models 30
4. Focal neighborhood settings for the ephemeral species group 31
5. Focal neighborhood settings for *C. melanura* 31
6. Summary of the HSI linear regression model for the ephemeral species group 38
7. Results of the HSI linear regression model for the ephemeral species group 38
8. Summary of the HSI linear regression model for *C. melanura* 39
9. Results of the HSI linear regression model for *C. melanura* 39
10. Summary of the WSC linear regression model for the ephemeral species 51
11. Results of the WSC linear regression model for the ephemeral species 51
12. Summary of the WSC linear regression model for *C. melanura* 52
13. Results of the WSC linear regression model for *C. melanura* 52

CHAPTER 1: INTRODUCTION

This chapter begins with an introduction to the mosquito research and its significance. This is followed by an overview of how GIS technology will be used in this mosquito study. A brief background on the mosquito species under investigation is then discussed. This chapter concludes with a brief overview of the methodology used to predict the risk of disease transmission from mosquitoes.

Vector-borne Diseases and Public Health

Infectious diseases continue to be a threat to populations around the world. Vector-borne diseases such as those transmitted by mosquitoes, contribute significantly to the total disease burden in developing countries. Currently, nearly half of the earth's people live in tropical or temperate regions where they may be at risk to one or more vector-borne diseases (Washino and Wood, 1994). Over one million people die from mosquito-borne diseases every year (American Mosquito Control Association, 2005). The increase in mosquito populations following extreme weather events poses a major threat to humans due to mosquitoes' ability to carry disease-causing pathogens. Environmental conditions such as increased rainfall and higher temperatures can lead to an increase in mosquito populations, commonly referred to as 'blooms'. Provided there is a disease reservoir population (e.g., birds), this can lead to an increase in vector-borne disease transmission such as Eastern Equine Encephalitis (EEE) and West Nile Virus (WNV). These diseases commonly increase following extreme weather events such as hurricanes and tropical storms (Noji, 1997).

In order to prevent the spread of disease, it is advantageous to first assess human risk of disease transmission, both spatially and temporally. Knowing where risk is highest can improve preparedness and response efforts to the disease (World Health Organization, 2004). According to Panditrao, Jeevan and Akbar (2006), the ability to predict outbreaks of vector-borne disease

will greatly enhance the efficacy of prevention efforts and will substantially reduce costs of prevention with efficient targeting of high-risk areas. Knowing where areas of high risk are located is important to public health officials because they can target where mosquito control needs to be implemented the most. This allows for increased interruption of the disease transmission as well as the saving of resources, personnel and control products, by directing their efficient application. Unfortunately, the environmental and ecological determinants of mosquito-borne diseases act in complex ways, and it is therefore hard to predict the epidemiology of mosquito-borne diseases (Gage et al., 2008).

GIS and Public Health

Geographic Information Systems (GIS) are a vital tool for assessing the spatial epidemiology of these diseases and analyzing human risk of infection. GIS facilitates emergency planning and response for incidents ranging from natural disasters to bioterrorism, and the rapid assessment of the impact of such disasters (Waring et al., 2005). GIS can also help with mosquito control by predicting vector abundance. Accordingly, this study uses a GIS to determine how human vulnerability to mosquito-borne diseases changes temporally and spatially across Chesapeake, Virginia. The purpose is to inform public health policy and improve GIScience methodology. Spatial models were created that identify the mosquito vector-borne disease hazard and quantify risk of disease transmission to humans. This study will potentially lend support to the growing body of GIScience assessing human vulnerability to infectious diseases. One major goal of this project is to develop a set of methods that are reproducible in other study areas. This will allow other regions to utilize these methods provided they have the necessary data.

Mosquito Species and Disease

The spatially distributed abundance of three mosquito species will be predicted in this study. These species include: *Culiseta melanura, Aedes vexans,* and *Psorophora columbiae. C. melanura* is an important species because it is the primary enzootic vector of Eastern Equine Encephalitis (EEE). According to the Centers for Disease Control and Prevention (CDC), EEE is a fatal virus with a 33% mortality rate (2009). The virus is maintained in a cycle between *C. melanura* and avian hosts. However, other mosquito species can create a 'bridge' between infected birds and humans. *C. melanura* is also a potential vector of West Nile Virus (WNV). *C. melanura* is found mostly in freshwater swamps, particularly subterranean crypts (Mahmood and Crans, 1998). *A. vexans* is another important species because it is a potential epizootic vector for WNV. WNV is a potentially serious epidemic affecting humans and animals throughout North America. The virus often flares up in the summer and continues into the fall (CDC, 2006). *P. columbiae* is also a potential vector for WNV as well as Venezuelan Equine Encepahlitis (VEE). Although human and animal cases of VEE have been reported in the U.S., this virus is mainly confined to equatorial South America and Central America. *A. vexans* and *P. columbiae* share a preferred habitat of ephemeral pools, particularly river floodplains (Crans, 2004). Due to differences in habitat preferences, the abundance of *C. melanura* will be predicted separately from the other two species. The abundance of *A. vexans* and *P. columbiae* will be predicted as a combined total. These species will often be referred to as the 'ephemeral group' throughout this thesis. The abundance of these mosquito species will be predicted for the months of June through August for the year 2003. The high temperatures and abundant precipitation from June through August create an ideal habitat for mosquito populations to thrive. The year 2003 was chosen for this study based on the ample mosquito trap data available for this year.

Predicting Risk of Vector-borne Disease Transmission

The presence of mosquitoes is dependent on many ecological factors. According to Gage et al. (2008), environmental variables such as temperature, precipitation, and humidity are known to affect the reproduction, development, behavior, and population dynamics of mosquito vectors. This is due to the fact that mosquitoes are ectothermic and subject to the effects of changing temperatures. These climatic factors can also increase the transmission of vector-borne diseases both directly and indirectly. For example, temperature can affect pathogen development within a mosquito and interact with humidity to influence vectorial capacity. These climatic factors determine how suitable a habitat is for breeding. Rainfall for instance, can strongly influence the availability of breeding sites for mosquitoes. To determine the suitability of areas within Chesapeake for mosquito habitation, a habitat suitability index (HSI) was calculated for each species. The HSI values can then be used along with additional environmental determinants that affect breeding patterns to predict mosquito abundance.

Vector-borne diseases are climatically driven; however, disease transmission is also influenced by other factors such as land use, water storage, and human vulnerability. To account for these multiple factors, this study will incorporate multiple causal factors of disease transmission, including human vulnerability. According to Wilson (2002), the spatial pattern of infectious and susceptible people to vector-borne diseases is a basic determinant of exposure and disease risk. Therefore, this study will assess the spatial distribution of vulnerability across Chesapeake in order to predict the risk of disease transmission. Using U.S. 2000 decennial Census data and ancillary vulnerable population data from the City of Chesapeake, the spatial vulnerability of the population was determined for the year 2003. Because the transmission of vector-borne diseases is partially dependent on the proximity of humans to the vector, the

monthly abundance values can be overlaid with the vulnerability patterns to predict the risk of disease transmission of vector-borne diseases.

CHAPTER 2: LITERATURE REVIEW

This chapter begins by giving an overview of the types of literature directly related to this study. These types of literature will then be discussed in more detail. First, literature associated with climate and vector-borne diseases is discussed. An overview of literature pertaining to disease surveillance is then provided. The various methods used to investigate vector-borne diseases are also addressed. Next, the literature pertaining to GIS and public health is examined. This chapter concludes by discussing how the literature discussed will be useful to this study.

Overview

There is an abundance of literature on the various types of vector-borne diseases and their impacts on human health. Much of the literature discusses how vector-borne diseases are related to the environment. There is also a great deal of literature on surveillance and epidemiology of vector-borne diseases. As Geographic Information Systems (GIS) are becoming more widely used, more literature is emerging that discusses how GIS is used to investigate vector-borne diseases. Much of this literature explains how GIS can be used for evaluating the spatial epidemiology of these diseases. A large portion of the literature also discusses how GIS is used to link climate and disease. Unfortunately, there is not a great deal of literature on how GIS can be used to both assess human vulnerability to vector-borne diseases and to model possible risk transmission to inform vector surveillance or control.

Climate and Vector-borne Diseases

Much of the literature discusses the effect of climate on vectors such as mosquitoes. Changes in temperature, precipitation, humidity and wind patterns can all affect a vector's reproduction, development rate and longevity (Martens et al. 1995). In the case of temperature, warming of the environment boosts mosquito reproduction rates and the number of blood meals

they take, prolongs their breeding season, and shortens the maturation period for the microbes they disperse (Epstein, 2005). Increased temperature also affects the susceptibility of a vector to pathogens, the incubation period of a pathogen, the seasonality of vector activity, and the seasonality of pathogen transmission (Hunter, 2003). Precipitation influences vector populations by increasing the number of breeding sites for vectors and increasing vegetation to allow expansion in vector populations. Flooding can also eliminate vector habitats and force hosts into closer contact with humans. Temperature and precipitation changes also affect the behavior and geographical distribution of vectors such as mosquitoes (Martens et al. 1995).

Gage et al. (2008) discuss how climate can contribute to outbreaks in vector-borne diseases such as malaria and West Nile Virus. Their work reveals how temperature can increase the transmission of arboviruses by decreasing the development time of mosquito vectors, increasing the extrinsic incubation period, and increasing the viral titer, or concentration, in mosquitoes. They also discuss how precipitation affects vector populations at the larval and adult stages. Caillouet et al. (2008) explain that at the larval stage, mosquitoes are very successful at colonizing newly-flooded habitats. For adult mosquitoes, the flood waters create potential breeding sites (Speilman and D'Antonio, 2001). Rainfall also increases the humidity which increases the longevity of the adult mosquito and reduces evapotranspiration, potentially sustaining active breeding sites (Martens et al., 1995). Hayes and Hess (1964) examined weather and disease data in order to investigate the relationship between Eastern Encephalitis and extreme weather in areas of the United States where both human and equine cases have occurred. The only region in which a temporal correlation was found between extreme weather and Eastern Encephalitis was Southeastern Massachusetts. Each outbreak occurred after there was unusually heavy rainfall.

One observation noted in much of the literature on vector-borne diseases is an emphasis that climate alone does not determine disease events. Gage et al. (2008) mention that the effects of climate change on these diseases are not easily predictable and the ecologic determinants of these diseases interact in complex ways. Other factors contribute to these diseases such as vector and host ecology, human culture and behavior, land use and other local conditions. Mather et al. (2004) also explain that although hazards can contribute to human health, its presence alone may not be enough to affect the health of a population. Dengue fever transmission, for instance, is influenced by rainfall and humidity, but is not directly related to these factors (Watson, Gayer, and Connely, 2007). The risk for outbreaks can be influenced by changes in human behavior, which can yield increased exposure to mosquitoes while being outside, movement from dengue-nonendemic to endemic areas, a pause in disease control activities, and overcrowding. Dengue transmission can also be influenced by changes in habitat that promote mosquito breeding such as landslides, deforestation, river damming and re-routing of water. Malaria outbreaks are often caused by humans as well. An article by Gratz (1999) discusses ecological changes associated with malaria. In many areas of the world, water development projects and increased irrigation have resulted in shifts from dry land to wetland rice cropping, resulting in an increase in vector populations. Portions of Turkey for instance, illustrate a strong link between water development, increased vector densities, and malaria resurgence. In Sri Lanka, pits dug to search for gem stones filled with water and became the source for dense populations of malaria-carrying mosquitoes. Martens et al. (1995) emphasize that not only are there multiple factors influencing disease, but the consequences of climate change on vector-borne diseases are poorly understood.

Surveillance and Control

In order to assess the population at risk for vector-borne diseases, as well as respond to illness, epidemiologic surveillance is important. Predicting risk to disease is important because it can improve epidemiologic surveillance and disease control efforts. According to Nasci and Moore (1998), four major arboviruses are of human and veterinary health importance. These include eastern equine encephalomyelitis (EEE), western equine encephalomyelitis (WEE), St. Louis encephalitis (SLE), and LaCrosse (LAC) encephalitis. In nine out of ten extreme weather events in which surveillance has been conducted, arbovirus activity was detected in surveillance programs initiated after the event. Because the factors controlling disease act in complex ways, public health agencies must not only monitor mosquito populations, but other factors such as drinking water, pesticide exposure, and pollutants (Gage et al., 2008). Glass and Noji (1992) explain the importance of epidemiologic surveillance and how it is performed. Following a natural disaster, epidemiological techniques have been incorporated into disaster relief operations. Epidemiologists must be able to define the nature and extent of the potential health problems, identify groups in the population at risk of adverse health events, optimize the relief response, monitor the effectiveness of the relief effort, and provide recommendations to decrease the consequences from future disasters.

Predicting human vulnerability to disease is important because it could guide officials on decisions of where to implement control efforts. Mosquito control is one common method for inhibiting the spread of disease. Aerial application of insecticide is often used to control mosquitoes because it is less prone to patchy coverage than ground-based applications. Aerial application is also capable of covering larger areas in shorter time periods than ground-based applications (CDC, 2003). In 2005, spraying at ten sites following Hurricane Katrina resulted in

a 91% reduction in expected mosquito density (Manuel, 2006). Although mosquito control techniques are widely used, control efforts are costly and at times ineffective. Mosquitoes can become resistant to insecticides, reducing their efficacy (Lacey and Lacey, 1990). Insecticide use can also pose health risks to humans, animals, and the environment. Adulticide applications pose acute health risks including neurological, allergic, and respiratory risks (Thier, 2001). Chronic health risks such as developmental toxicity, endocrine disruption, carcinogenicity, genotoxicity, and immune system damage also have been related to adulticide use. Peterson, Macedo, and Davis (2006) assessed the human-health risk for West Nile Virus and compared the results to the health risk of insecticide use. The results indicate that the risks from WNV exceed the risks from exposure to mosquito insecticides. Source reduction is another effective method for reducing mosquito vectors. Source reduction consists of the removal of larval habitats or rendering of such habitats unsuitable for larval development (Rose, 2001). Ways to reduce larval pools include cleaning rain gutters, bird baths, and unused swimming pools (CDC, 2003). In areas where source reduction is not feasible, larvicides can be used to prevent the emergence of mosquito vectors. This method is often less controversial than adulticide use (Rose, 2001). Bacterial control agents such as *Bacillus thuringiensis* and *Bacillus sphaericus* are common types of larvicide (Becker, 2000). These bacteria serve as a toxin which disrupts the gut of the mosquito when ingested. Biological controls such as predators can also be used to reduce populations of mosquito larvae. Predators of mosquito larvae and pupae such as dragonfly nymphs or the mosquito, *Toxorhynchites* spp., are commonly used to control vector populations. The mosquito fish, *Gambusia affinis* and *G. holbrooki* are the most commonly used biological control for mosquitoes (Rose, 2001).

Methods Used to Research Vector-borne Diseases

Various methods are used investigate the transmission of vector-borne diseases. Many of these approaches attempt to link climate with the presence of vector-borne diseases. Statistical analyses are a common method for determining the relationship between the environment and disease. Biological (or process-based) models are another approach for modeling the impact of the environment on transmission of diseases such as malaria. These models can exist in many different forms. These models measure the extent to which the natural world would allow the transmission of disease if there were no other human-induced constraints on transmission (McCarthy et al., 2001). Another type of modeling investigates the change in distribution of vectors as an indicator of disease risk. Each of these approaches for investigating disease is unique, however, these approaches are often used together to accurately estimate the distribution of vector-borne diseases.

Statistical analyses are a commonly used mechanism for determining the relationship between the environment and disease. Mather et al. (1995) explain that three types of statistical analyses are typically applied to health and hazards. The first method is to track trends and analyze them. The second is ecologic analysis, which describes the coexistence of risk factors with disease between and within populations. The third type of statistical analysis is epidemiologic studies which associate exposure in individuals to health outcomes by means of case-control studies in rare disease and cohort studies. Lawson (2001) also explains how statistical methods can be used in spatial epidemiology. In particular, this book discusses how to model infectious diseases, particularly the space-time behavior of infectious disease. Statistical analyses are often used in accordance with GIS techniques to determine the relationship between

environmental variables and vector-borne diseases. Because they are of focal interest here, studies that use this approach will be discussed in a subsequent section.

Biologicals models are another method for investigating the association between climate and disease. Martens et al. (1995) investigated the effects of temperature and precipitation changes on mosquito reproduction rates based on global climate models (GCMs). Climate scenarios were created by modeling changes in temperature and precipitation data for the period 1961-1990. Model simulations indicated that variation in precipitation and temperature resulted in minor changes in the potential areas at risk for malaria. This study also estimated the number of people at risk of disease transmission based on anthropogenic climate change. However, this model is based solely on climatic factors and does not take into account population data. Martens et al. (1999) also used GCMs to calculate the global impact of climate change on malaria transmission. Using climate change scenarios and vector distribution data, they predicted the number of people at risk of malaria. The model took into account population growth data in order to estimate the risk of transmission but did not take vulnerability data into account. In an effort to control mosquitoes and mosquito-borne diseases, Shaman et al. (2002) used a dynamic hydrology model to predict mosquito abundances in flood and swamp water. The model provides both hourly and daily time series of hydrologic variables including water table depth, percent surface saturation, and total surface runoff. By providing variables which can affect surface wetness, the model can capture the expansion and contraction of breeding pools at rates that impact mosquito development. Hoshen et al. (2005) used a biological model to determine vector capacity of mosquitoes in Africa based on climatic parameters. The model used equations to incorporate the stages of the malaria vector and their dependence on temperature and rainfall and parts of the within-host parasite population dynamics. The results

of the model indicate that the rate of maturation of mosquito larvae is directly related to temperature. The model also indicated that the wetter regions of Africa had a higher prevalence of malaria compared to the drier regions.

Vector modeling estimates the spatial distribution of disease vectors in order to assess the transmission of disease risk. Sutherst (1998) used the CLIMEX model to estimate changes in global and national (Australia) distribution of malaria vectors using a range of climate scenarios. The CLIMEX model is designed to extract maximum information from spatially distributed observational data on the distribution of species or other biological factors. Bryan et al. (1996) also used the CLIMEX model to investigate the present and future distribution of malaria vectors in Australia. Schaeffer, Mondet, and Touzeau (2008) also built a climate-dependent model that predicts the abundance of *Aedes* mosquito species. The model takes into account dynamic population information such as reproductive rate, growth, and death. Brownstein, Holford, and Fish (2003) used climate data within a statistical model to predict the abundance of the Lyme disease tick vector, *Ixodes scapularis*. A logistic regression model was derived for the relationship between environmental variables and established tick populations, and was used with GIS techniques to predict the abundance of *I. scapularis*.

GIS and Public Health

Medical geography is both a venerable and new specialization (Meade and Earickson, 2005). Medical geography uses geographic techniques to study health and the spread of disease. This sub-discipline of Geography can be concerned with the impact of climate and location on an individual's health as well as the distribution of health services. One of the first studies which used geographic techniques to study disease was performed by Dr. John Snow in the mid 1800s (Cameron and Jones, 1983). Snow isolated the source for Cholera in London by mapping

Cholera-related deaths. He found a large number of deaths centered on a water pump on Broad Street and determined that pump to be the source for the deadly bacterium. Today, medical geography has advanced greatly with the use of GIS. The resurgence of infectious disease, particularly vector-borne disease, has led public health agencies to use GIS for the purpose of investigating these diseases (Cromley and McLafferty, 2002). According to Albert, Gesler, and Levergood (2000), GIS is often used for many applications in medical geography. Some common uses are emergency response, AIDS prevention, catchment area studies, monitoring and surveillance, and cancer-related research. GIS is also used in the context of epidemiology for disease mapping, disease pattern recognition, and exploration of disease correlates (Ray, Randolph and Rogers, 2000). Much of the literature on mosquito-borne diseases discusses how GIS is used for the purpose of medical geography. Gatrell and Loytonen (1998) explain that GIS is used in medical geography for the purpose of environmental and spatial epidemiology. Environmental epidemiology focuses on links between disease and the environment. This can be contrasted with spatial epidemiology where description, exploration, and modeling of disease incidence does not necessarily involve investigating links with the environment.

Assessing Vector-borne Diseases using GIS Technology

As GIS is becoming more commonly used, literature is emerging that discusses how GIS is used to map and assess patterns of disease infection. Some studies evaluate patterns of vector or human case distributions, while others calculate risk of disease transmission based on entomological, epidemiological and environmental determinants (Kitron, 2000). One limitation is that many risk assessment studies use either environmental variables or vector abundance as the only indicators of disease risk, and do not take into account population vulnerability. Another shortcoming is that these studies are often static and only predict abundance or risk at

one particular time and place. According to Ceccato et al. (2005), epidemic risk mapping should be dynamic and updated frequently to reflect the changes in vulnerability factors.

Geospatial technology is often used for assessing and mapping disease patterns. Albert (2000) discusses how a GIS has been used for thematic mapping in order to describe patterns of environmental variables contributing to Lyme disease, tick distributions, or human cases of Lyme disease. Albert used a GIS to track the distribution of Lacrosse Encephalitis in Illinois and Human Babesiosis in the northern United States. Gatton et al. (2004) also used a GIS to investigate spatial and temporal patterns of the Ross River (RR) virus in Queensland, Australia by mapping incidence rates within each Local Government Area (LGA) for the years 1991 to 2001. Kitron et al. (1997) used a GIS and spatial statistics to map the distribution of Lacrosse Encephalitis in Illinois. Human cases of Lacrosse encephalitis were mapped at the county, town and address level from 1988 to 1994. Rather than mapping disease cases, Shone et al. (2001) mapped mosquito vectors as an indicator of the risk of WNV. Using light trap data, a GIS was utilized to map the temporal and spatial abundance of mosquito species across Maryland.

Multiple studies have used environmental characteristics associated with vector presence as a measure of disease risk. Guerra et al. (2002) used GIS techniques to predict the abundance of the tick vector *Ixodes scapularis*, as well as the risk of Lyme disease in parts of Wisconsin, Illinois, and Michigan. Logistic regression analysis determined the relationship between tick presence and habitat attributes. The logistic equation was then used to calculate the probability of the tick vector in each cell of a grid. The abundance of the vector was then used to map the risk of Lyme disease transmission from *I. scapularis*. Glass et al. (1995) used GIS techniques to identify environmental risk factors for Lyme disease in Baltimore County, Maryland. A logistic regression model was used to determine the relationship between environmental attributes and

cases of Lyme disease. The results were used to create a risk map of Lyme disease. Craig et al. (1999) used a GIS-based model to predict malaria transmission in Sub-Saharan Africa. Vector and climate data were incorporated into a mathematical model using a GIS in order to predict the risk of transmission. Brownstein et al. (2002) mapped West Nile Virus cases in New York City to determine areas at high risk. A SATscan statistic creates a window around each Census tract centroid and a likelihood ratio is calculated for each window to identify the most likely clusters. A logistic model was used to extrapolate all the Census tracts to create a map of risky Census tracts. A threshold probability level was applied to each tract so that tracts above the cutoff value were classified as high risk.

Remote sensing techniques are commonly used to inventory environmental variables associated with vector presence and disease. Glass et al. (2006) predicted risk of hantavirus pulmonary syndrome (HPS) transmission using remote sensing techniques. Using Landsat satellite data of environmental attributes, logistic regression was used to model the odds that a site was at risk of HPS. Beck et al. (1994) used remote sensing and GIS technology to identify villages at high risk for malaria transmission in southern Chiapas, Mexico. Stepwise linear regression was used to determine the relationship between environmental attributes and abundance of the malaria vector, *Anopheles albimanus*. The linear regression equation was then used to predict the abundance of *A. albimanus.* The results of the abundance model were used to discriminate between areas of high and low risk of malaria transmission. Ceccato et al. (2005) discuss how GIS and remote sensing models can be used to assess risk in order to create an early warning system for malaria outbreaks. Remotely sensed images can also be used to map vector borne disease indicators such as land cover and rainfall. The indicator variables can then be incorporated into a GIS-based model to predict the risk of malaria. Thomson et al. (1997)

applied remote sensing techniques to observe environmental changes related to vector change and abundance in Africa with the goal of implementing an early warning system for malaria.

Despite advances in predicting vector and pathogen abundances, few studies also incorporate population vulnerability data when predicting risk of disease transmission. According to Ahern et al. (2005), not much effort has been made by public health agencies to target vulnerable groups. One of the few studies to use population data in order to calculate disease risk was performed by Hassan et al. (2003). This study used a GIS along with epidemiological, environmental, and socioeconomic data to predict the risk of malaria in Egypt. Socioeconomic data included governorate-level information on the total population, average number of households, crowding index, and sanitary conditions. Discriminant analysis was used to identify the variables that best predicted malaria risk. GIS spatial analysis was utilized with the predictor variables to map the risk of malaria across Egypt. Hu et al. (1998) used a GIS and multiple regression analysis to determine the nature and extent of factors influencing malaria transmission in Yunnan Province, China. This study discovered that the combined effects of the physical environment, the presence of competent vectors and the degree of population mobility had the largest influence on malaria transmission. Allen and Wong (2006) used the kernel density estimation (KDE) method to explore the spatial pattern of potential risk for WNV in Fairfax County, Virginia, combining population and dead bird data collected in 2002. Using vulnerable locations such as elderly care facilities and day cares, a density surface of the vulnerable population was created. The population density map was then overlaid with the dead bird density map to create a risk map of the study area. Sutherst (2004) developed a mathematical model that calculates disease risk based on climatic factors as well as human

vulnerability. Human vulnerability was calculated using a mathematical model that incorporates variables such as exposure and sensitivity to pathogens.

Synthesis of the Literature

The diverse literature on vector-borne diseases and GIS has provided a broad range of resources to assist with this thesis. Much of the literature addresses how the environment is related to mosquito populations and vector-borne diseases. These types of studies are important as they provide the necessary background to situate the methodology of this study. The literature relating to GIS and public health provides many useful approaches that could be applied to this particular analysis. The most noticeable gap in the literature is the lack of work that attempts to predict risk to disease infection using population vulnerability. Many studies have assessed disease and vector patterns, but few have used GIS-based modeling to predict transmission risk over space and time. This study will try to fill this gap by using dynamic predictive modeling along with interacting variables to quantify risk of disease infection. According to Sutherst (2004), few climate change risk assessments have been reported for diseases other than malaria. By predicting the risk of EEE and WNV infection, this study will strive to fill this gap in the literature.

CHAPTER 3: DATA AND METHODS

This chapter provides an overview of the methodology involved in predicting the risk of mosquito-borne disease transmission to humans. The data and steps used to predict mosquito abundance are discussed in detail. Next, the data and methods used to estimate human vulnerability across Chesapeake are explained. The chapter concludes by explaining how mosquito abundance and human vulnerability are integrated and used to predict the risk of disease transmission.

Overview

Several GIS-based models were created that were used for predicting mosquito abundance and ultimately, risk of disease transmission. The first step was to create a model that estimates the habitat suitability for both groups of mosquitoes across Chesapeake. The model used mosquito trap data along with environmental attributes, to calculate a city-wide habitat suitability index (HSI) for *C. melanura* and the ephemeral species, *A. vexans* and *P. columbiae*, that indicates where these species are most likely to occur. The HSI values along with other environmental variables were then used in a predictive model that estimates the monthly abundance of both mosquito groups from June through August of 2003. The methods used for predicting habitat suitability and abundance were based on the methodology used by Bellows (2007). Bellows predicted the abundance of *C. melanura* across Chesapeake, Virginia for the years 2003 and 2004. This thesis takes Bellows' study a step further by incorporating human vulnerability and dasymetric mapping techniques to predict the risk of disease transmission.

Once mosquito abundance is predicted, the vulnerability of the Chesapeake population to disease can be assessed. The number of vulnerable individuals was estimated and then mapped according to land cover using dasymetric mapping techniques. Finally, the results of the abundance model and vulnerability mapping were overlaid to predict the risk of disease

transmission from both groups of mosquitoes from June to August of 2003. An overview of the steps used in predicting risk of disease transmission is provided in Figure 1.

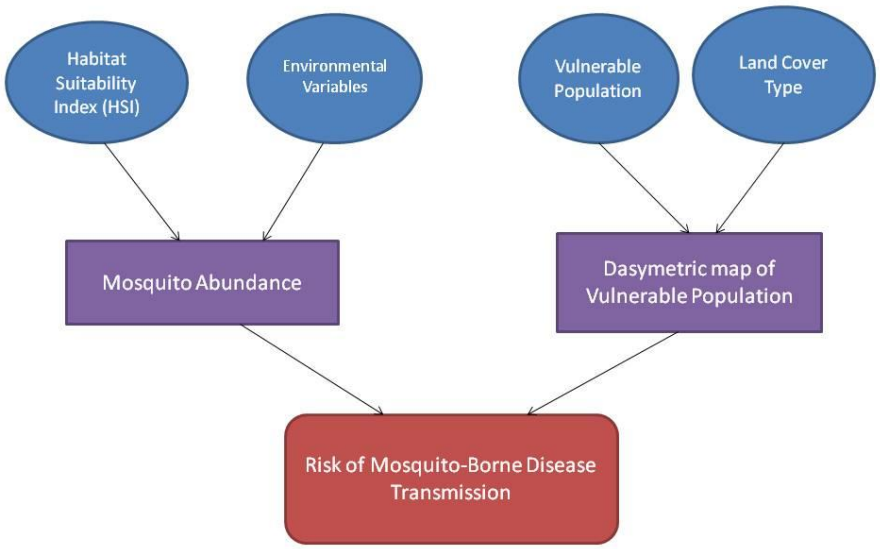

Figure 1: Overview of the steps involved in predicting the risk of disease transmission across Chesapeake.

Study Area

Chesapeake is an independent city which comprises 340 square miles (2000) of Southeastern Virginia and has a population of 220,111 (2008). The city is located in the coastal plain of Virginia and contains the northeastern portion of the Great Dismal Swamp (Figure 2). Although it serves as a large reservoir of bird and mosquito vectors, the Great Dismal Swamp was excluded from the study area because there are no permanent residents in the swamp. Therefore, it would be irrelevant to predict the risk of disease transmission to residents in this

region. The prominent wetlands and creeks within Chesapeake are conducive to mosquito breeding and therefore provide a suitable habitat for mosquitoes. The proximity of these mosquito habitats to the metropolitan areas of Chesapeake allows mosquitoes to easily transmit diseases to humans. Chesapeake was selected as the study area because of its extensive mosquito trap data. Other areas in coastal North Carolina were considered for this study, however, these regions lacked the quality of data that Chesapeake holds. The trap data were acquired from the City of Chesapeake Mosquito Control Commission (CMCC).

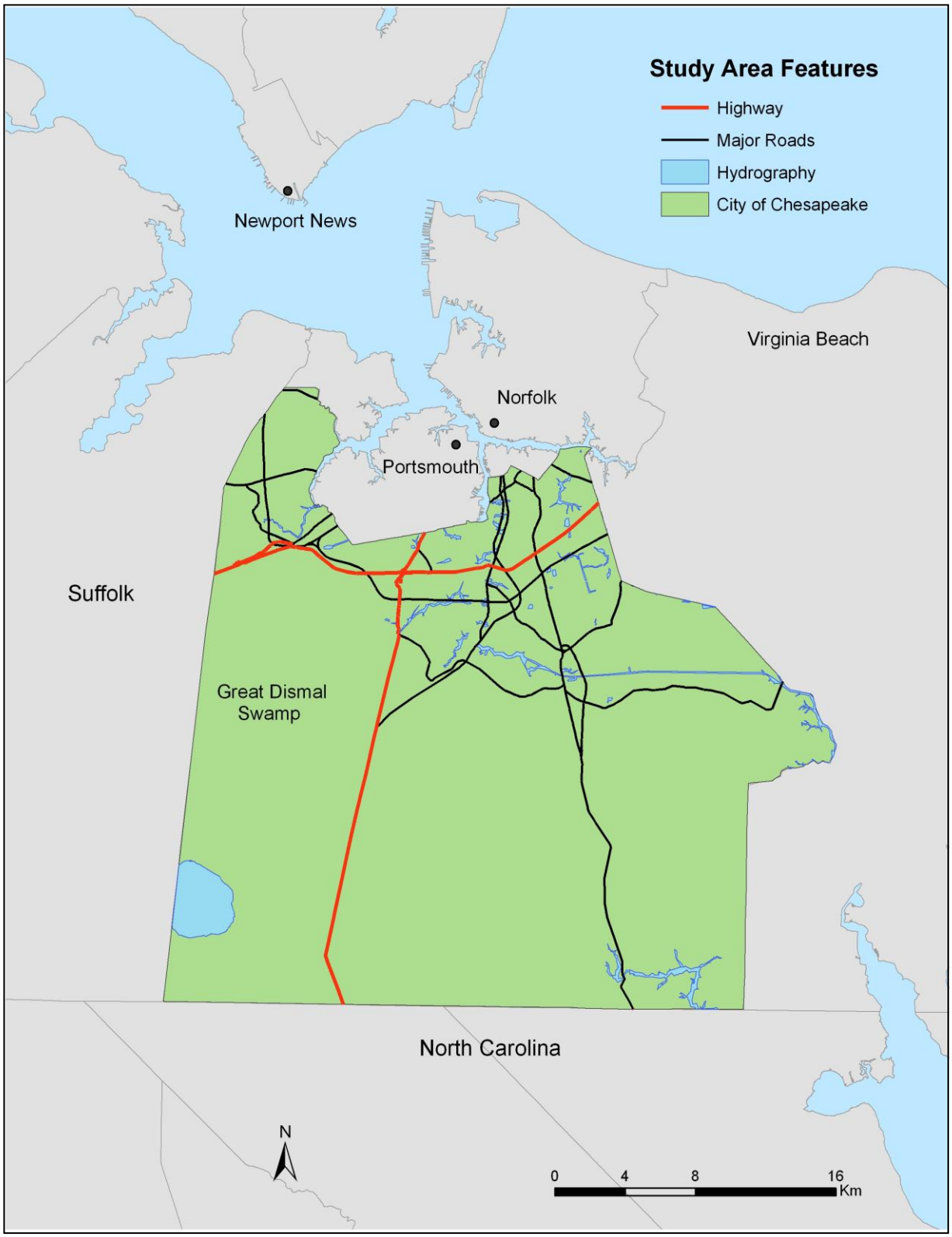

Figure 2: Map of Chesapeake, Virginia and its surrounding jurisdictions.

Habitat Suitability Index

In order to predict mosquito abundance, a habitat suitability index (HSI) is calculated for each mosquito species group. Linear regression models were used to quantify the HSI for each group. Assuming that mosquito abundance is a function of environmental variables, certain habitat attributes were used as independent variables to explain the spatial variation in mosquito capture data. Because the predictor variable data is time invariant across the year, a single habitat suitability index was calculated for each mosquito group to represent the entire breeding season. The habitat attributes (X) are weighted using the corresponding regression coefficient (b) and incorporated in a regression equation to calculate habitat suitability (Equation 1). The final HSI's were created on the basis of a 30 meter pixel grid, which serves as the unit of observation.

Equation 1: $HSI = a + b_1(X_1) + b_2(X_2) \ldots b_p(X_p)$

Dependent Variables

CO_2-baited CDC light traps were placed at 40 locations across Chesapeake, Virginia in 2003 (Figure 3). A point shapefile of the trap sites containing capture data was obtained from the Chesapeake GIS office. Mosquito numbers were counted weekly at each trapping site from April through November. Only female captures were used in this study as male mosquitoes do not bite. Capture data includes the number of each species counted in the traps per week. The cumulative counts of the ephemeral species, *A. vexans* and *P. columbiae* were summed for each month as well as for the entire season. *Culiseta melanura* counts were also aggregated accordingly. To take into account the variation in trap nights (i.e. trapping effort), the capture data were normalized by dividing the total season's captures by the total number of trap nights. The monthly totals were also divided by the number of monthly trap nights. To display how the

dependent variables vary spatially, inverse distance weighting (IDW) methods were used to interpolate a surface of the normalized trap counts. Figures 4 and 5 illustrate the interpolated surfaces of the monthly trap counts. The trap points were overlaid onto the interpolated surfaces. These surfaces can later be compared to the predicted mosquito abundance values.

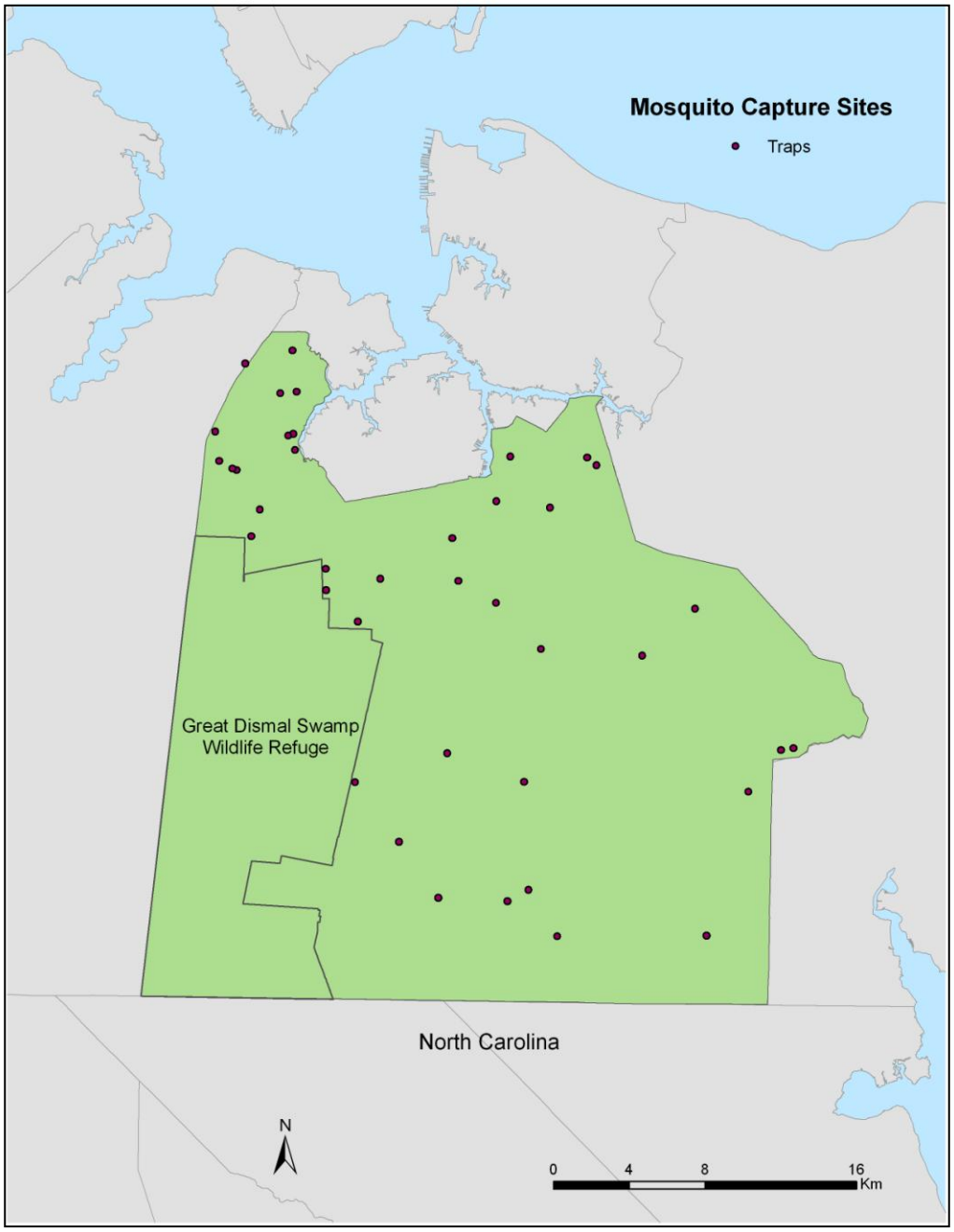

Figure 3: Light trap locations throughout Chesapeake in 2003.

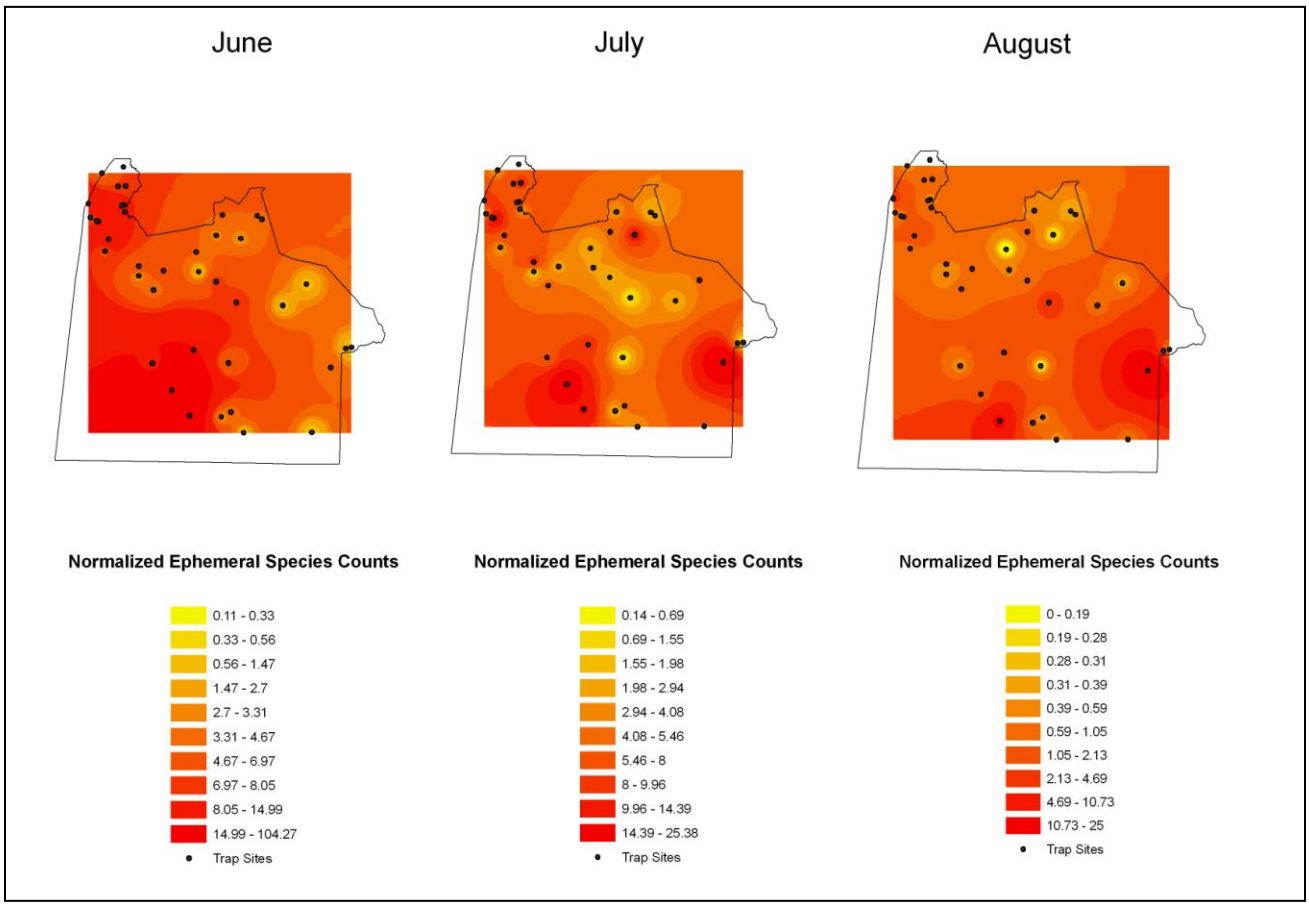

Figure 4: Interpolated surfaces of the normalized monthly trap counts for the ephemeral species. Surfaces were created using IDW. Values are symbolized using a quantile classification.

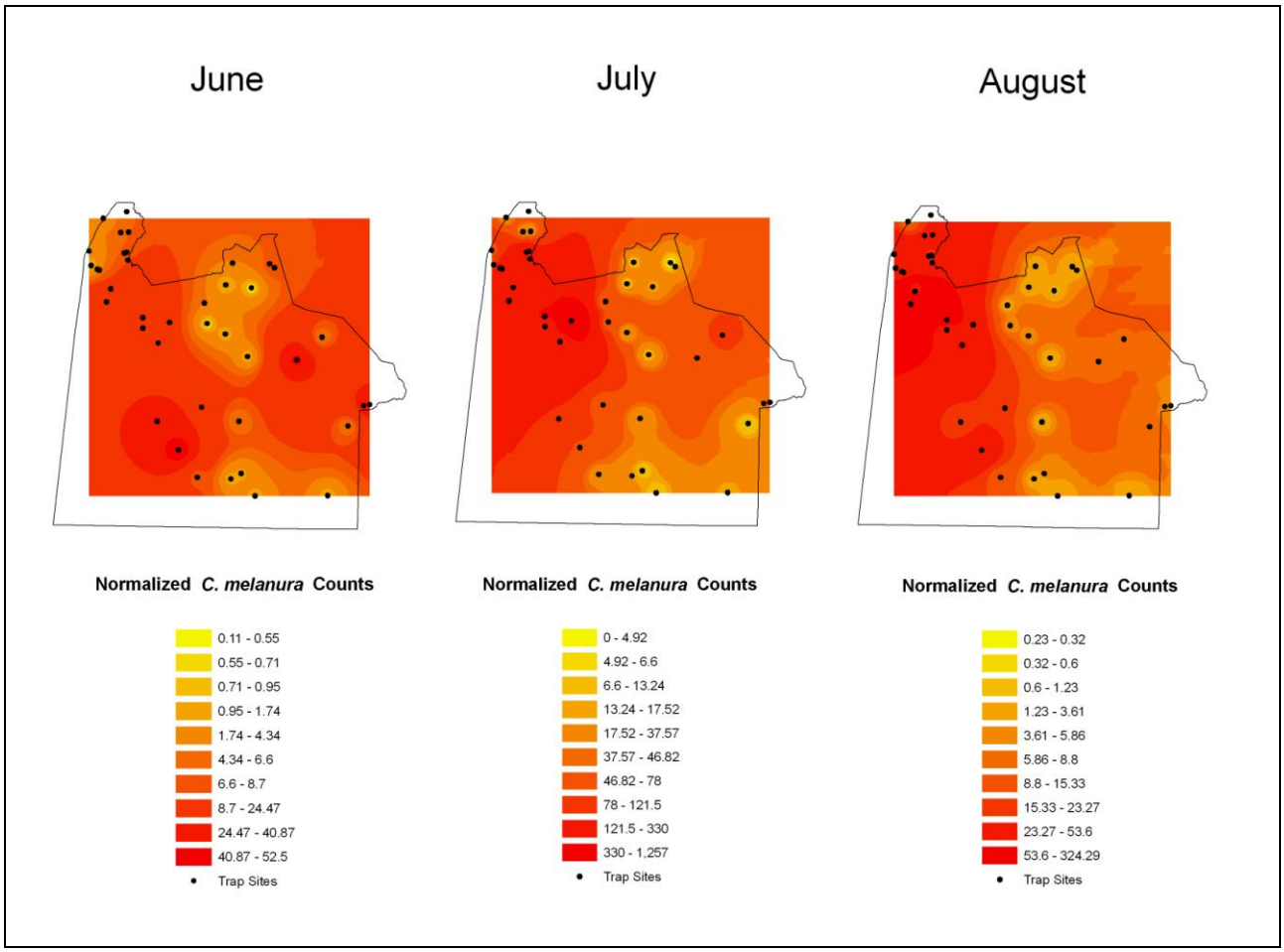

Figure 5: Interpolated surfaces of the normalized monthly trap counts for *C. melanura.* Surfaces were created using IDW. Values are symbolized using a quantile classification.

Independent Variables

The habitat variables expected to best predict the spatial variation in mosquito capture data were chosen as the independent variables in the linear regression models (Table 1). These variables were chosen based primarily on methods developed by Bellows (2007). Each independent variable required some manipulation before being used in the regression models. Each habitat attribute was converted into a 30 m pixel grid format. A model was created using

the ArcGIS 'Model Builder' application that included pre-processing of the variables as well as the final HSI calculation for both species groups (Figure 12).

Landsat satellite imagery was used to produce landscape-scale evaluation of habitat suitability. A Tasseled-Cap transformation was calculated from a 2002 Landsat image acquired from the United States Geologic Society (USGS). The Tasseled-Cap transformation is used to separate brightness, greenness, and wetness bands within satellite imagery (Crist and Cicone, 1984). Brightness, greenness, and wetness indices are useful for characterizing spatial patterns associated with habitat suitability. Brightness is a measure of reflectance and is correlated to the texture and moisture content of soils (Guerra et al., 2002). Greenness is a measure of the density of green vegetation present, while wetness is a measure of the moisture in soils and vegetation. The transformed values are reprojected onto three orthogonal axes (TC1-TC3). TC1-TC3 were used as the independent variables in the linear regression equations (Figure 6).

Soil survey data was acquired from the United States Department of Agriculture (USDA) National Resources Conservation Service's (NRCS) soil data mart. Chesapeake soil data for 2002 was exported into SSURGO format (Soil Survey Geographic Data). The SSURGO soil data is presented in the form of ArcGIS polygon shapefiles. Various soil attributes were chosen to be used as explanatory variables in the habitat suitability model. The variables were chosen based on their relationship to mosquito habitat preferences. The soil attributes chosen are each associated with soil moisture. According to Tanser, Sharp, and le Sueur (2003), soil moisture is an important factor in mosquito survival. Once the soil variables were converted into grid format, the variables were reclassified into numeric values (Table 2). These numbers are standard values used by SSURGO. The soil variable grids are shown in Figures 7-11.

Variable	Code	Data Type	Source	Description
Tasseled-Cap	TC1-TC3	Raster: Landsat-7 ETM+	USGS	TC1 (Brightness) TC2 (Greenness) TC3 (Wetness)
Hydrologic	HYD	Vector (polygon)	NRCS	Presence of water
Percent Hydric Composition	HYDRIC	Vector (polygon)	NRCS	Soil meets requirements for hydric soil
Drain Potential	DRAIN	Vector (polygon)	NRCS	Degree of hydraulic conductivity and low water-holding capacity
Runoff Potential	RUNOF	Vector (polygon)	NRCS	Degree of potential water loss by overland flow
Water Table Depth	WTD	Vector (polygon)	NRCS	Minimum value for the range in depth to the seasonally high water table (April-June)
Available water storage (25 cm)	AWS25	Vector (polygon)	NRCS	Maximum value for the range of available water in plant root zones

Table 1: Habitat attributes used as independent variables in habitat suitability regression model

Soil Attribute	Values
HYD	0 = no water 1 = water
HYDRIC	0 = not hydric 1 = hydric
DRAIN	1 = well drained 2 = moderately well drained 3 = somewhat poorly drained 4 = poorly drained 5 = Very poorly drained 6 = water
RUNOF	1.00 = neglible 0.75 = very low 0.50 = low 0.25 = medium 0 = water
WTD	Continuous
AWS25	Continuous

Table 2: Soil attributes used as independent variables in habitat suitability regression models.

Not every habitat attribute was used in each linear regression model. The variables used in each model were chosen based primarily on work by Bellows (2007). Bellows used multiple regression models to calculate a HSI for the same species included in this thesis, using equivalent trap data for Chesapeake, Virginia. Bellows used all possible regressions (APR) to select the independent variables that best explain the spatial variation in trap data. The variables chosen by Bellows were used as the independent variables in the corresponding linear regression models to predict mosquito abundance (Table 3).

Ephemeral Species Model	***C. melanura* Model**
TC1	TC2
TC2	TC3
HYD	DRAIN
DRAIN	RUNOF
RUNOF	AWS25
WTD	

Table 3: Independent variables chosen to be used in linear regression models to predict HSI.

The effect of variables influencing landscape and ecosystem-level patterns, processes, and functions is scale-dependent (Turner, 1989). Therefore, the spatial scale used for each habitat attribute was not the same in every case. For each habitat attribute, the spatial scale that is most strongly correlated with mosquito captures for each species group was used. The spatial scales were chosen based on research by Bellows (2007). Bellows used Pearson's correlation analysis to determine the spatial scale most strongly correlated with mosquito captures for each independent variable. ArcGIS Spatial Analyst tools were used to replace the raster values for each attribute with the focal neighborhood mean of the pixels with the corresponding spatial scale. The spatial scales for each habitat attribute are included in Tables 4 and 5. In order to associate the predictor variables with the mosquito counts at each trap site, the corresponding predictor variable data were spatially joined to the attribute table of each trap point.

Independent Variable	Neighborhood Settings
TC1	17 x 17
TC2	21 x 21
HYD	3 x 3
DRAIN	5 x 5
RUNOF	19 x 19
WTD	1 x 1

Table 4: Focal neighborhood settings (height x width) for the ephemeral species group.

Independent Variable	Neighborhood Settings
TC2	21 x 21
TC3	21 x 21
DRAIN	17 x 17
RUNOF	17 x 17
AWS25	7 x 7

Table 5: Focal neighborhood settings (height x width) for *C. melanura.*

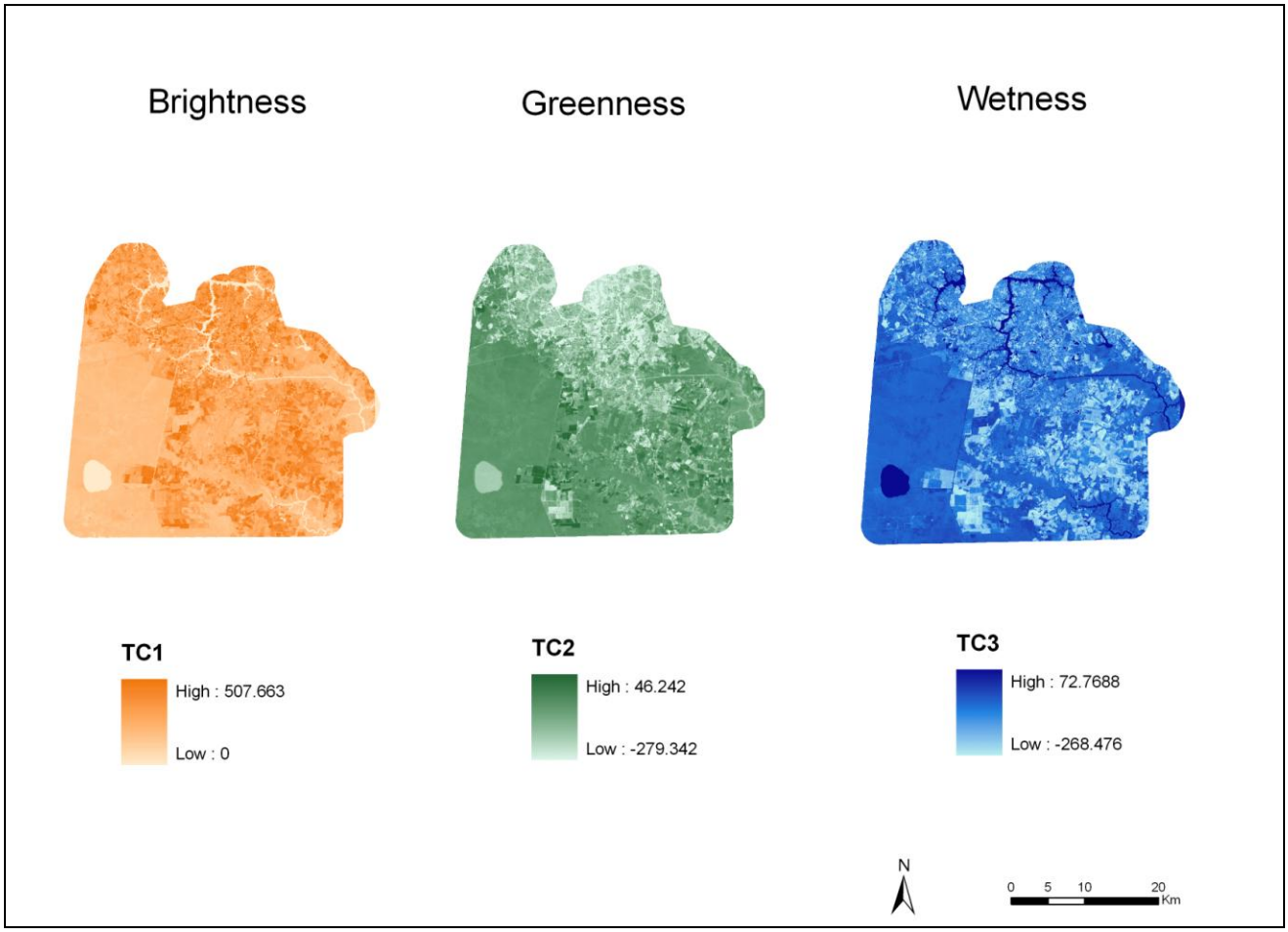

Figure 6: Tasseled-cap indices.

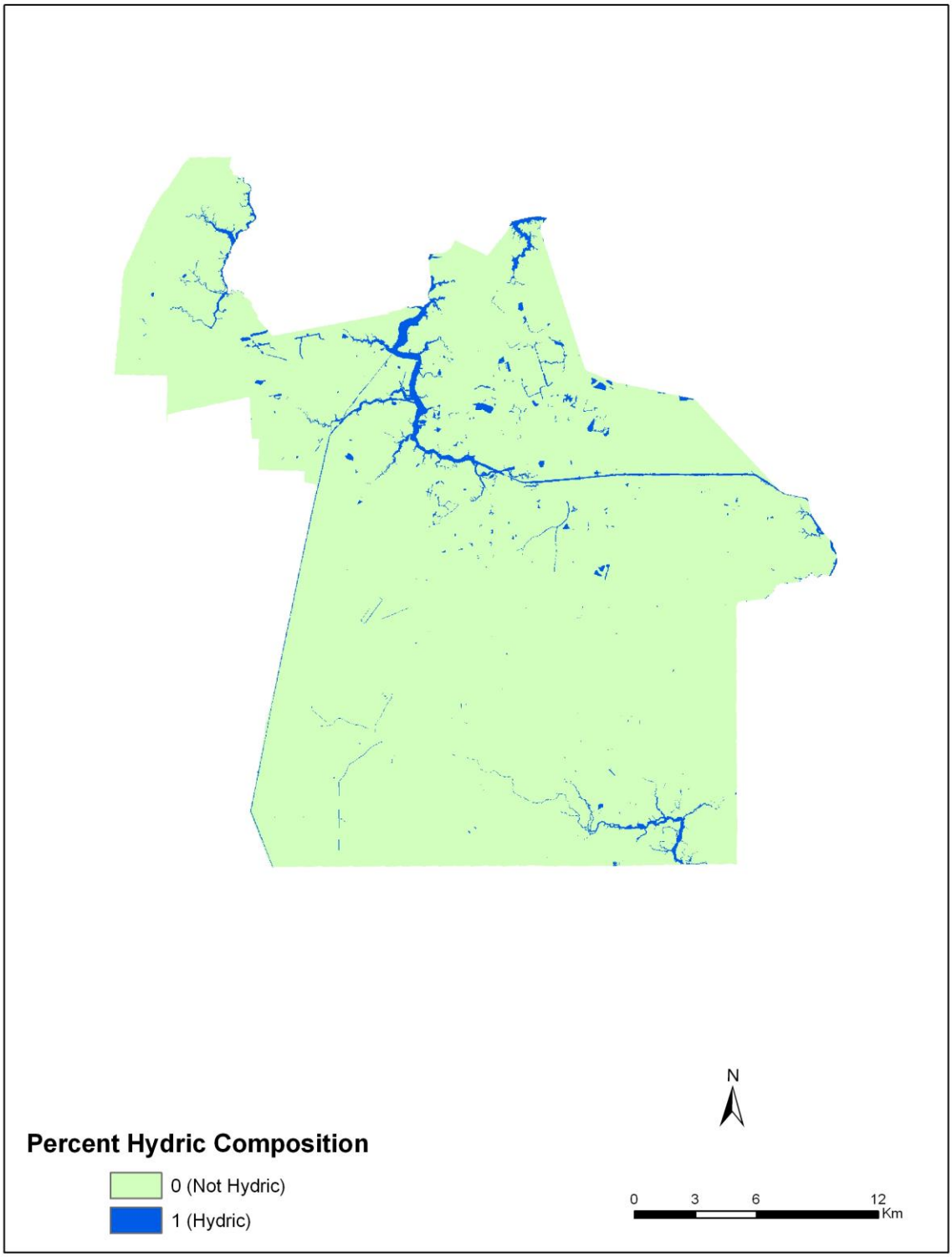

Figure 7: Percent hydric composition of the soil. Soil that meets the hydric percentage requirements were classified as 'hydric'.

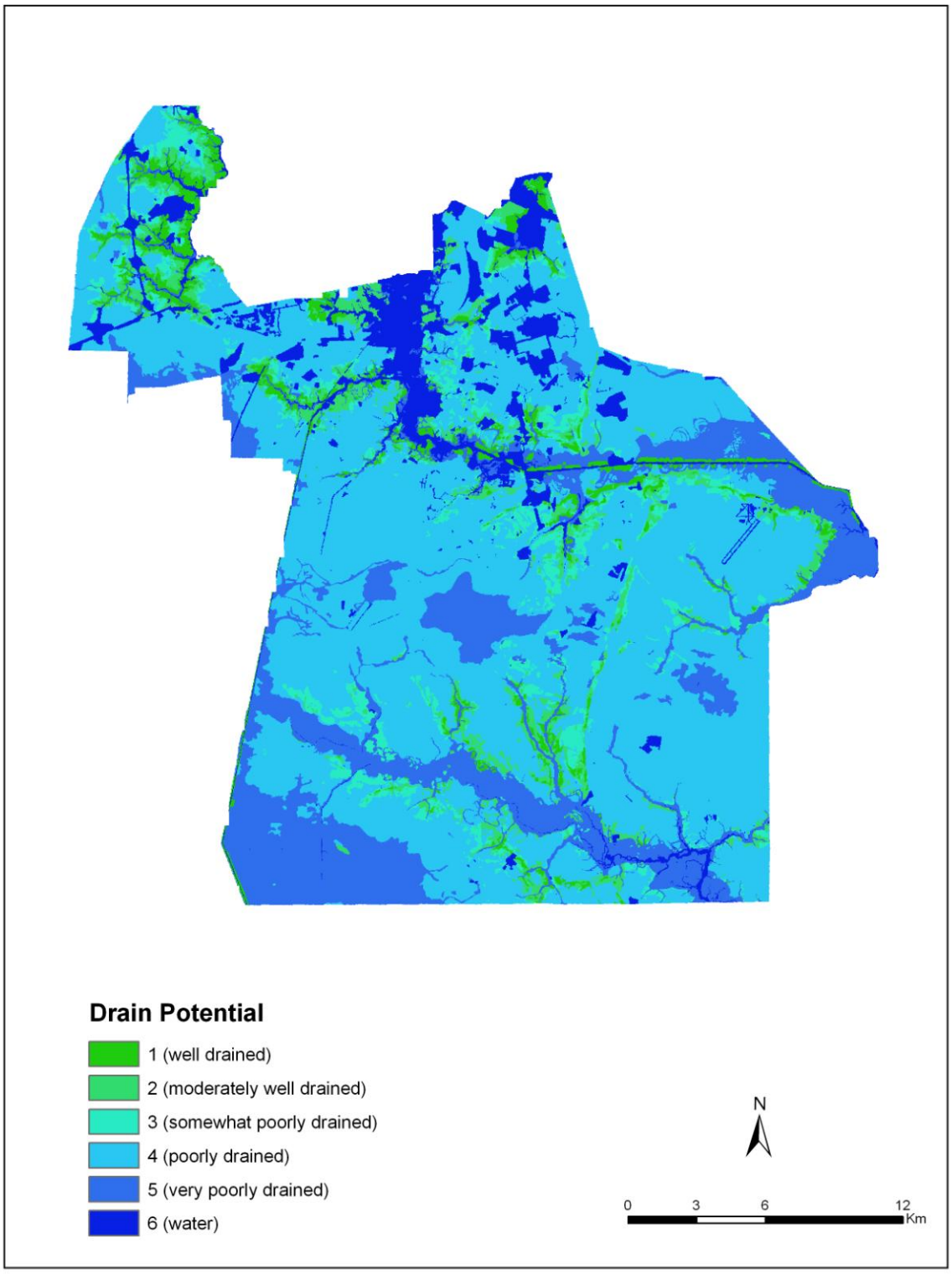

Figure 8: Soil drainage potential. Values are based on standard numbers used by SSURGO.

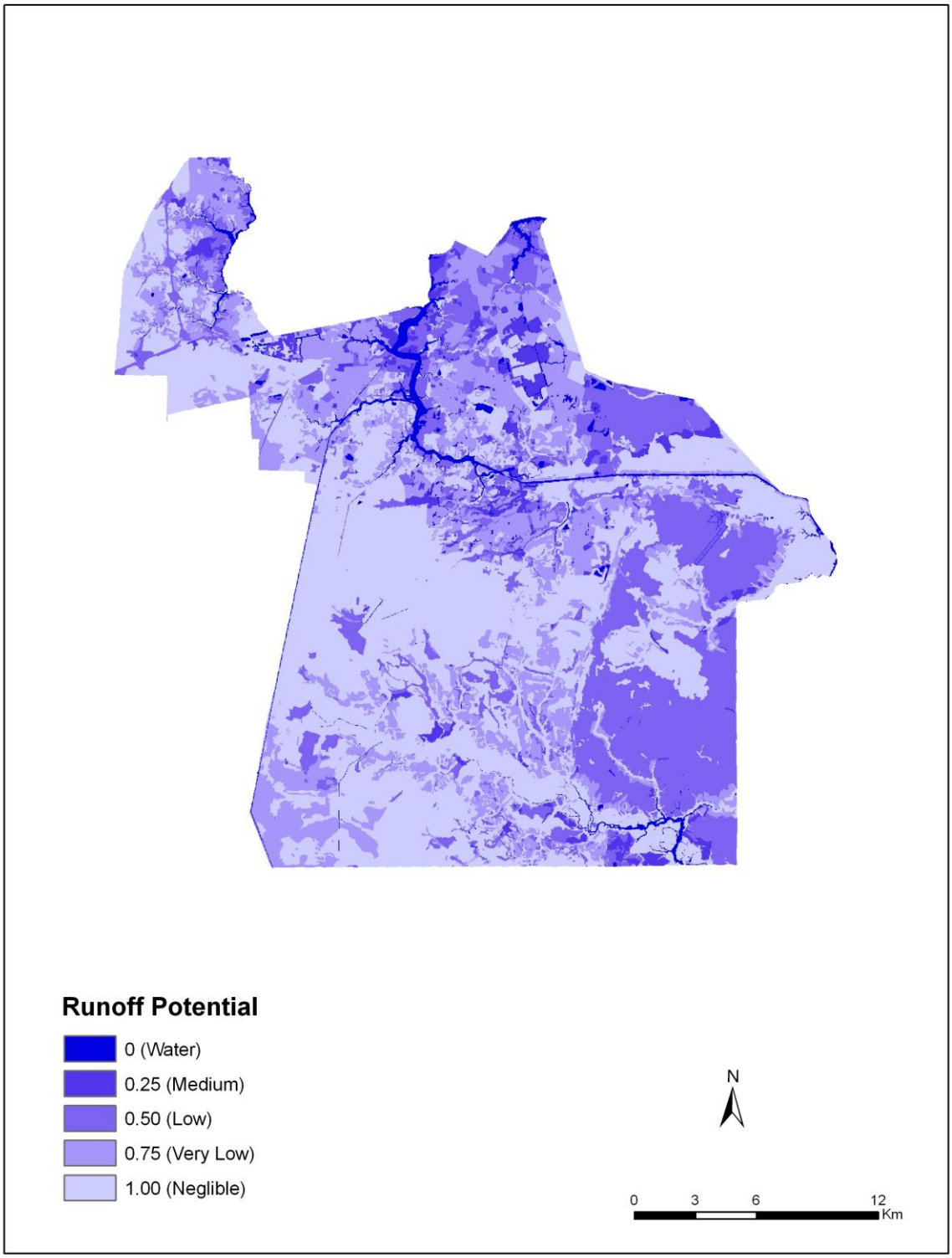

Figure 9: Soil runoff potential. Values are based on standard indices used by SSURGO.

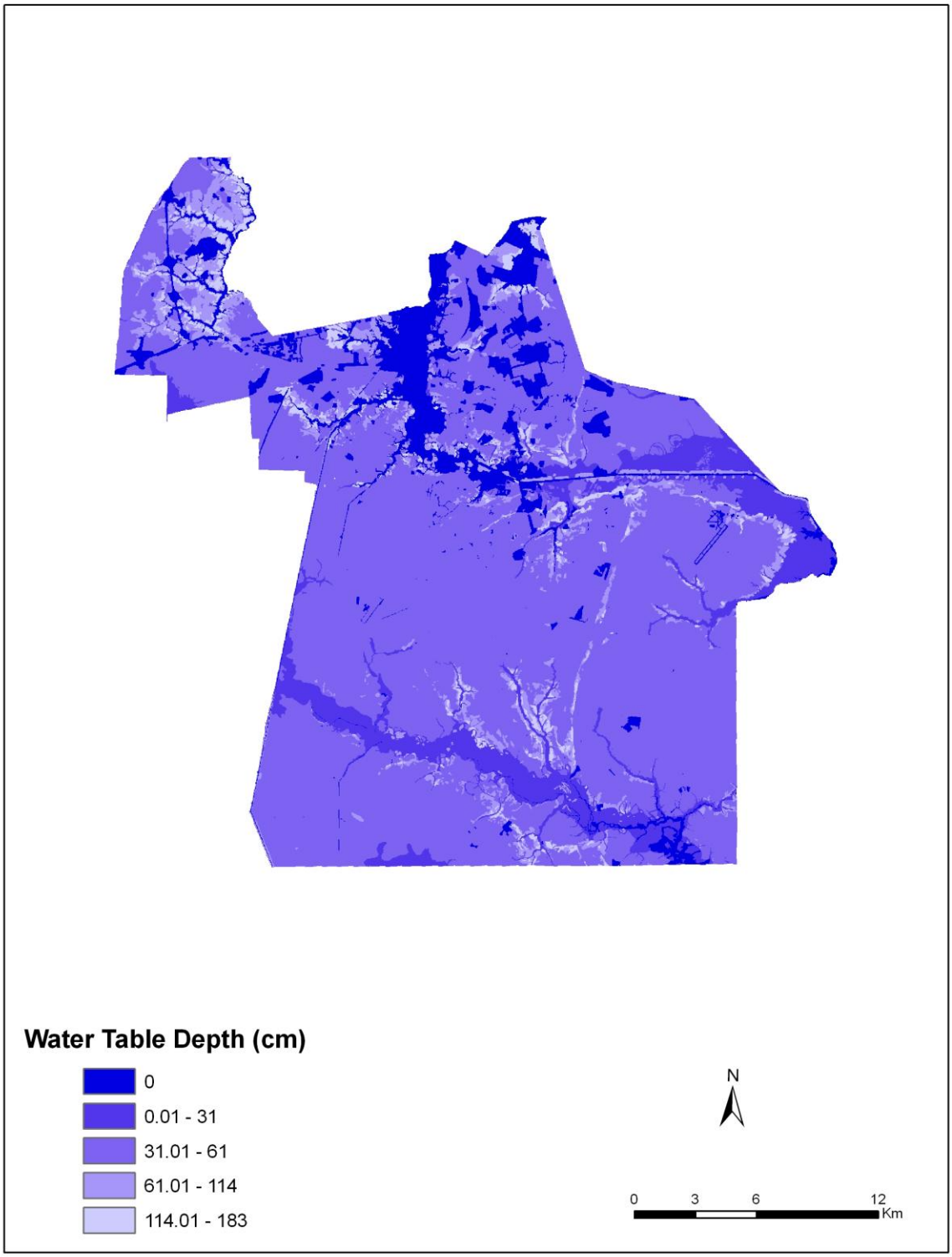

Figure 10: Water table depth. Values represent the depth in cm to the water table.

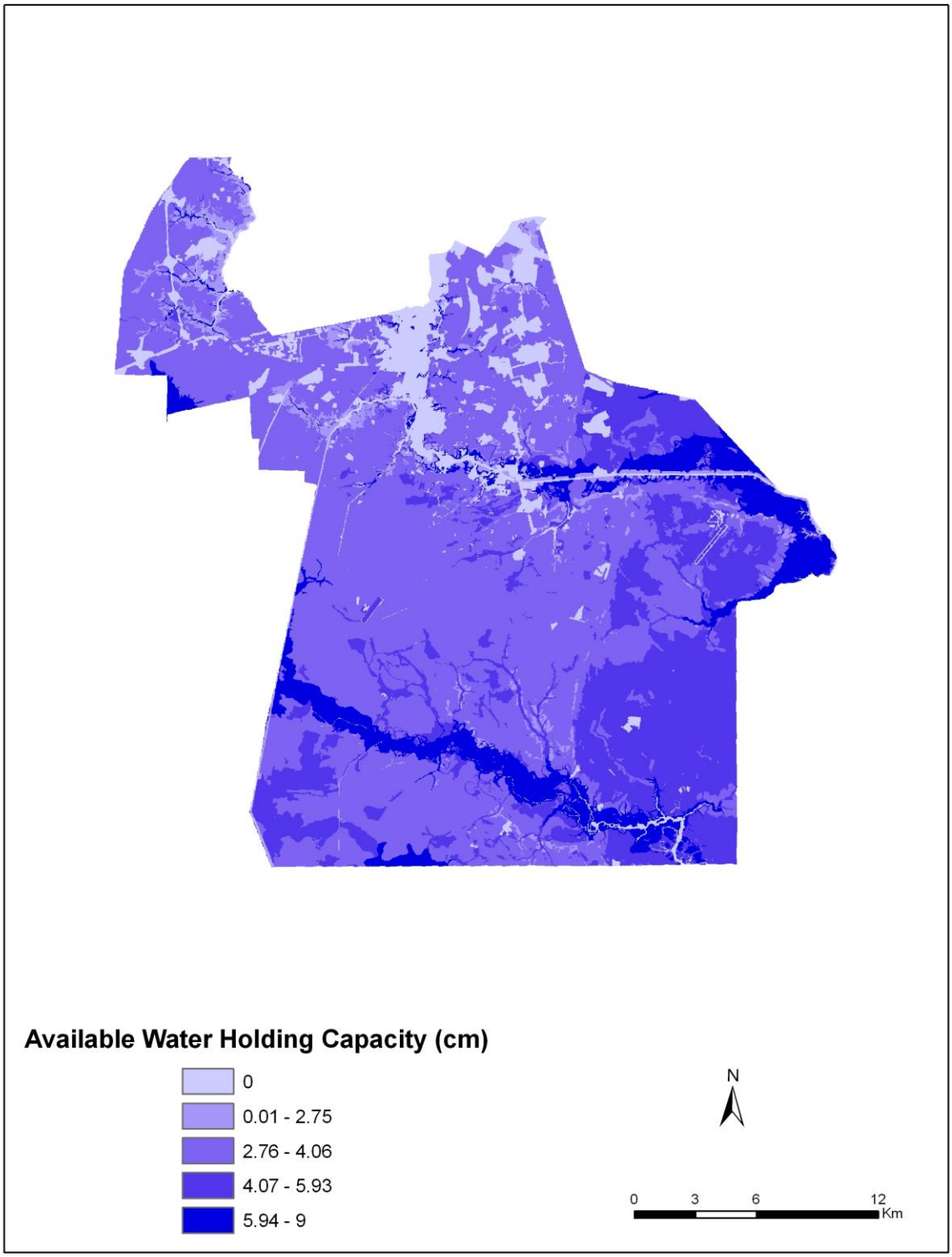

Figure 11: Available water holding capacity of the soil at 25 cm. Values represent volume of water in cm.

Linear Regression Models

Using the statistical software PASW Statistics 17.0, linear regression models were calculated for each species group which model the effect of the independent variables on mosquito counts. For each group of species, the total normalized mosquito count for all months was regressed upon the corresponding predictor variables. Because there are 39 traps and the study period covers three months, ideally the sample size (n) should have been 117 traps. However, not every trap was counted each month, reducing the sample size to 93 traps. In order to obtain the regression equation of best fit, two outliers were removed from the *C. melanura* regression model. The results of the linear regression models for both species groups are shown in Equations 2 and 3.

R^2	Adjusted R^2	F	Sig
0.356	0.238	3.035	.018

Table 6: Summary of the linear regression model for the ephemeral species group.

Variable	B	t	Sig
Constant	-111.719	-1.629	0.113
TC1	1.065	3.106	0.004
TC2	0.517	1.805	0.080
HYD	20.807	0.762	0.452
DRAIN	-7.925	-1.212	0.234
RUNOF	20.730	0.904	0.373
WTD	-0.283	-1.266	0.215

Table 7: Results of the linear regression equation for the ephemeral species group.

Equation 2: Regression equation to calculate HSI for the ephemeral species.

HSI_{Ep} = -111.719 + 20.730 (RUNOF) – 0.283 (WTD) + 0.517 (TC2) + 1.065 (TC1) + 20.807 (HYD) - 7.925 (DRAIN)

R^2	Adjusted R^2	F	Sig
0.339	0.236	3.287	.017

Table 8: Summary of the linear regression model for *C. melanura*.

Variable	B	t	Sig
Constant	-532.162	-2.818	0.008
TC2	-5.357	-2.599	0.014
TC3	0.193	0.059	0.953
DRAIN	11.926	0.531	0.599
RUNOF	510.400	3.096	0.004
AWS25	51.574	1.924	0.063

Table 9: Results of the linear regression equation for *C. melanura*.

Equation 3: Regression equation to calculate HSI for *C. melanura.*

HSI_{Cm} = -532.162 + 510.400 (RUNOF) + 51.574 (AWS25) – 5.357 (TC2) + 0.193 (TC3) + 11.926 (DRAIN)

Once the linear regression models were calculated, the regression equations could be encoded into the spatial model to calculate the HSI value in each grid cell. Each independent variable was inserted into the regression equations using the 'Map Algebra' tool (Figure 12).

The raw HSI values were separated into five equal interval classes to represent the percent suitability (Figure 13).

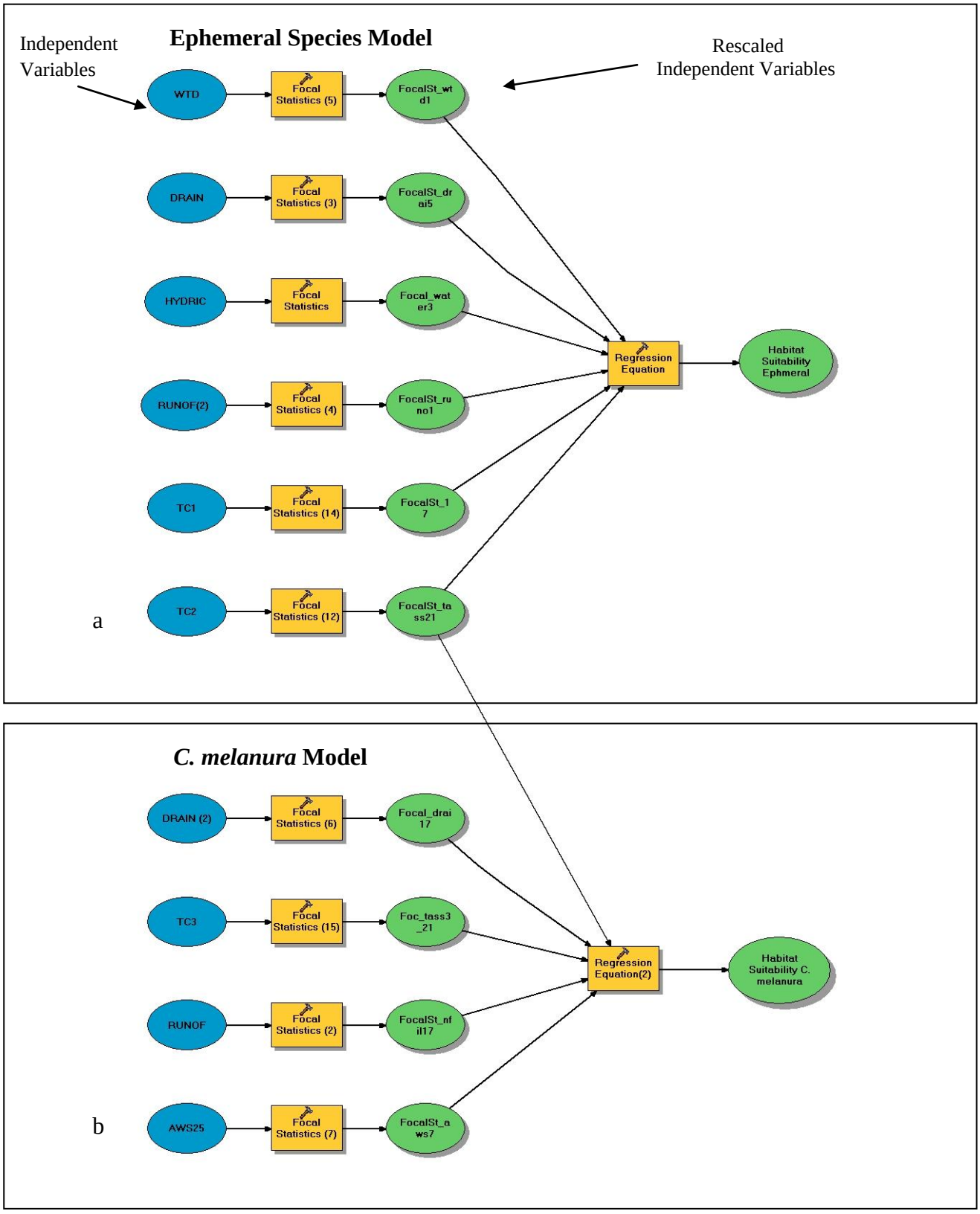

Figure 12: Model that calculates HSI for the ephemeral species (a) and *C. melanura* (b).

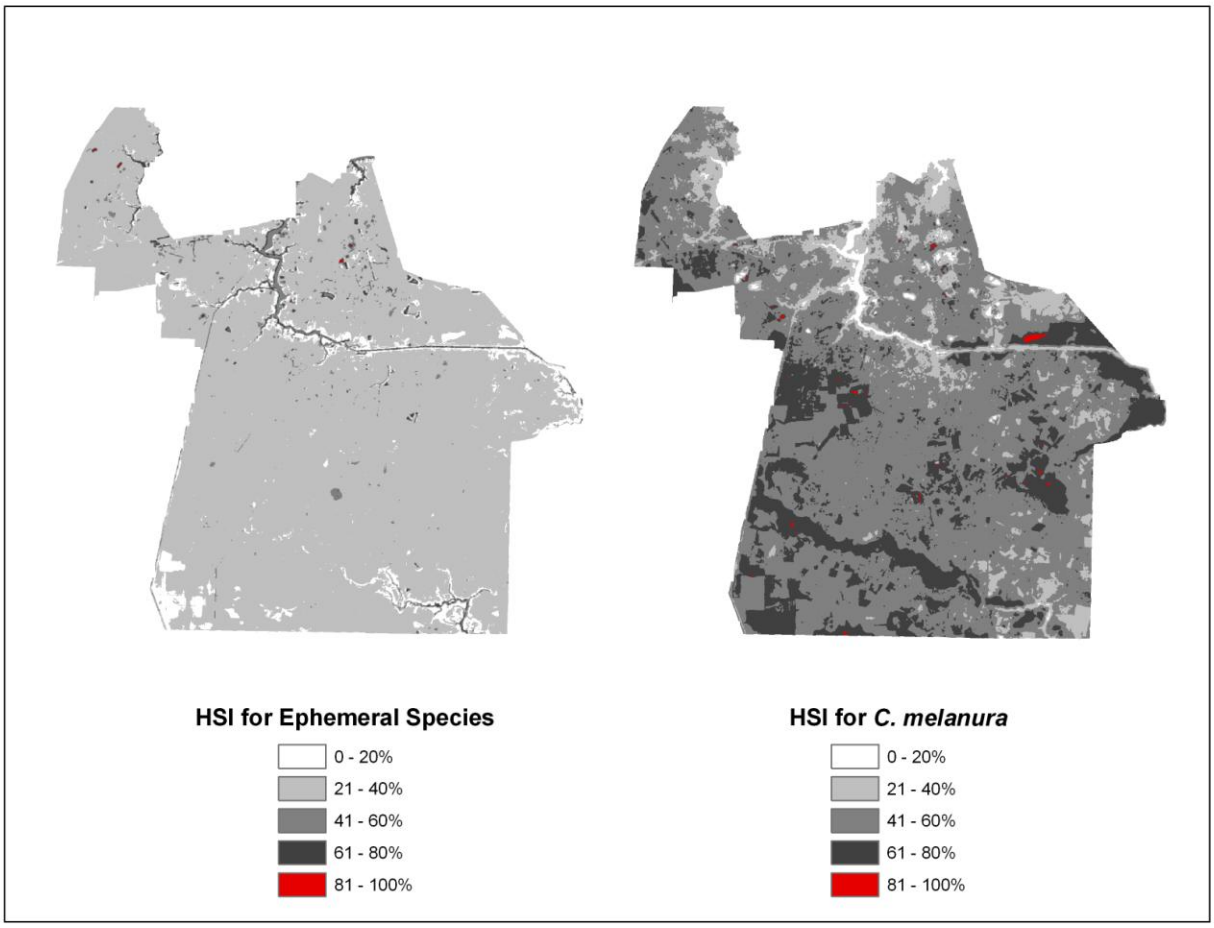

Figure 13: HSI for ephemeral species group and *C. melanura*. The HSI values were calculated using equations 2 and 3. Values were classified into 5 equal interval classes.

Mosquito Abundance Models

Using the Model Builder function, an equation was built for both groups of mosquitoes which predicted mosquito abundance for each month from June to August of 2003. Linear regression models were used to quantify the effect of certain climate variables on mosquito trap counts for each month. The regression equations were then used to calculate monthly indices to represent the weighted effects of the variables on mosquito captures for both mosquito groups. The indices representing the weighted spatial coefficients for each climate variable were

abbreviated as 'WSC'. The WSC monthly indices were each overlaid with the corresponding HSI grid to calculate the monthly mosquito abundance.

Independent Variables

Topographic Soil Moisture Index (TMI), monthly precipitation, and Average Weekly Air Temperature (AWAT) were used as the explanatory variables in the linear regression models. The product of temperature and precipitation were also used as an independent variable in the models to account for possible interaction. Each variable was aggregated to a 30 m x 30 m pixel grid. Each grid cell is representative of the corresponding month's environmental conditions. In other words, there will be three grids for each variable representing each month in the study period.

Topographic Soil Moisture Index (TMI) Grid

The Topographic Soil Moisture Index (TMI) is a derivative of slope (Figure 14) and flow accumulation (Figure 15). Using a ArcGIS hydrology tools, flow accumulation and slope were calculated using a 2-ft interval Digital Elevation Model (DEM) of Chesapeake. TMI was calculated using an equation derived from Beven (1997) which is shown below.

Equation 4: $TMI = \ln (A / \tan \beta)$

Where A = flow accumulation surface and β = slope surface. The Map Algebra tool was used to calculate this equation and create a 30 m TMI grid. The TMI grid was normalized and rescaled using the following equation:

Equation 5: $$TMI_r = \frac{(TMI_O - TMI_{min})}{(TMI_{max} - TMI_{min})} \times 100$$

Where TMI_r = normalized and rescaled TMI pixels, TMI_O = calculated TMI values (Equation 4), TMI_{min} = the lowest pixel value in the calculated TMI surface, and TMI_{max} = the highest pixel value in the calculated TMI surface. The final rescaled TMI surface is shown in Figure 16.

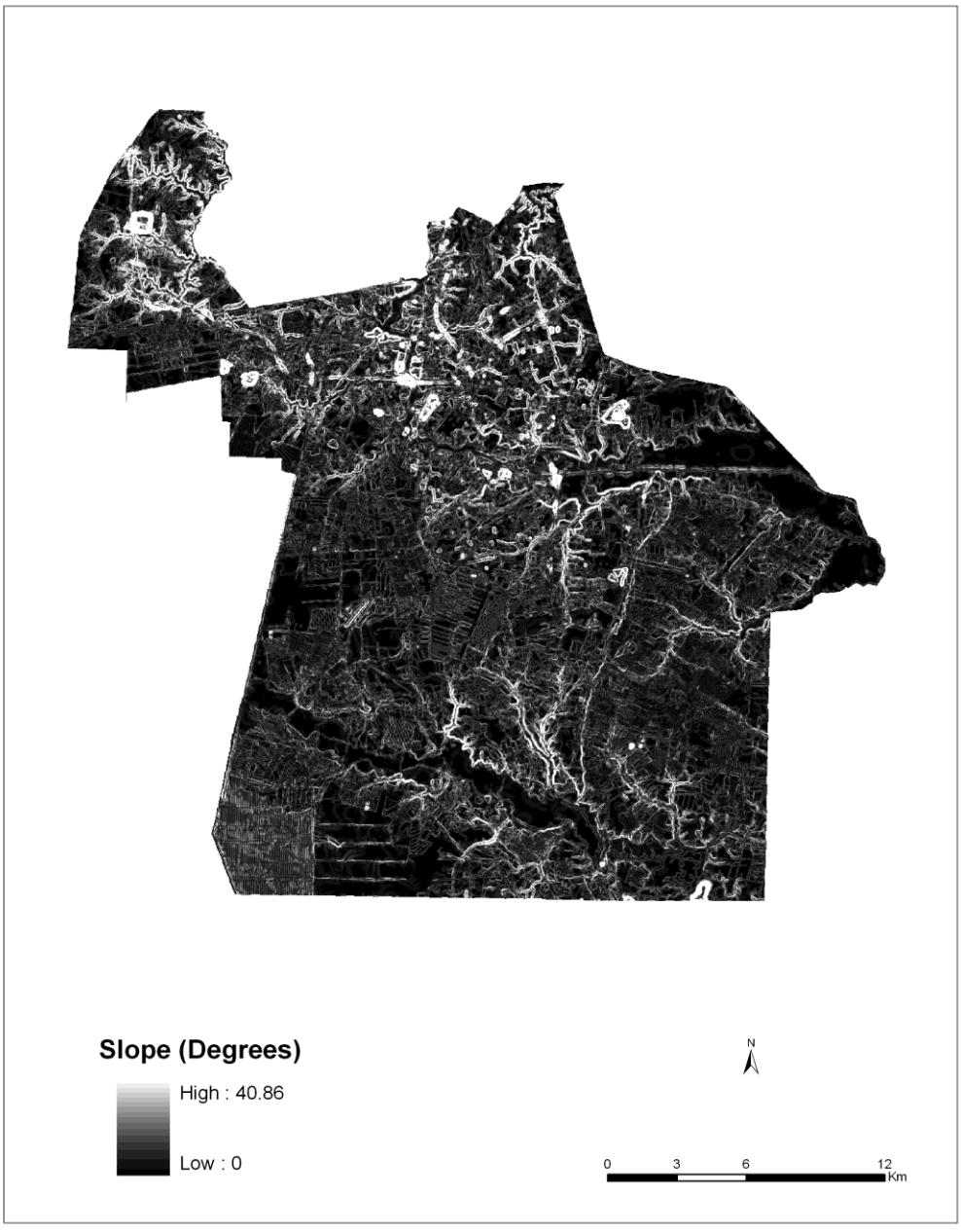

Figure 14: Slope surface of the DEM.

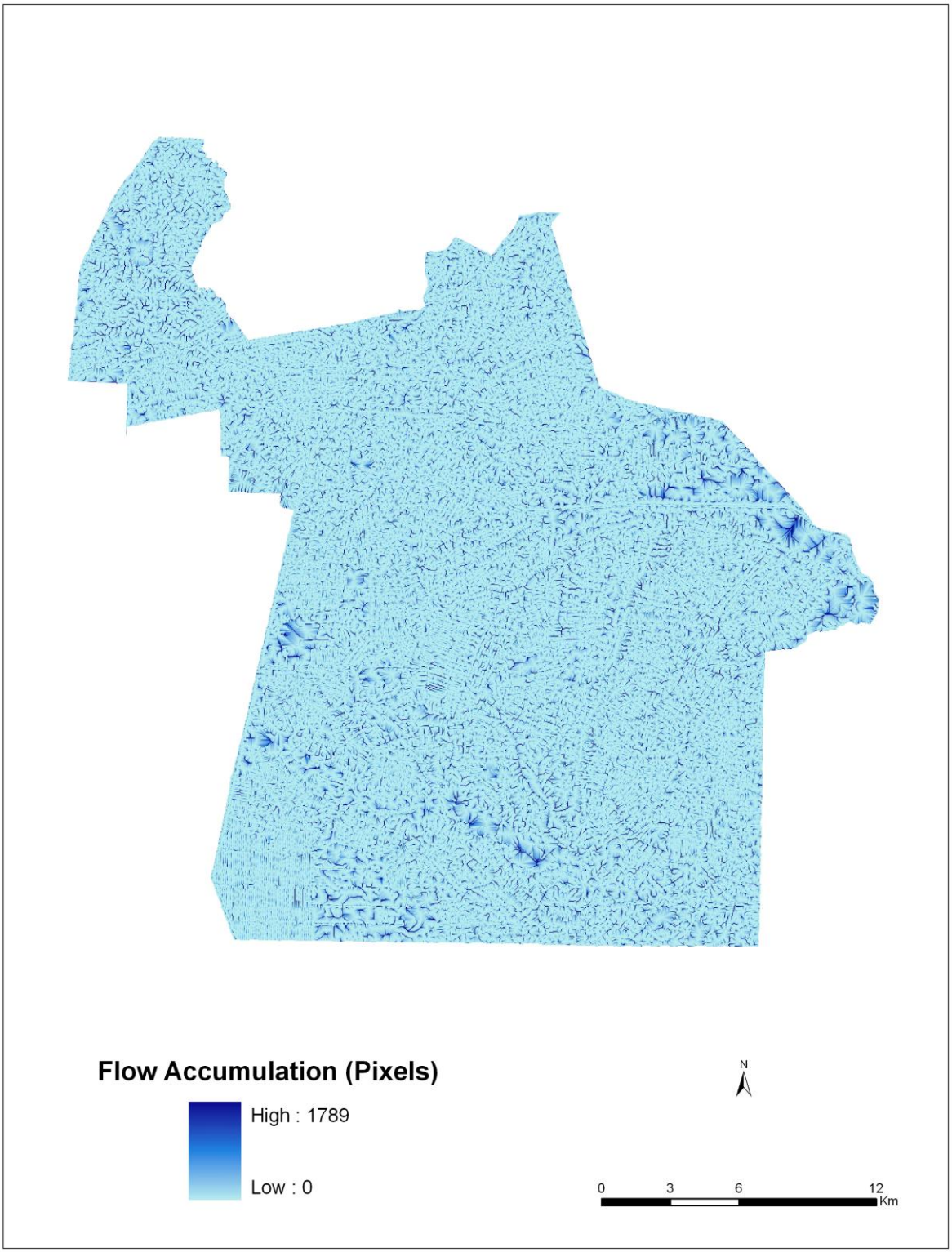

Figure 15: Flow accumulation surface of the DEM. Values represent the number of pixels flowing into each cell.

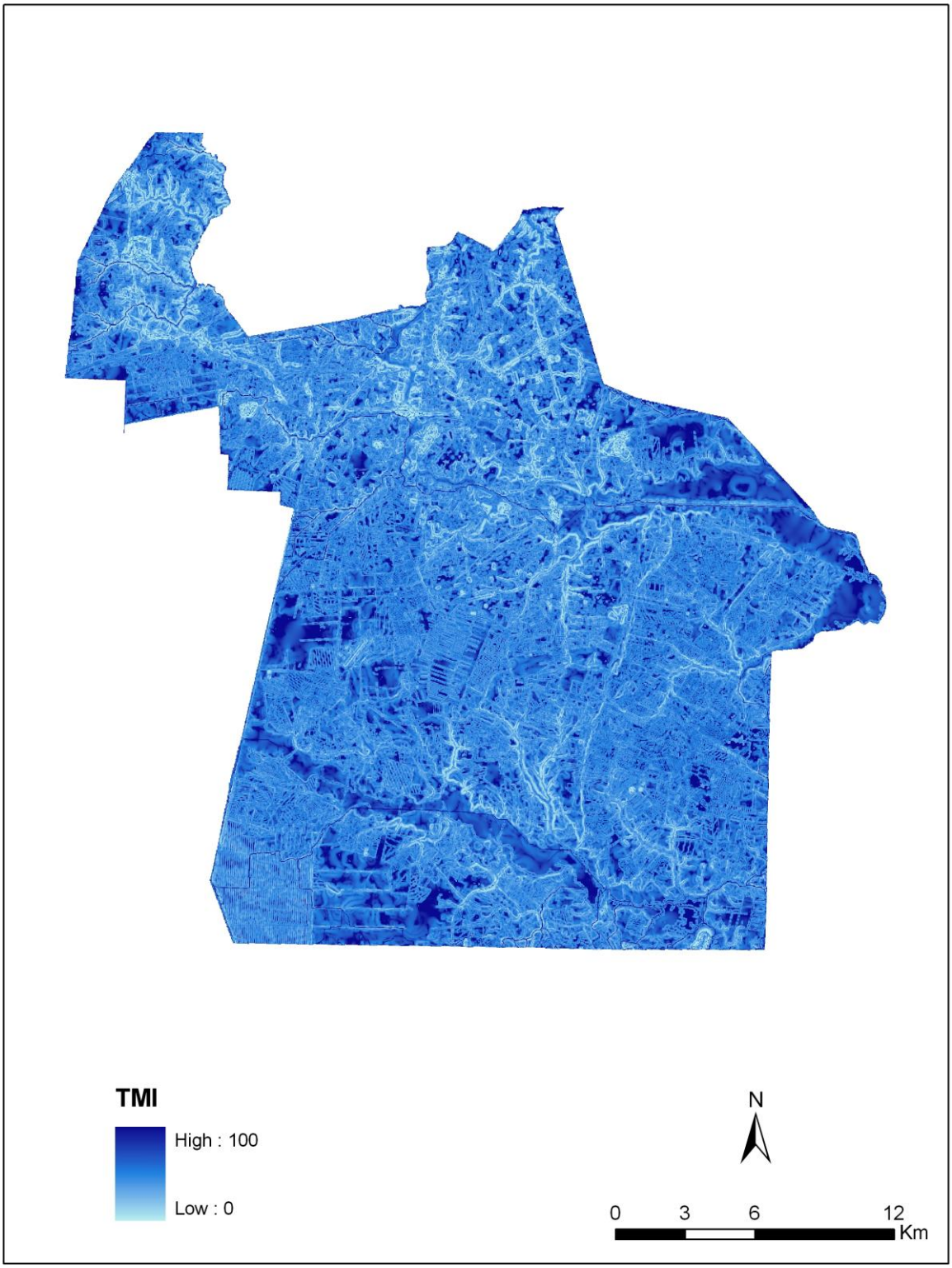

Figure 16: Topographic soil moisture index (TMI). Values calculated using Equation 5.

Weekly Average Air Temperature (AWAT) Grids

Unfortunately, spatially dependent temperature grids for Chesapeake, Virginia are not available for 2003. AWAT constant-value grids are available from the National Climatic Data Center (NCDC), collected at the NWS Station at Chesapeake Regional Airport (KCPK). Each grid displays the mean weekly temperature in Fahrenheit degrees across Chesapeake. Rather than using weekly temperature grids, AWAT temperature data was obtained and aggregated to the month. For each month, the weekly average temperatures were averaged and attributed to the grid (Figure 17). The temperature values were normalized and rescaled using the following equation:

Equation 6: $$X_r = \frac{(X_O - X_{min})}{(X_{max} - X_{min})} \times 100$$

Where X_r = the normalized and rescaled monthly temperature value (0-100), X_O = the observed temperature value, X_{min} = the minimum monthly temperature value, and X_{max} = the maximum monthly temperature value.

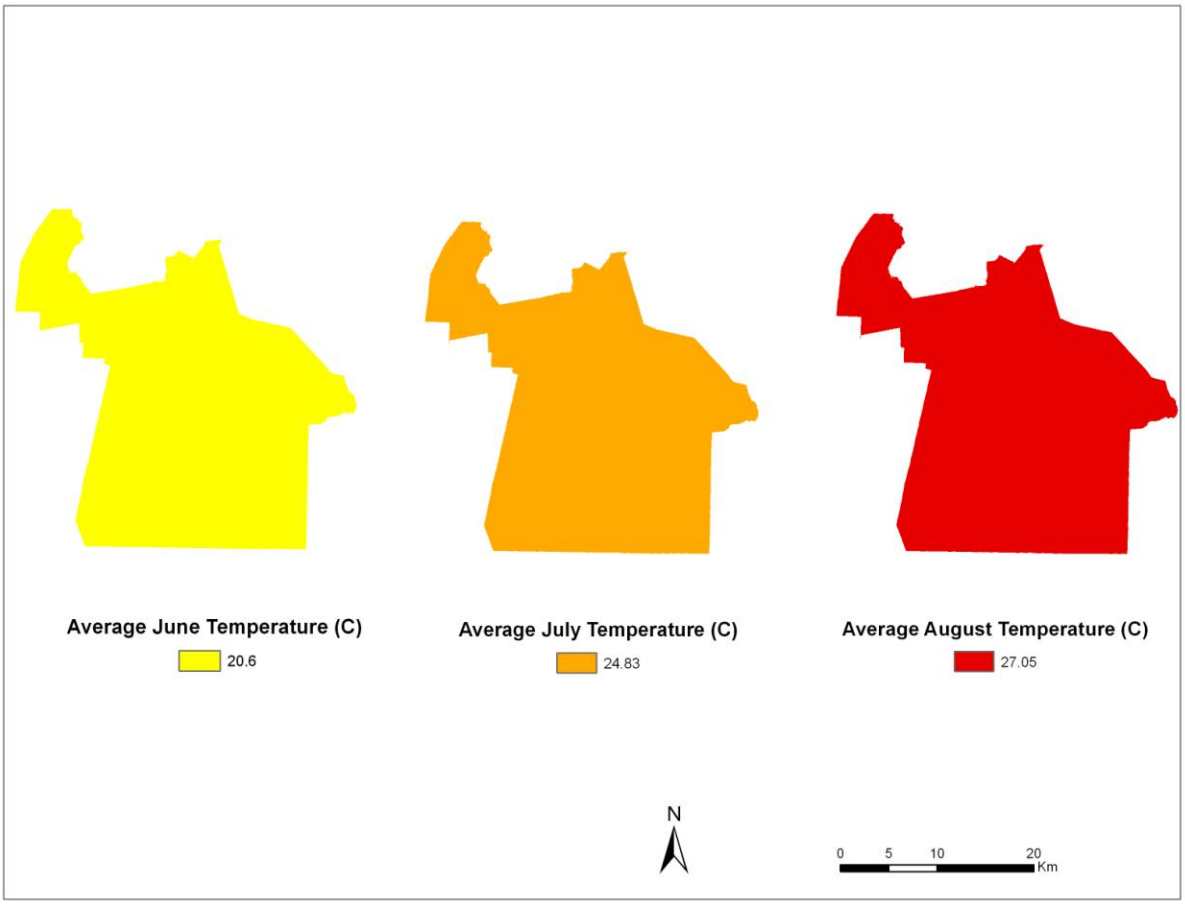

Figure 17: Monthly average air temperature grids. The values were rescaled from 1 to 100 using Equation 6.

PRISM Precipitation Grids

Monthly precipitation grids were obtained from the PRISM Climate Group. The precipitation data sets are created using the Parameter-elevation Regressions on Independent Slopes Model (PRISM) climate mapping system. Chesapeake experienced a particularly wet summer in 2003 due to Hurricane Isabel which made landfall in North Carolina on September 18, 2003 (Smith and Graffeo, 2005). PRISM grids display the nationwide average rainfall in millimeters for each month of the study period. Grids were downloaded in ASCII format and converted to raster format (Figure 18). Each monthly grid was clipped to the full extent of the

study area and the values were normalized and rescaled from 1 to 100 using the following equation:

Equation 7: $X_r = (X_O / X_{max}) \times 100$

Where X_r = the normalized and rescaled monthly temperature value (0-100), X_O = the observed value, and X_{max} = the maximum value. To take into account the combined effect of temperature and rainfall on mosquito counts, the corresponding monthly precipitation and temperature grids were multiplied using the equation:

Equation 8: $X_{pt} = X_{prec} \times X_{temp}$

Where X_{pt} = the product of the average monthly precipitation and average monthly temperature, X_{prec} = the rescaled monthly precipitation values, and X_{temp} = the rescaled monthly temperature values. The resulting grids are shown in Figure 19.

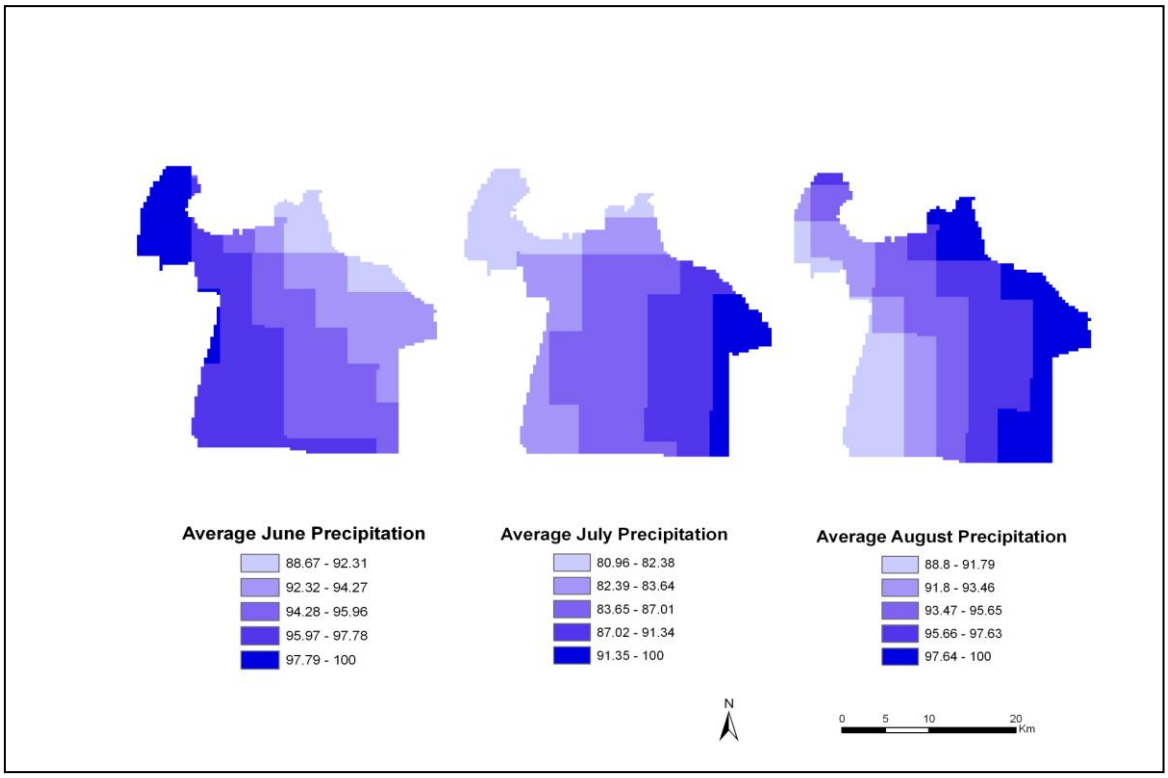

Figure 18: Monthly average rainfall. Values were rescaled from 1 to 100 using Equation 7.

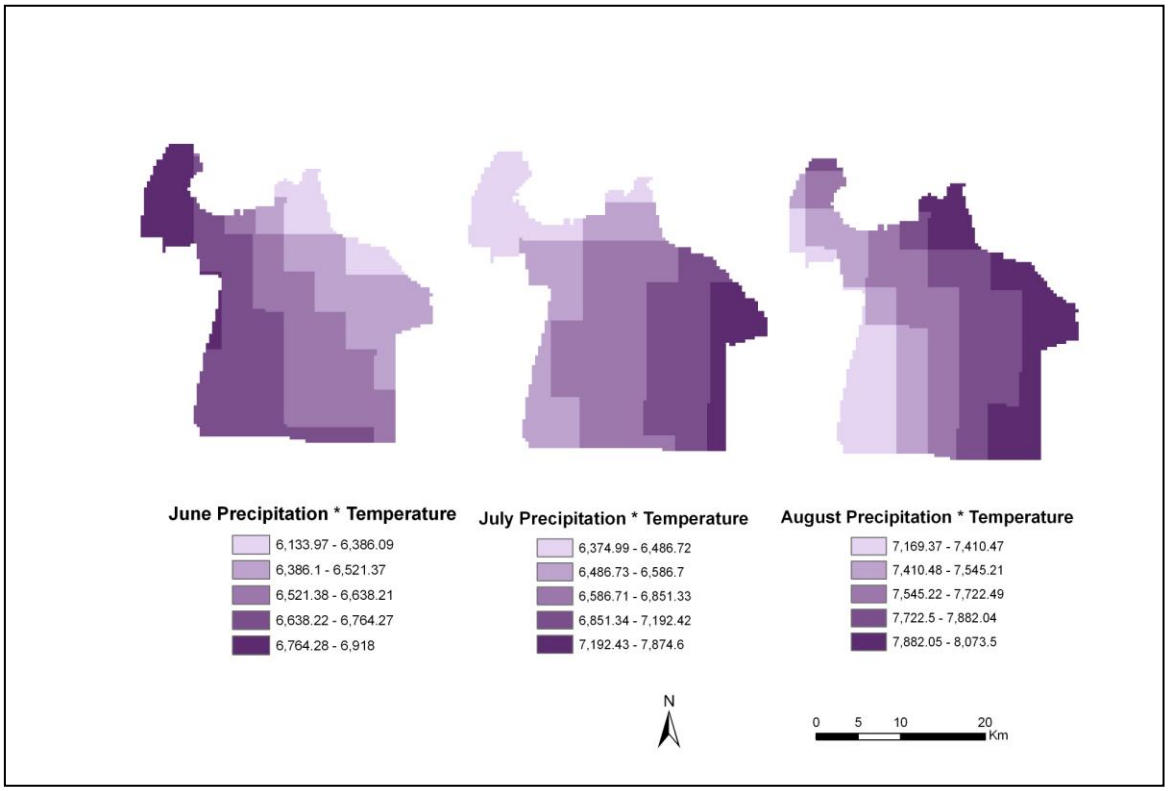

Figure 19: The product of average monthly temperature and average monthly precipitation for each month within the study period. Values were calculated using Equation 8.

Predicting Monthly Mosquito Abundance

Using the software program, PASW Statistics 17.0, a linear regression model was created for both species groups that use the independent variables to explain the variation in monthly mosquito trap data. Spatial Analyst tools were used to extract the independent variable data for each coinciding trap point into a database. The resulting table could then be used in PASW to calculate the regression equations. In order to normalize the mosquito capture data, the mosquito counts were log transformed to calculate the natural log of the values. A separate model was created for each species in which the log transformed capture value at each trap site was regressed upon the corresponding monthly independent variables. The results of both linear regression models are shown below.

R^2	Adjusted R^2	F	Significance
0.270	0.235	7.846	0.000

Table 10: Summary of the linear regression model for the ephemeral species.

Variable	B	t	Significance
Constant	-104.888	-2.875	0.005
Precipitation	1.144	2.989	0.004
Temperature	1.399	2.987	0.004
Precip_Temp	-0.015	-3.108	0.003
TMI	0.000	-0.006	0.995

Table 11*:* Results of linear regression model for the ephemeral species.

R^2	Adjusted R^2	F	Significance
0.405	0.377	14.793	0.000

Table 12: Summary of linear regression model for *C. melanura.*

Variable	B	t	Sig
Constant	-138.191	-3.298	0.001
Precipitation	1.444	3.295	0.001
Temperature	1.881	3.508	0.001
Precip_Temp	-0.020	-3.498	0.001
TMI	0.016	1.224	0.224

Table 13*:* Results of linear regression model for *C. melanura*.

Because environmental variables often affect the subsequent month's mosquito counts, a temporal lag model was also considered as a method for predicting abundance. For each of these models, the monthly mosquito abundance was regressed upon the preceding month's independent variables. This lag model however, did not significantly diverge from the relationships in the linear regression models already calculated and therefore were disregarded.

Once the linear regression equations were calculated for both species groups, the equations could be used to calculate monthly WSC. The regression coefficients from each equation were used to calculate the weighted influence of the independent variables on the mosquito trap counts. The equations were calculated using the 'Map Algebra' tool and incorporated into each abundance model (Figure 20). The equations for the linear regression models are revealed below:

Equation 9: WSC_{Ep} = -0.016 (Temperature x Precipitation) + 1.462 (Temperature) + 1.193 (Precipitation)

Equation 10: WSC_{Cm} = -0.020 (Temperature x Precipitation) + 1.883 (Temperature) + 1.444 (Precipitation) + 0.016 (TMI)

Where WSC_{Ep} = the weighted influence of the independent variables on ephemeral species abundance for a particular month, and WSC_{Cm} = the weighted influence of the independent variables on *C. melanura* for a particular month. The monthly values were each represented as a 30 m grid (Figure 21). Within each model, the monthly WSC grids were used along with the HSI grids to predict abundance. Abundance was predicted for each month on a pixel-by-pixel basis using the equation:

Equation 11: $Abundance_{Cm} = HSI_{Cm} \times WSC_{Cm}$

Where $Abundance_{Cm}$ = total *C. melanura* abundance for a particular month. For each month, the abundance values were rescaled to reflect the season's overall abundance using the equation:

Equation 12: $$Abundance_r = \frac{Abundance_O - Abundance_{min}}{Abundance_{max} - Abundance_{min}} \times 100$$

Where $Abundance_r$ = the rescaled abundance for a particular month, $Abundance_O$ = the observed abundance for the month, $Abundance_{min}$ = the minimum abundance for the month, and $Abundance_{max}$ = the maximum abundance for all months within the study period.

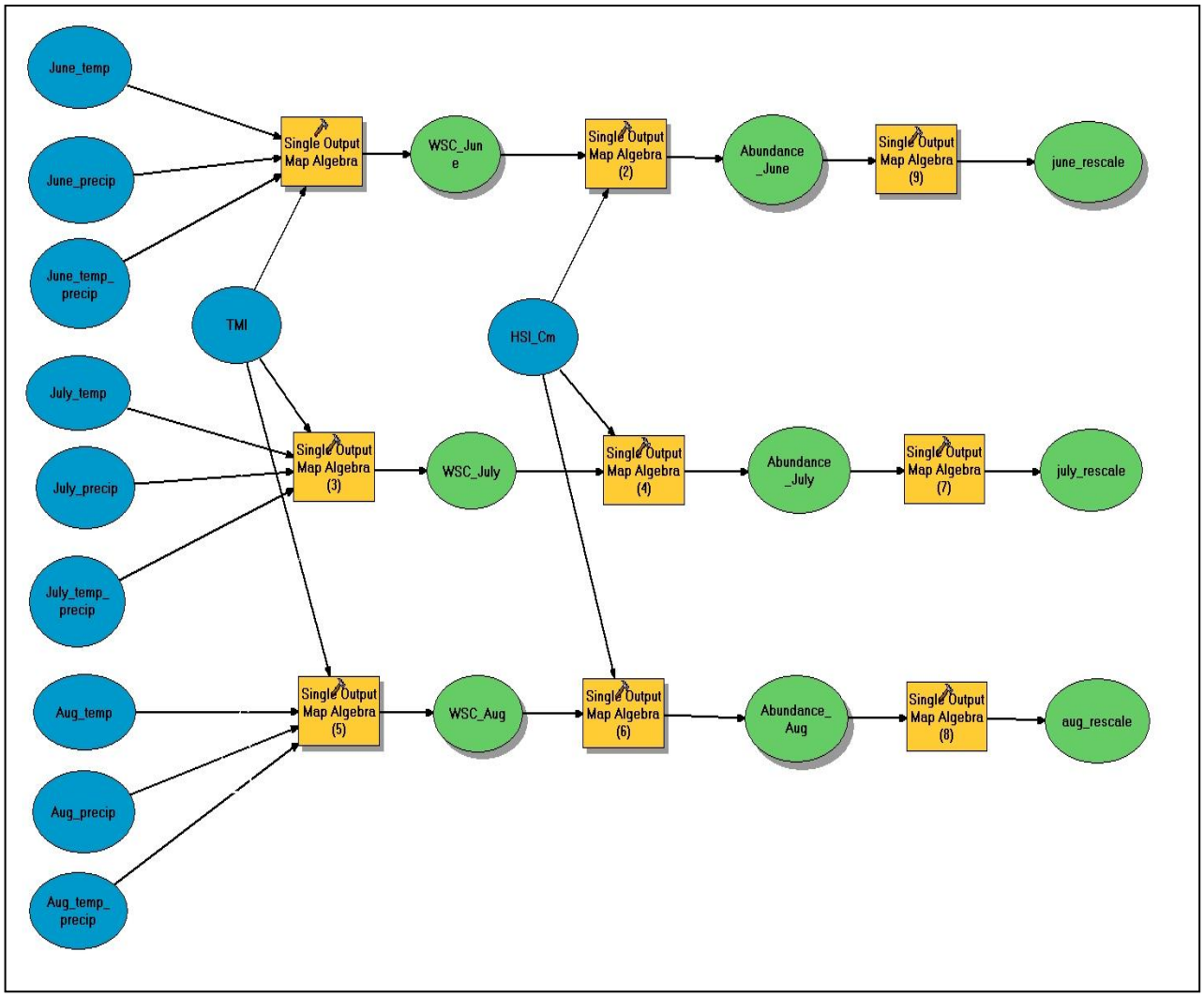

Figure 20: Abundance model for *C. melanura* created using Model Builder. The model predicts the abundance of *C.melanura* for each month from June to August.

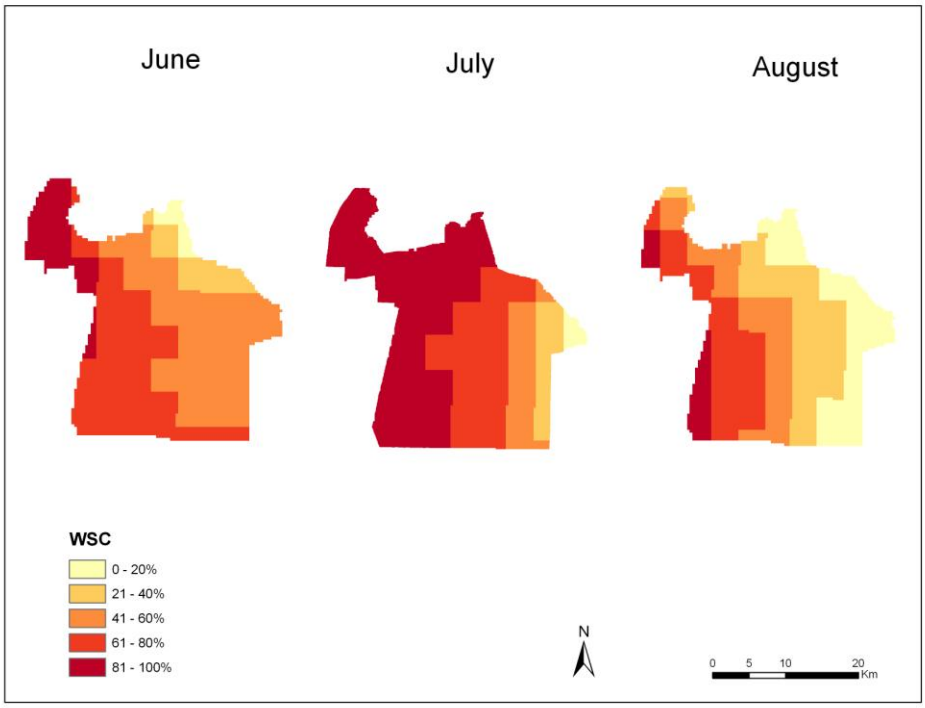

a)

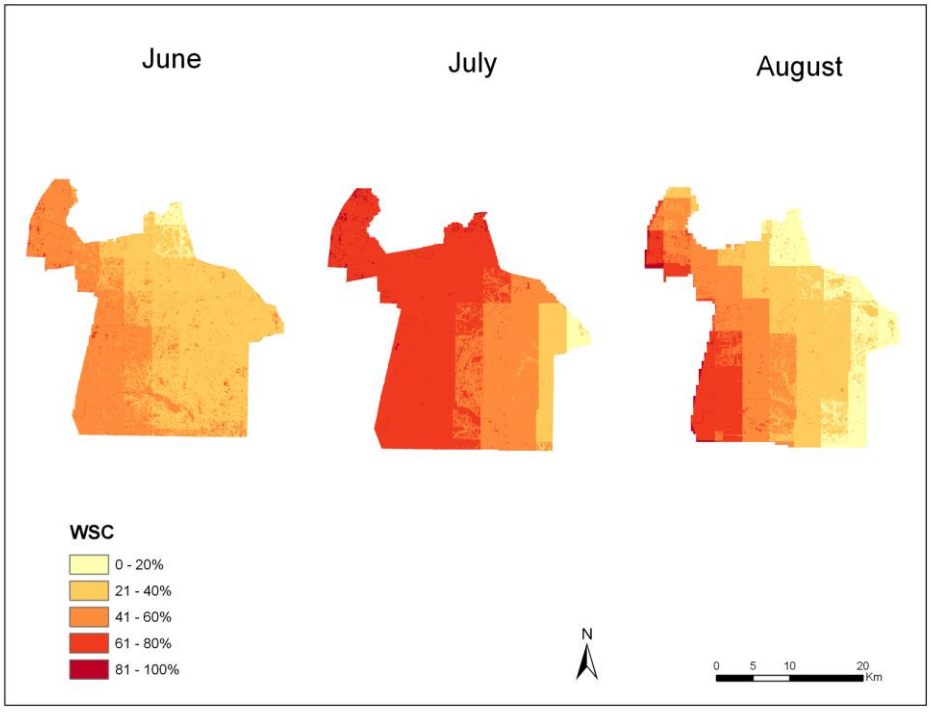

b)

Figure 21: The weighted influence of the independent variables on ephemeral species abundance (a) and *C. melanura* (b). Values were separated into five equal interval classes that represent the percent effect on abundance.

Predicting Human Risk of Mosquito-Borne Disease Transmission

In order to calculate a disease transmission risk index, the population that is most vulnerable to mosquito-borne diseases must first be determined. Using U.S. decennial Census data for 2000 and GIS data from the Chesapeake Information Technology Department, a vulnerable population was initially inventoried across Chesapeake. Population data is often mapped according to enumeration units such as Census blocks, which do not reflect the actual distribution of the population. Rather than mapping the vulnerable population according to an enumeration unit, a dasymetric map was created that displays the vulnerable population according to land cover classes. This will allow the vulnerable population to be distributed in a more accurate and finer resolution than other methods based on less meaningful observational units. The predicted vulnerable population can then be used with the previously calculated mosquito abundance to predict the risk of disease transmission for each month within the study period.

Dasymetric Mapping of the Vulnerable Population

This study utilizes the Intelligent Dasymetric Mapping (IDM) approach developed by Mennis and Hultgren (2006). This automated approach uses the cartographer's domain knowledge and the relationship between the enumeration units and the ancillary information (Slocum et al, 2009). The IDM approach takes data mapped to a set of source zones and a categorical ancillary data set, and redistributes the data to a set of target zones formed by the intersection of the source and ancillary zones. In this case, Census block groups will serve as the source zones, while the land cover data will serve as the ancillary data. A 30 m pixel land cover grid from NOAA's Coastal Change Analysis Program (C-CAP) for 2001 was used as the ancillary layer for the dasymetric map. The data are redistributed based on a combination of

areal weighting and the relative densities of ancillary classes. The formula for calculating the estimated count of the target zone is:

Equation 13: $$\hat{y}_t = y_s \left[\frac{A_t \hat{D}_c}{\sum (A_t \hat{D}_c)} \right]$$

$\hat{y}_t$ = the estimated count for target zone *t*
y_s = the count of a source zone, which overlaps the target zone
A_t = the area of the given target zone
$\hat{D}_c$ = the estimated density of ancillary class *c* associated with the target zone

In some cases, cartographers may use their own domain knowledge to specify the value of D_c. In this case, the dasymetric tool computed the value of D_c using the percent cover method. This option allows the cartographer to select a threshold percentage and selects the zones whose percentage of coverage equals or exceeds that threshold. Once the zones are selected, the estimated density of the ancillary class is selected using the equation:

Equation 14: $$\hat{D}_c = \sum_{s=1}^{m} y_s \Big/ \sum_{s=1}^{m} A_s$$

$\hat{D}_s$ = the estimated density of ancillary class *c*
Y_s = the count of a source zone
A_s = the area of a source zone

Predicting the vulnerable human population consisted of two major steps. The first step was to calculate the vulnerable population within each Census block group. Because Census data reflects only a "nighttime" population distribution, points of higher possible vulnerable

populations, such as hospitals, day cares, elder care facilities, and schools were also included in the vulnerable population analysis. The second phase of vulnerability prediction was to add these points of high vulnerability to the vulnerable population within each Census block group.

To predict the vulnerable population, a U.S. Census polygon shapefile was obtained from ESRI and clipped to the extent of Chesapeake, Virginia. Unfortunately, Census population data was not available for the year 2003. The Census data displays various population variables according to Census block groups estimated for the year 2004. ArcGIS tools were used to calculate the vulnerable population within each block group. According to the CDC (2009), persons over age 50 and under age 15 are at greatest risk for developing severe disease when infected with EEE and WNV. Based on this information, the 'field calculator' function was used to sum the population less than 5 years of age and greater than 50 years of age within each Census block group (Figure 22). Children between 5 and 15 years of age were not included in the categorization because the Census data did not have a classification that matched this age range.

To complete the second step of vulnerability prediction, vulnerable location data was obtained from the City of Chesapeake Information Technology Department. The data was obtained in the form of a point shapefile in which each point represents a vulnerable location (Figure 22c). The population for each elderly care facility was already included in the shapefile and required no research. The population of Chesapeake General Hospital was calculated by summing the total number of inpatients and outpatients. Unfortunately, not every school and daycare center contained population data in the corresponding attribute tables. Therefore, the population of these locations had to be determined through additional research. By making phone calls and utilizing Internet resources, the population of the schools and daycares was

determined. Analysis was limited to primary, elementary, and intermediate schools. Determining the population of every daycare was cost prohibitive of this study (there are over 250 facilities). To calculate the final vulnerable population within each block group, ArcGIS was used to add the population of each vulnerable point to the previously calculated block group vulnerable population. The final output was processed in the form of a polygon shapefile. In order to reflect the total population in each block group, the vulnerable population was normalized using the following equation:

Equation 15: $$Population_n = \frac{Population_v}{Population_{Total}}$$

Where $Population_n$ = the normalized vulnerable population per block group, $Population_v$ = the calculated vulnerable population per block group, and $Population_{Total}$ = total population of the block group. The final vulnerable population is shown in Figure 23.

In order to distribute the population into dasymetric zones, the land cover classes were divided into categories. Initially, the land cover data set consisted of 22 land cover classes. The land cover types were separated into four classes: highly intensity developed, low intensity developed, non-urban, and water (Figure 24). This method has been used by Sleeter (2004) to map the San Francisco Bay according to land cover. Using the dasymetric mapping extension downloaded from the U.S. Geological Society (http://geography.wr.usgs.gov/science/dasymetric/data.htm), $population_n$ was mapped according to the reclassified land cover (Figure 25). The output was a 30 m pixel grid. In order to clearly represent the population across Chesapeake, the grid units were converted to persons per hectare using the following equation:

Equation 16: $\text{Population}_h = \text{Population}_p \times 10{,}000$

Where Population_h = the population per hectare and Population_p = the population per pixel.

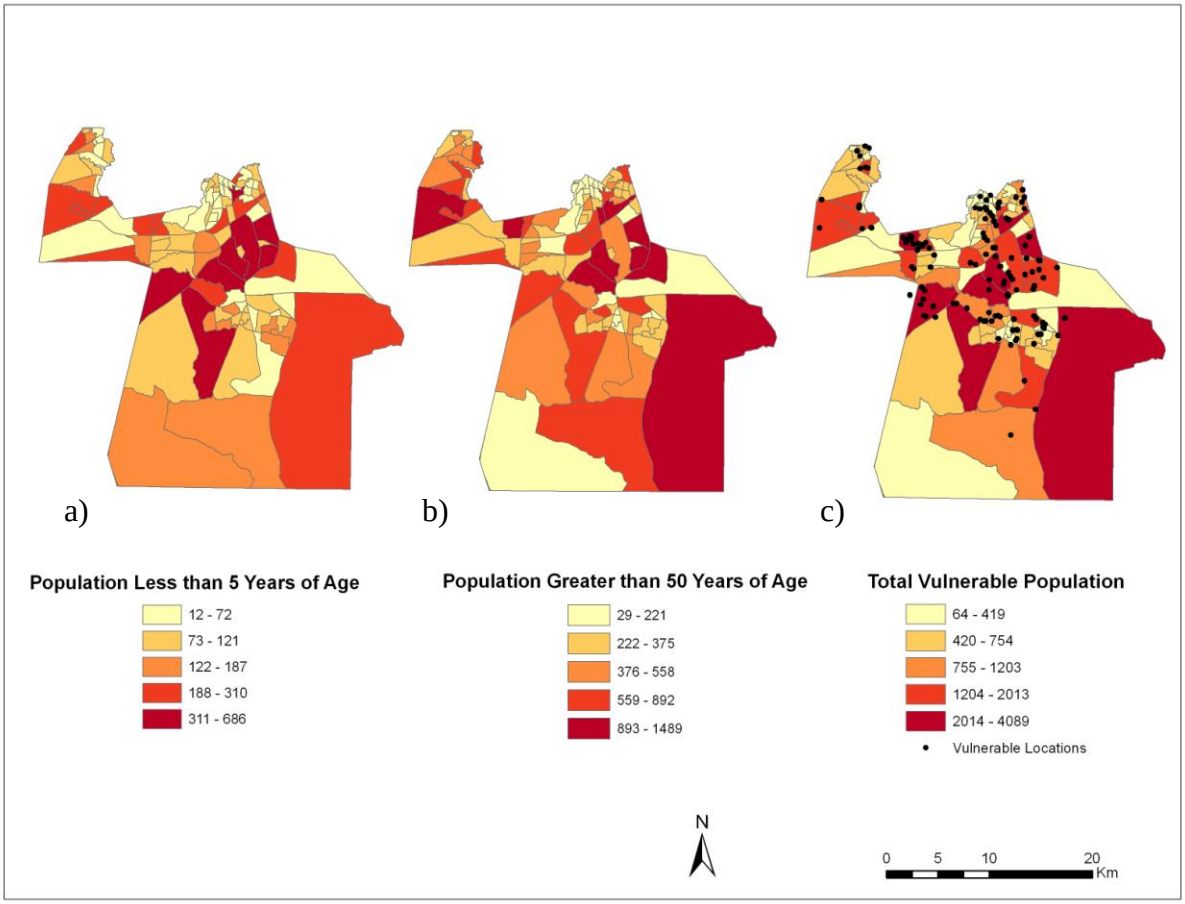

Figure 22: The population that is most vulnerable to mosquito-borne diseases using Census block groups. The maps show the population of children less than 5 years of age (a), the population greater than 50 years of age (b) and the sum of the children and elderly overlaid with the vulnerable locations across Chesapeake, VA (c).

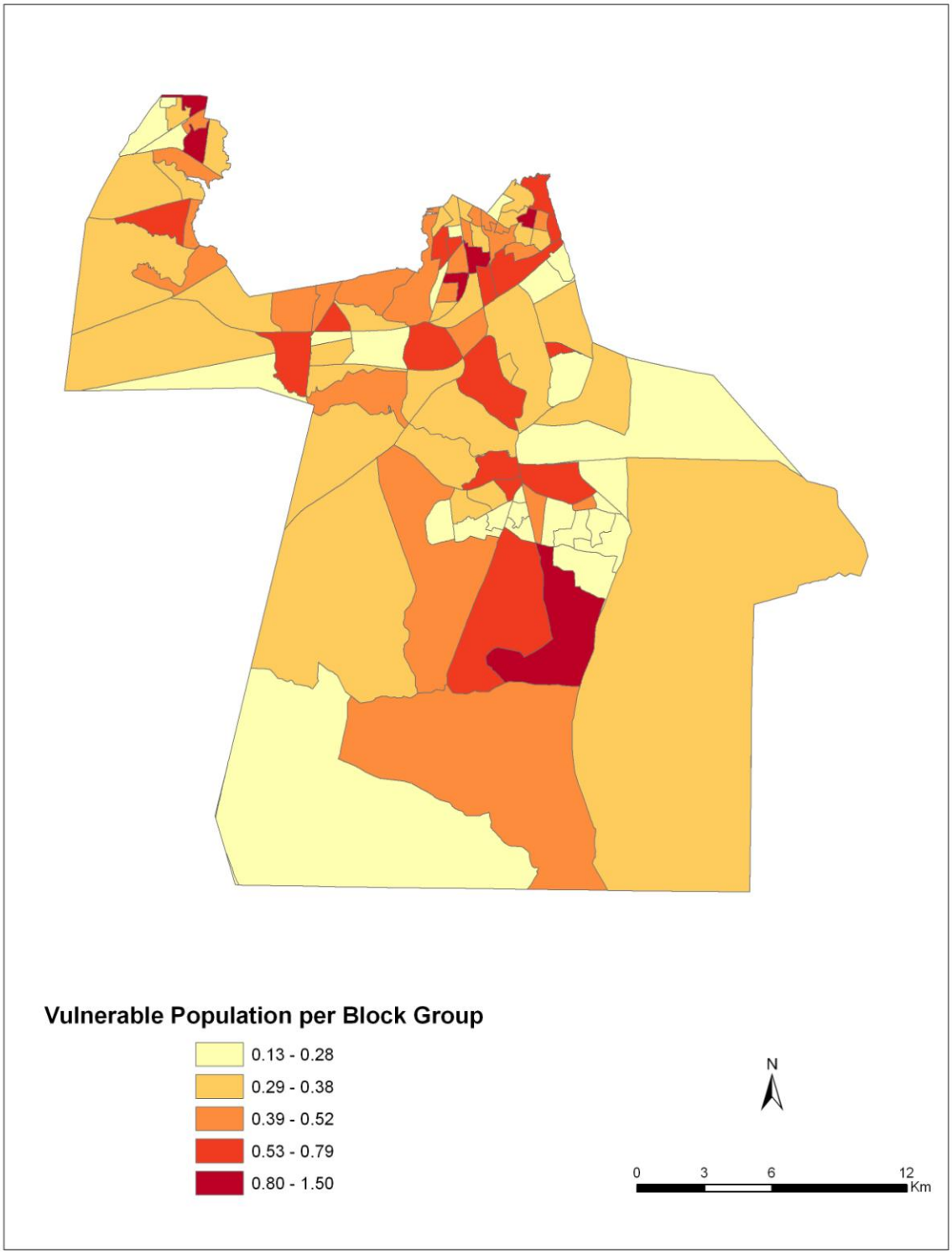

Figure 23: Vulnerable population density per block group. Values were calculated using Equation 15.

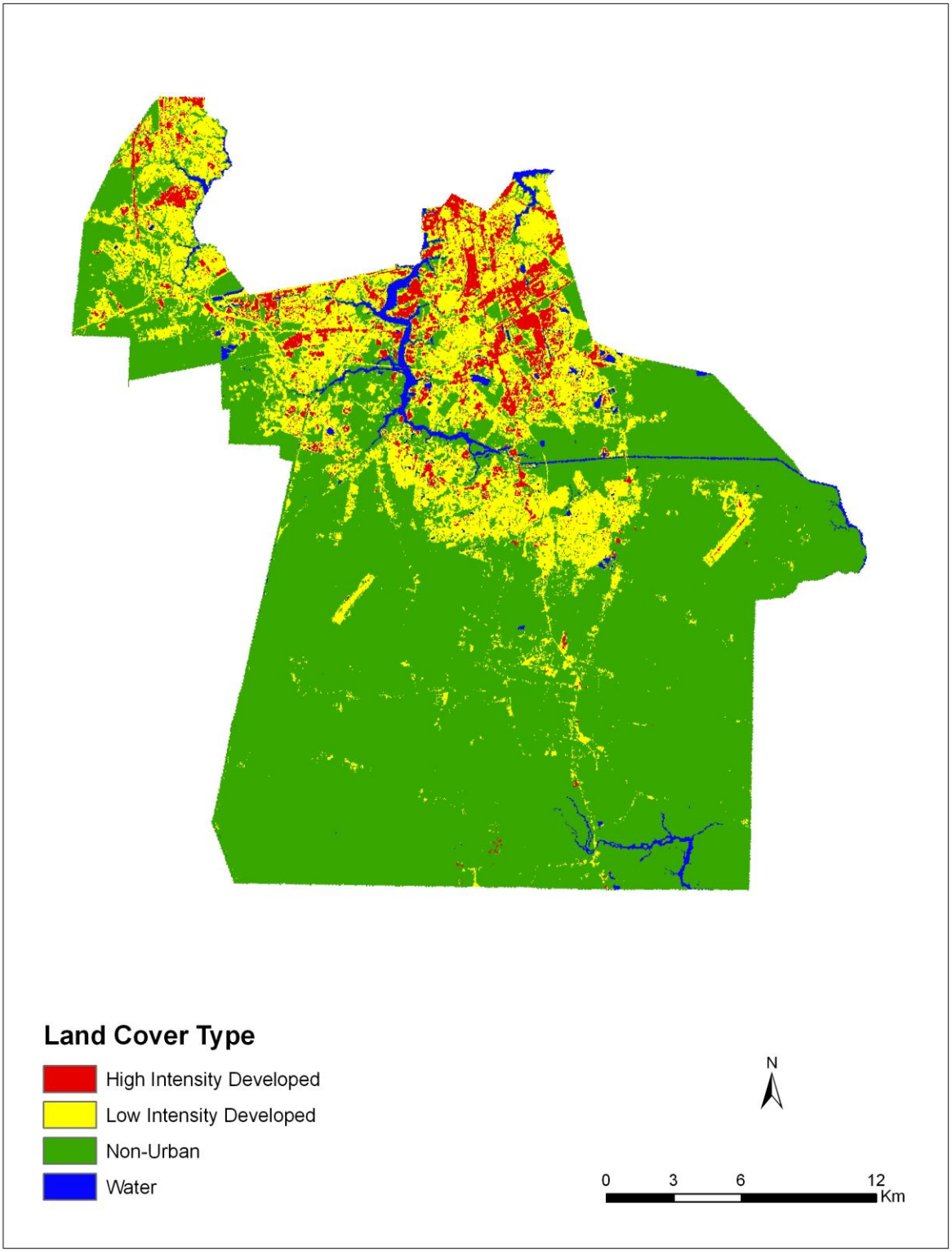

Figure 24: Reclassified land cover types used as the ancillary units in dasymetric map.

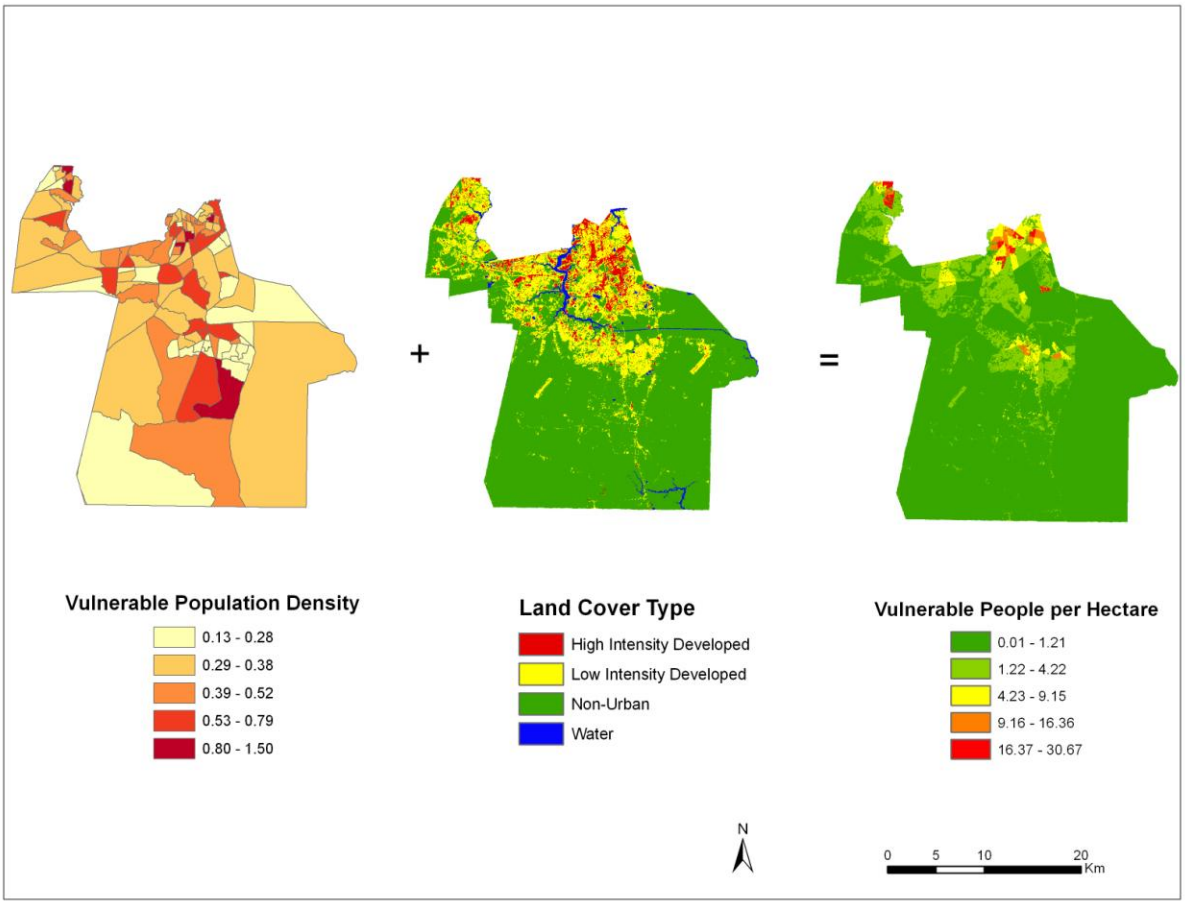

Figure 25: Spatial overlay of the vulnerable population and land cover. The image to the far right represents the dasymetric map of the vulnerable population mapped according to land cover. Values were calculated using Equation 16.

Predicting the Risk of Mosquito-Borne Disease Transmission

Using the monthly mosquito abundance values and the dasymetric map of the vulnerable population, a monthly risk index could be calculated that indicates the risk of disease transmission from the corresponding mosquito species to humans. The units of risk are arbitrary and merely represent an index ranging from low to high risk. Spatial Analyst tools were utilized to overlay the dasymetric map with the mosquito abundance grids (Figure 26). The outputs were created in the form of 30 m pixel grids. The final risk values were calculated using the equation:

Equation 17: $Risk_{ep} = (Population_h \times Abundance_r)$

Where $Risk_{ep}$ = the risk of disease transmission from the ephemeral species for a particular month, $Population_h$ = the vulnerable population per hectare, and $Abundance_r$ = the rescaled abundance of the ephemeral species for the corresponding month.

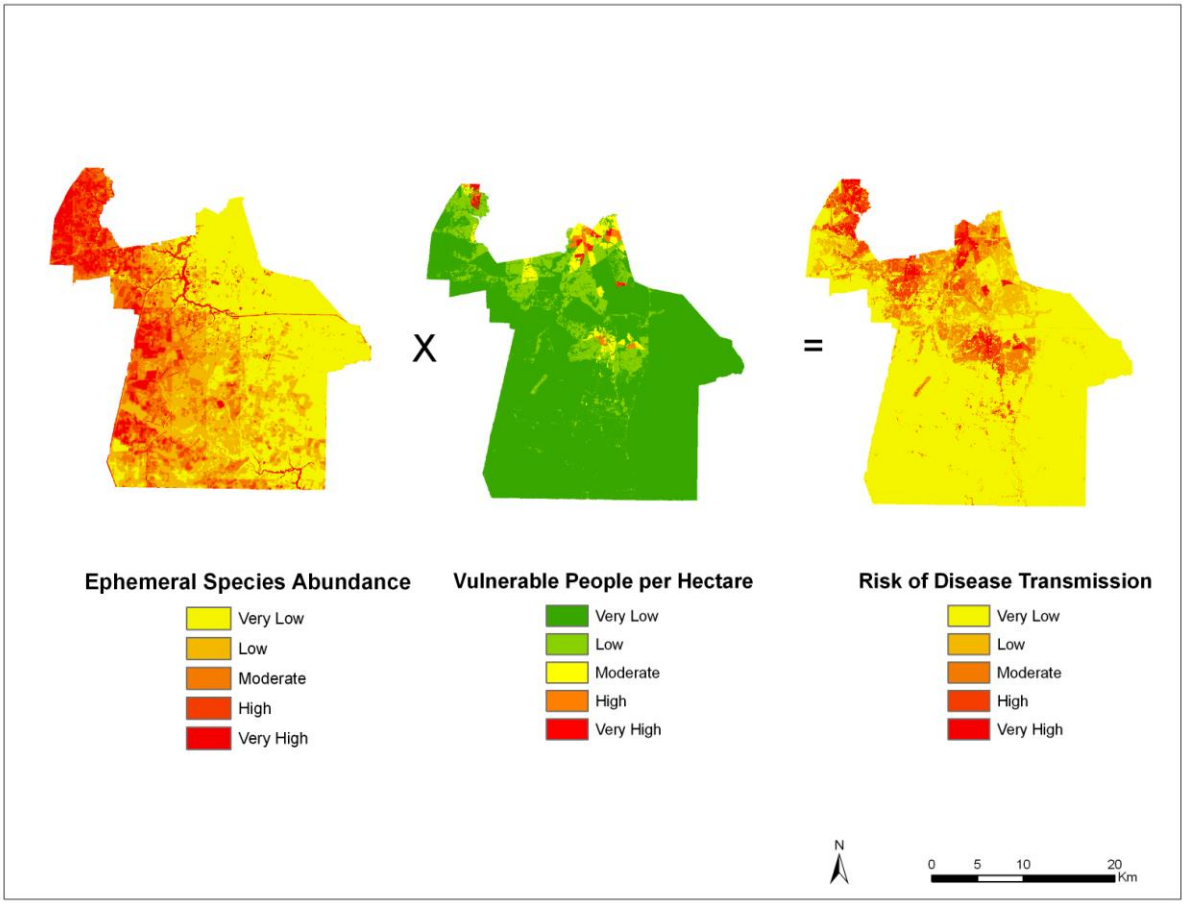

Figure 26: Visual representation of the spatial overlay used to predict the risk of disease transmission. This example represents the risk of disease transmission from the ephemeral species for June of 2003. The abundance and risk values were classified using a quantile classification, while the vulnerable population values are classified using natural breaks.

CHAPTER 4: RESULTS

This chapter begins by discussing the results of the habitat suitability index and the influence of the independent variables on mosquito trap data. The chapter then discusses the results associated with the mosquito abundance models. The chapter concludes with a discussion of the human vulnerability patterns and the risk of disease transmission predictions.

Habitat Suitability Index (HSI)

The habitat suitability maps for both groups of mosquitoes are each unique and representative of the corresponding mosquito preferences. First the results of the habitat suitability model for the ephemeral species will be evaluated. The R^2 value for the habitat suitability regression model indicates that independent variables explain 35.6% of the variation in mosquito trap data (Table 6). The model indicates that TC1 or brightness is the most significant variable in predicting the suitable habitat for ephemeral species. With a regression coefficient of 1.065, the model indicates that brightness and habitat suitability are positively correlated. Since the regression coefficient for TC1 is relatively small, the correlation between brightness and habitat suitability is not particularly strong. By overlaying the brightness variable onto the HSI map, it is clear that the correlation between habitat suitability and brightness is not very prominent. Because high brightness values represent a lack of vegetation, this weak correlation between HSI and TC1 is expected. The preferred habitat of *A. vexans* and *P. columbiae* is ephemeral pools which do not correspond with regions of high brightness. A few of the highly suitable regions do in fact overlay with bright regions. These regions may represent suburban areas where mosquitoes may be breeding in containers. According to the regression model, TC2 or greenness is another important variable in predicting habitat suitability. The model indicates that greenness is positively correlated with habitat suitability. However, habitat

suitability actually appears to be inversely correlated with greenness. Like the brightness variable, the regression coefficient for the greenness variable is small. This low coefficient of 0.517 would explain the lack of correlation between HSI and TC2. Overall, the most suitable habitat for *A. vexans* and *P. columbiae* appear to be regions covered in open water such as rivers and lakes. There is no distinct pattern between unsuitable regions and land cover. The highly unsuitable regions coincide with many land cover types.

The habitat suitability model results for *C. melanura* vary considerably from the ephemeral species model. The R^2 value indicates that independent variables explain 33.9% of the variation in *C. melanura* trap data (Table 8). With a significance value of 0.004 (Table 9), the soil runoff variable proved to be the most significant attribute in the habitat suitability model for *C. melanura*. According to the linear regression model, runoff and suitability are positively correlated. Because higher runoff values actually represent less runoff potential, it is expected that highly suitable areas should overlay with high runoff values. The habitat suitability map confirms the significance of the runoff variable. By overlaying the runoff variable onto the habitat suitability map, it is clear that the regions with the highest suitability appear to have either soils with low runoff potential or are covered by water. Available water holding capacity is another significant variable in predicting habitat suitability for *C. melanura*. The linear regression results (Table 9) indicate that soil water holding capacity and habitat suitability are positively correlated. An overlay of the two variables confirms that as water holding capacity increases, so does habitat suitability. Because *C. melanura* prefer a moist habitat, it makes sense that a lack of runoff and increase in available water holding capacity are associated with an increase in habitat suitability. In general, the most suitable areas for *C. melanura* habitation appear to be swamps and marshes. This observation is expected since swamps are the preferred

habitat for these species. Open water areas such as rivers were predicted to be very unsuitable for *C. melanura*. This prediction contrasts with the HSI results for the ephemeral species.

Weighted Influence of Independent Variables on Mosquitoes (WSC)

The results of the linear regression models (Tables 10-13) reveal the relationship between the environmental variables and mosquito trap data. For the ephemeral species, the model indicates that the independent variables explain 27.0% of the variation in ephemeral species counts (Table 10). Temperature, precipitation, and the combined effects of temperature and precipitation are all significant variables in the ephemeral species abundance model. With a regression coefficient of 0.000 and a significance value of 0.995, the TMI variable is not a significant variable in predicting ephemeral species abundance. Temperature and precipitation are both positively correlated with mosquito abundance. This was expected since an increase in these conditions often produces habitats conducive to mosquito breeding. On the other hand, the interaction of temperature and precipitation had a negative correlation with mosquito abundance. However, with a regression coefficient of -0.015, the negative influence of this variable on abundance is minimal.

The monthly WSC grids (Figure 21a) illustrate the weighted impacts of the environmental variables on ephemeral species counts. The WSC values were scaled from 0 to 100 to represent the percent influence of the variables on mosquito captures. From June through August, WSC values increase moving from east to west. The effect of the independent variables on mosquito counts is particularly high in western Chesapeake across all months. In July, the WSC values are especially high across Chesapeake. The environmental variables were predicted to have more than an 80% influence on mosquito numbers across a large portion of the city.

The results of the regression model for *C. melanura* are quite similar to the ephemeral species regression results. According to the model results for *C. melanura* (Tables 12 and 13), temperature and precipitation are significant variables in predicting abundance and are positively correlated with mosquito numbers. The combined effects of temperature and precipitation are also significant variables for predicting *C. melanura* presence, but are negatively correlated with abundance. However, the regression coefficient for this variable is close to 0, indicating that the product of precipitation and temperature does not have a strong influence on abundance. Unlike the other independent variables, TMI is not a significant variable in predicting abundance. The low regression coefficient of 0.016 and significance value of 0.224, indicate that TMI does not have a strong influence on abundance.

The WSC indices for *C. melanura* (Figure 21b) show similar patterns to the values for the ephemeral species. The WSC values were again scaled from 0 to 100. After experimenting with different classification schemes, the WSC values were classified into equal intervals. For all months, the influence of the environmental variables on mosquitoes increases going east to west. Compared to the WSC values for the ephemeral species, the WSC values for *C. melanura* are relatively lower. There are very few regions where the independent variables have more than an 80% influence on *C. melanura* captures. June in particular has low WSC values compared to July and August. July on the other hand, exhibits very high WSC values across much of Chesapeake. One major difference between WSC grids for both mosquito groups is that the influence of the TMI values can be seen in the WSC grids for *C. melanura.* As mentioned earlier however, the effect of this variable on *C. melanura* abundance is negligible.

Mosquito Abundance

As predicted, the abundance results for both groups of mosquitoes are relatively distinctive. The abundance results appear to be representative of each species' breeding and habitat preferences. The rescaled abundance values for both groups of mosquitoes were classified into quantiles to represent different levels of abundance. The abundance values for both mosquito groups were rendered on the same scale across all months. Although there is significant variation in abundance between the mosquito groups, similar spatial and temporal patterns can be seen among both groups.

Ephemeral Species Abundance

The abundance model results for the ephemeral group (Figure 27) shows a strong relationship between HSI values and abundance. As the HSI model suggested, ephemeral species abundance is very high in rivers and open water regions from June through August. In general, abundance values are highly reflective of the WSC grids (Figure 21). The patterns seen in the monthly WSC maps are also seen in the abundance grids. For the most part, regions with high WSC values have correspondingly high numbers of ephemeral species. Like the WSC values, monthly abundance appears to increase going from east to west across Chesapeake. For all three months, the western side of Chesapeake was predicted to have a large abundance of these species. In June, abundance is highest in the western portion of Chesapeake and gets progressively lower going east. Overall, July is predicted to have a very broad distribution of high abundance regions. In August, Chesapeake is predicted to have many low abundance regions, particularly on the eastern side of the city. Unlike the other months, August abundance was predicted to be concentrated and very high on the western side of Chesapeake.

By displaying the trap data in relation to the abundance results, we can determine the predictive ability of the trap data. Figure 28 displays the trap sites across Chesapeake and the number of ephemeral species counted at each site. The trap counts were symbolized using a quantile classification in order to give the abundance data an even distribution. In many regions, the trap data for all three months appear to be indicative of the final abundance results. In June and July, traps on the western side of the city that had a large number of mosquitoes correspond to high abundance results for those months (Figure 29a). The wetlands at the southern end of Chesapeake also show a positive correlation between trap data and abundance (Figure 29b). At other sites however, there appears to be no relationship between trap counts and predicted abundance. Figure 29c shows a trap point with a high number of ephemeral species but a low predicted abundance across all months. This point is on the edge of the city, therefore, it is possible that some mosquitoes were dispersed to Chesapeake by wind.

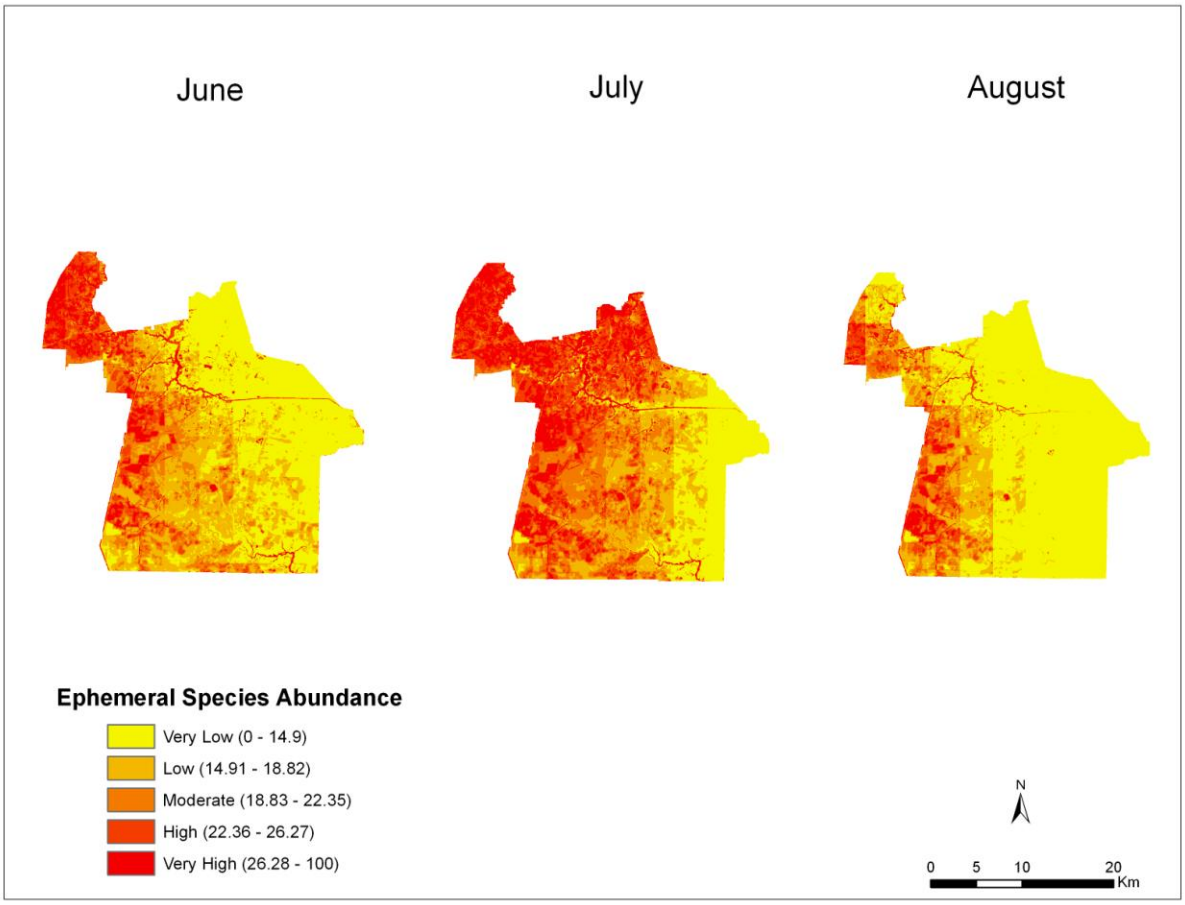

Figure 27: Monthly abundance of the ephemeral species for each month. Values were classified into quantiles.

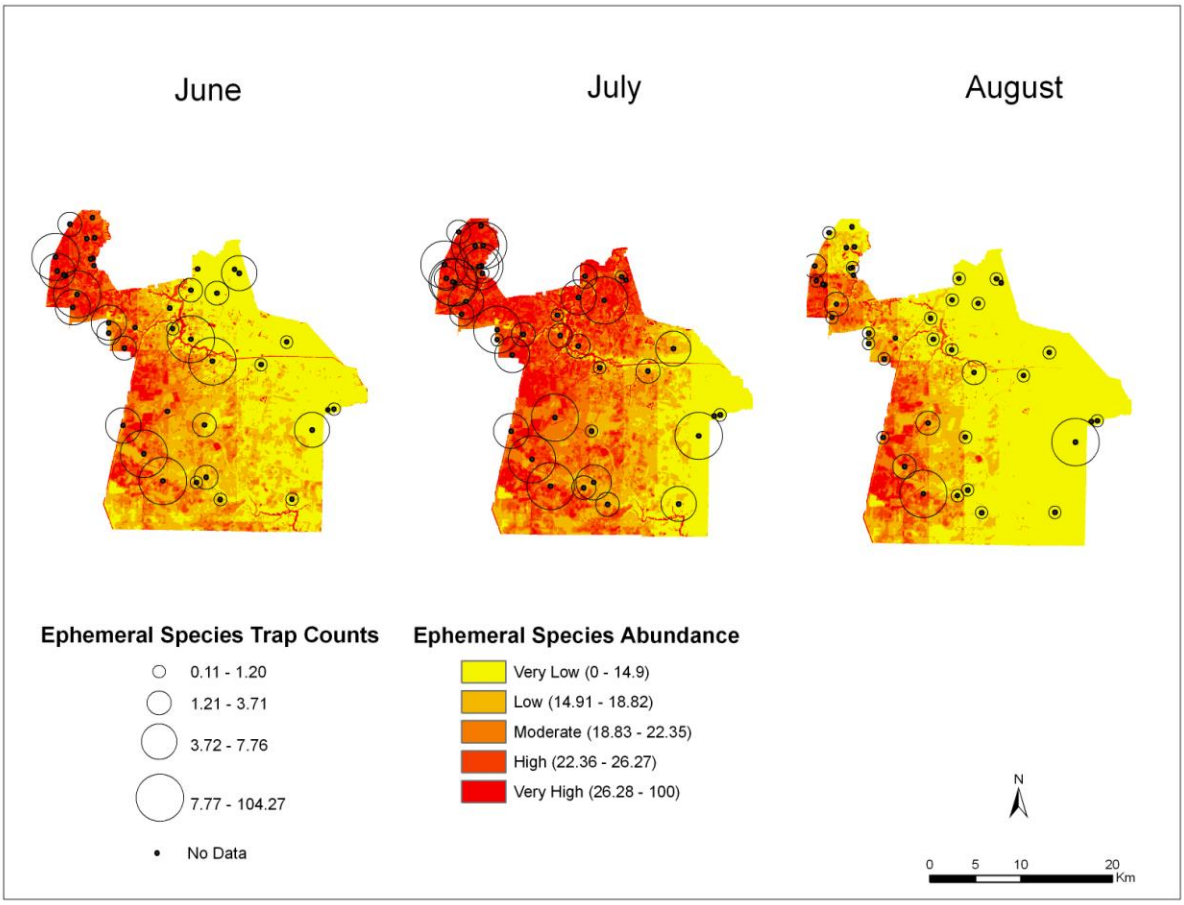

Figure 28: Trap sites overlaid onto the monthly abundance maps of the ephemeral species. Graduated symbology is used to display the monthly mosquito counts for the corresponding trap sites. Points with no graduated symbology represent traps where no data was collected for that month.

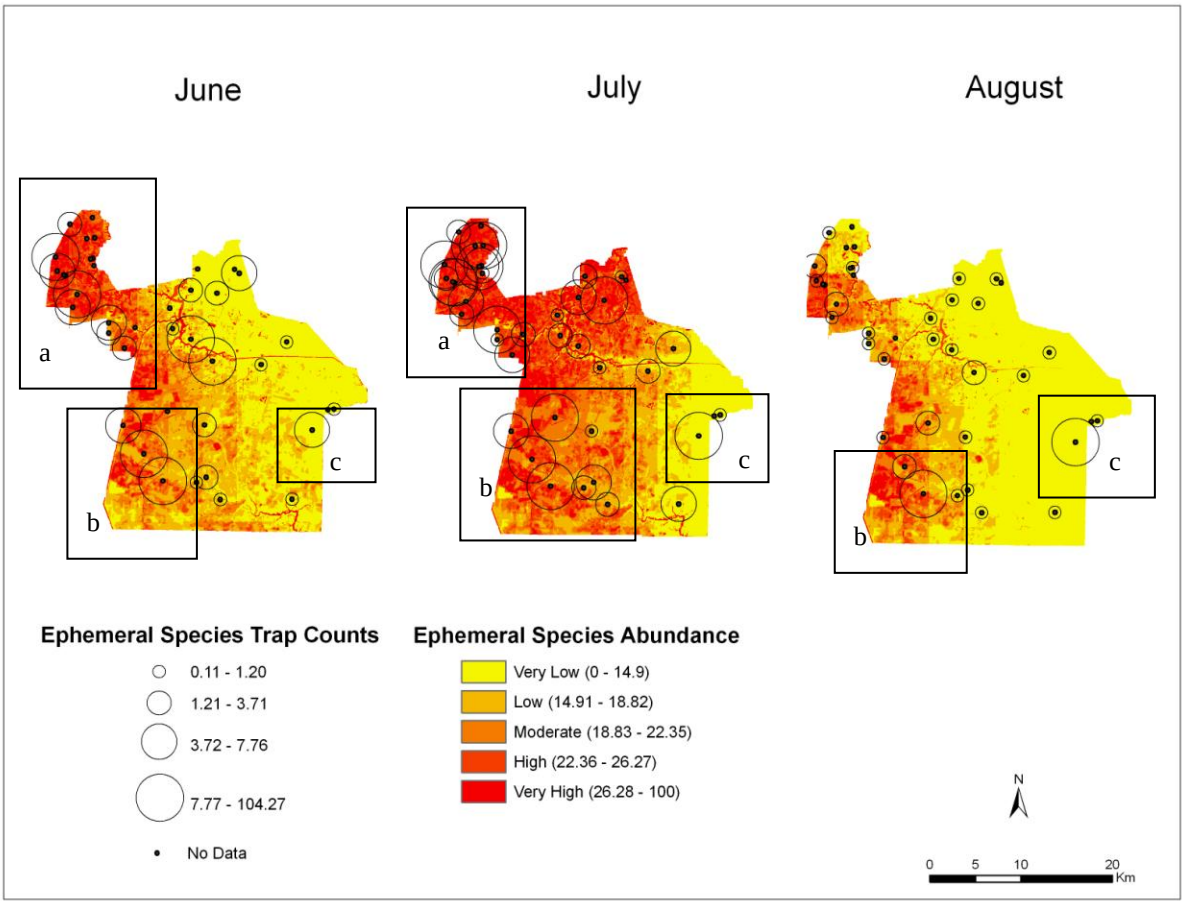

Figure 29: Trap sites overlaid onto the monthly abundance maps of the ephemeral species. Regions a and b indicate areas where trap data and abundance values are positively correlated across all months. Region c shows a trap point where mosquito counts and calculated abundance values are negatively correlated.

C. melanura Abundance

The abundance results for *C. melanura* (Figure 30) show patterns consistent with the HSI results. The HSI model predicted that open water areas such as rivers would be unsuitable for *C. melanura*. Accordingly, the abundance model predicted that there would be a very small number of these species in open water areas. Based on the HSI results, the model predicted a high abundance of *C. melanura* in wetlands. The predicted high abundance of this species in wetlands is no surprise since swamps are the preferred habitat of this species.

Overall, *C. melanura* abundance is very high across most of Chesapeake from June through August. For all three months, abundance was predicted to be especially high on the western side of the city, adjoining the Great Dismal Swamp. Central Chesapeake was also predicted to have a high abundance of *C. melanura*. This can be partly attributed to the impact of the environmental variables on mosquito counts, which increases going from east to west (Figure 21b). In June and July, abundance is very high across most of the city. The abundance patterns for these months are highly reflective of the corresponding WSC grids. In August, abundance is very high on the western half of the city and very low on the eastern side. One obvious similarity between June and August is that the northern tip of Chesapeake was predicted to have a very low abundance of *C. melanura.*

To determine how well the predicted *C. melanura* abundance reflects the trap data, the trap counts were overlaid with the abundance results (Figure 31). Many of the trap counts are in fact suggestive of the calculated abundance values. Trap values along the river for instance are relatively low in June and August (Figure 32a). Accordingly, the abundance model predicted that there would be a low number of *C. melanura* in this region. The correlation between trap data and abundance is especially obvious in the western portion of Chesapeake for July and August (Figure 32b). Across all three months, abundance was predicted to be high on the western side of the city. Trap data for *C. melanura* is proportionately high in these regions in July and August. There is also a positive correlation between trap data and abundance along the southern wetlands of Chesapeake (Figure 32c). Conversely, there are traps along this region where trap data is not proportionate to the calculated abundance values (Figure 32d). Perhaps these differences in mosquito abundance could be attributed to the fine scale of the abundance

grids. The spatial variation in monthly abundance values may be too detailed to compare to the trap data.

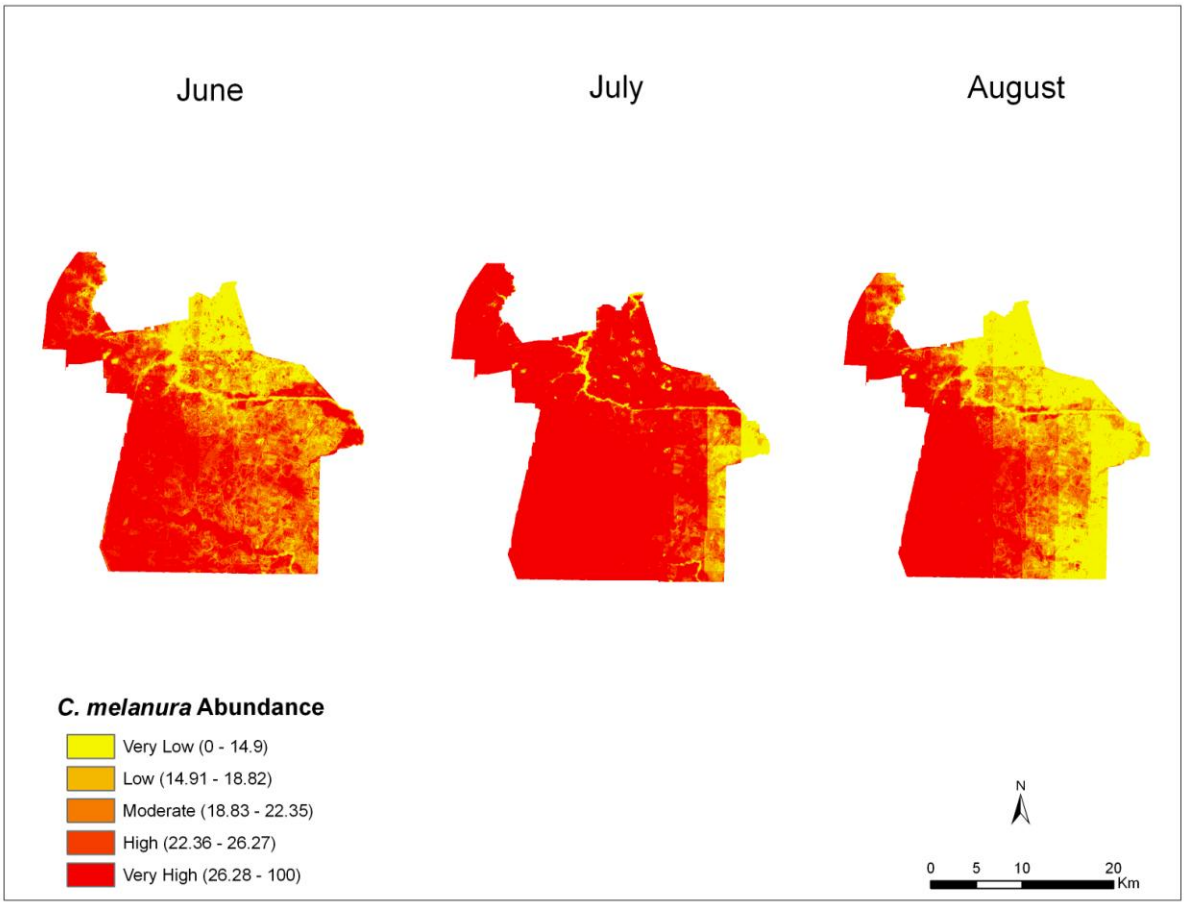

Figure 30: Monthly abundance of *C. melanura.* Values were separated into quantiles.

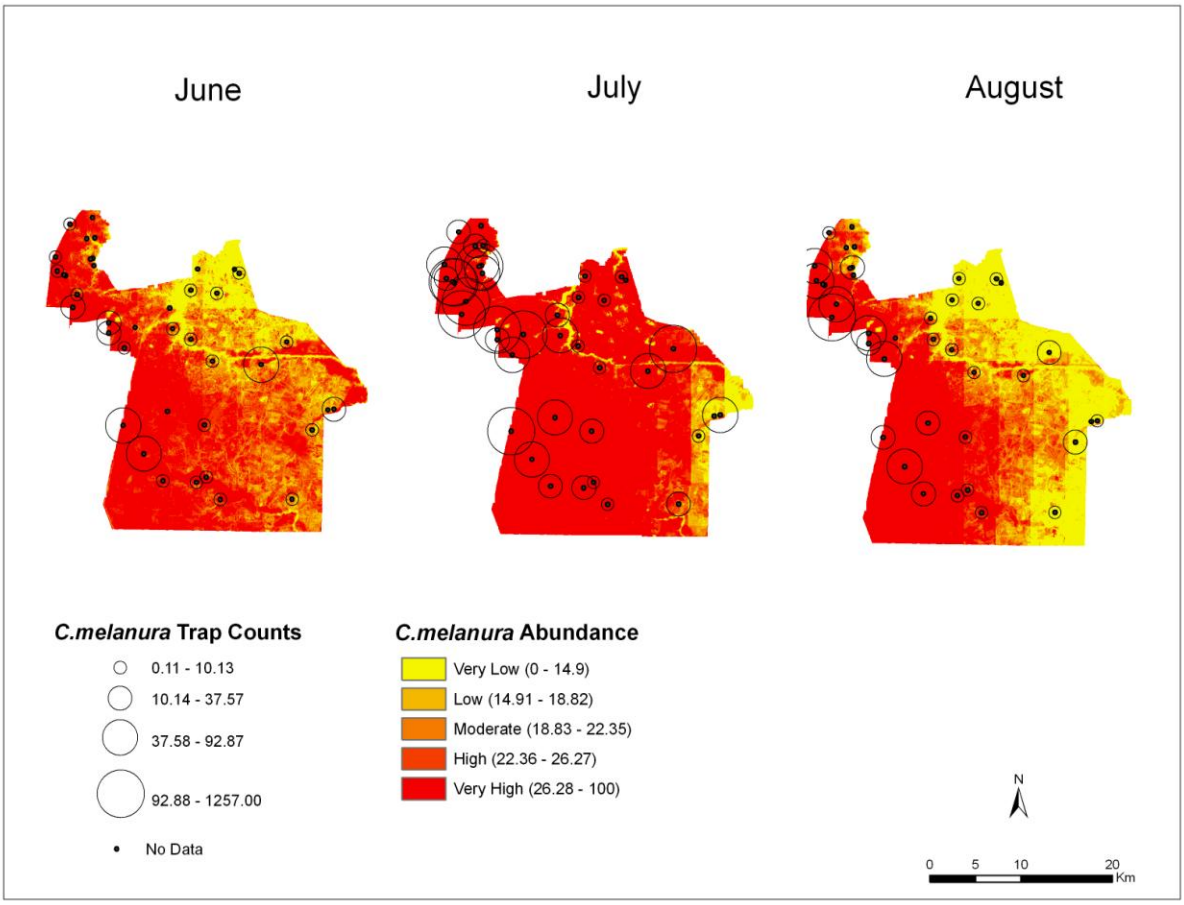

Figure 31: Trap sites overlaid onto the monthly abundance maps of *C. melanura*. Graduated symbology is used to display the monthly mosquito counts for the corresponding trap sites. Points with no graduated symbology represent traps where no data was collected for that month.

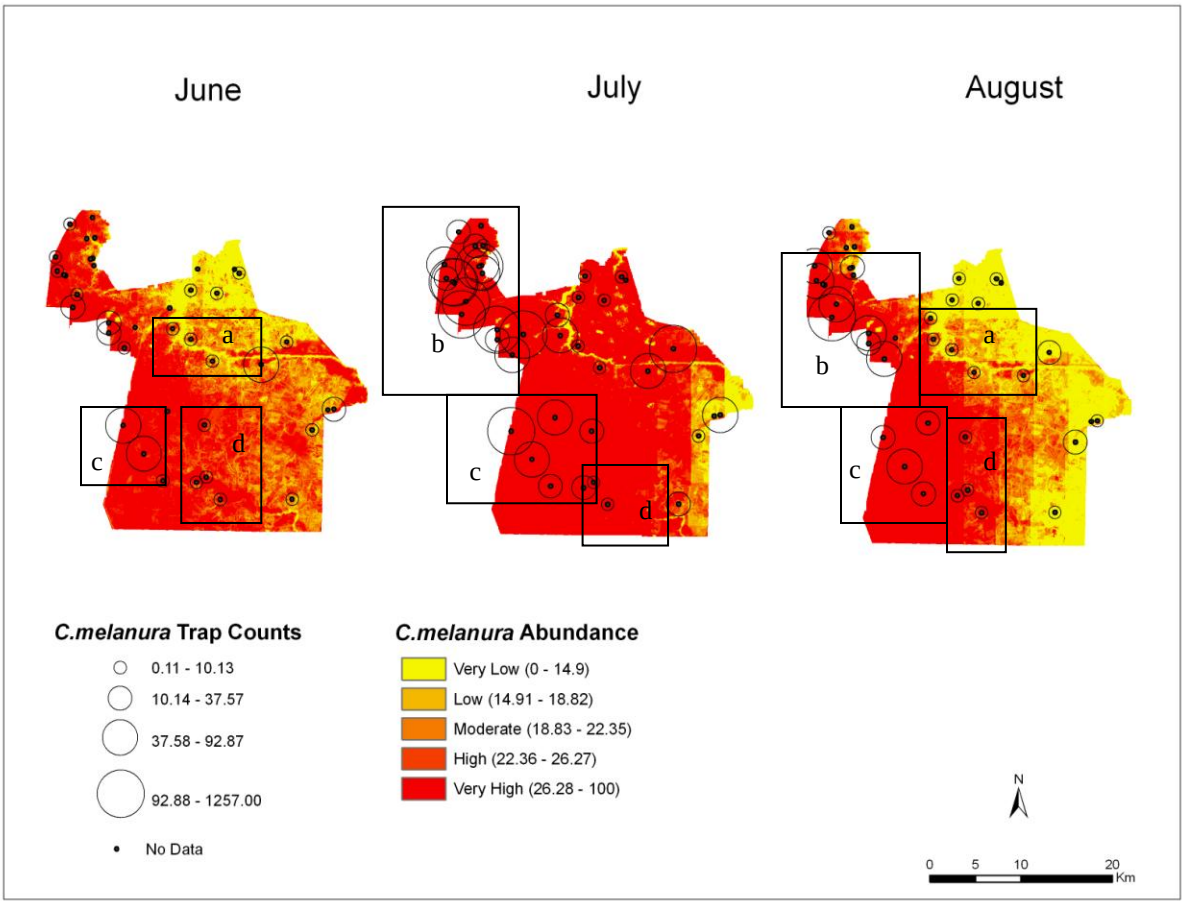

Figure 32: Trap sites overlaid onto the monthly abundance maps of the ephemeral species. Regions a,b, and c are areas where trap data and abundance values are positively correlated. Region d shows trap points where mosquito counts and calculated abundance values are negatively correlated.

Model Results vs. Interpolated Surfaces

To determine the predictive nature of the trap data and evaluate the accuracy of the model, the results of the abundance model can be compared to the surfaces interpolated from the trap data. Figure 4 illustrates the surfaces created from the ephemeral species monthly trap data. The patterns displayed in the interpolated surfaces differ significantly from the monthly abundance results (Figure 27). Compared to the model results, the interpolated surfaces show more temporal variation in abundance. The interpolated surfaces also show more spatial

variation. Rather than abundance increasing continuously from east to west, abundance varies across the city. The interpolated surfaces for the *C. melanura* trap data (Figure 5) also vary significantly from the abundance results (Figure 30) both spatially and temporally. One similarity is the concentration of high abundance regions predicted in western Chesapeake. Like the abundance results, western Chesapeake was interpolated to have a high abundance of *C. melanura* for all three months.

Human Vulnerability

By mapping the vulnerable population according to Census block groups (Figure 23), patterns of vulnerability are visible across Chesapeake, Virginia. The highly vulnerable regions seem to be concentrated in the northern portion of the city. This can be attributed to the clustering of vulnerable locations in northern Chesapeake (Figure 22c). There are also several block groups scattered throughout the city that are classified as highly vulnerable. However, these patterns of vulnerability are not as meaningful as the dasymetric map of population vulnerability (Figure 33). The dasymetric map of vulnerability displays the number of vulnerable people within each hectare. The vulnerable population values were classified using a natural breaks classification to represent areas ranging from very low to very high vulnerability. This map indicates that the highly vulnerable regions are mainly concentrated in the northern portion of the city. Areas of moderate vulnerability are also limited to the northern portion of the city, as well as to central Chesapeake. Most of Chesapeake is classified as having a low population vulnerability to mosquito-borne diseases.

By overlaying the dasymetric map with the land cover classes (Figure 24), the relationship between human vulnerability and land cover can be seen. For the most part, regions covered in water or non-urban areas are populated with a small number of vulnerable people.

This was expected since there are less vulnerable locations in these regions compared to other areas. In general, moderately vulnerable regions are classified as low intensity developed. The highly vulnerable regions are classified as either low intensity or high intensity developed. This observation was expected since these developed regions have more points of vulnerability such as schools and daycare centers. Although the low and high intensity developed regions are populated with a high number of vulnerable people, the vulnerability patterns vary across these land cover classes. Vulnerable population values range from very low to very high across the developed regions.

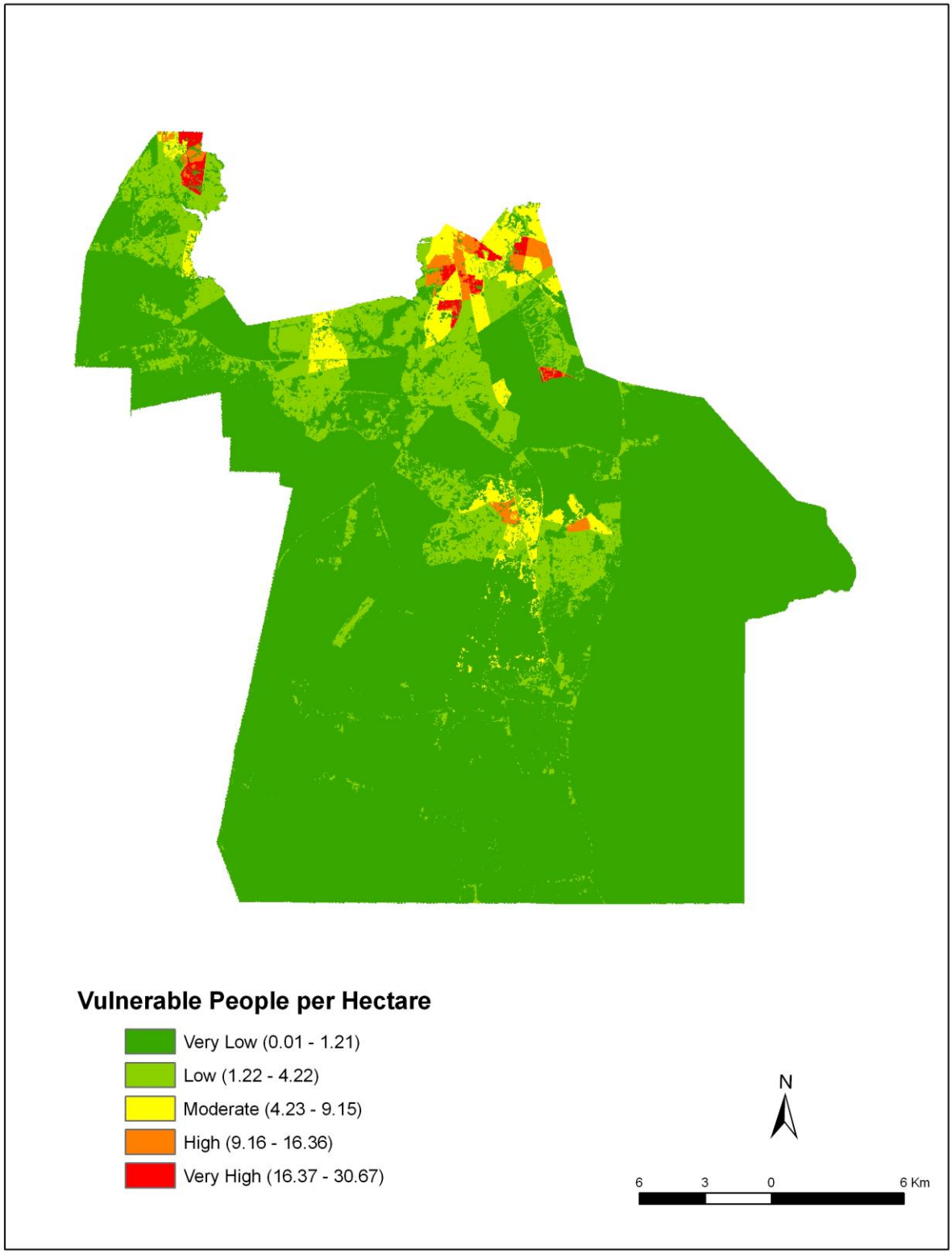

Figure 33: Dasymetric map of the population that is most vulnerable to mosquito-borne diseases. The vulnerable population data was mapped according to C-CAP land cover classes.

Risk of Mosquito-Borne Disease Transmission

By overlaying the monthly mosquito abundance grids with the habitat suitability indices, the risk of disease transmission from both groups of mosquitoes is predicted across Chesapeake. The results represent an index of the risk of disease infection from the corresponding mosquitoes for June through August of 2003. Due to the normalization of the abundance values used to calculate risk, the risk indices are relative values. The risk indices were classified to represent a scale of the level of risk of infection from mosquitoes for a particular month.

Risk of Disease Infection from the Ephemeral Species

The risk of disease transmission across Chesapeake from both *A. vexans* and *P. columbiae* is shown in Figure 34. To provide an effective visualization of the risk indices, the risk values were classified into quantiles. Each month's index was represented on the same scale. It is apparent in looking at the maps that July has the widest spatial distribution of high risk areas. In particular, northern Chesapeake has a very high potential risk of disease transmission in July. The risk of disease transmission was predicted to be high across northern Chesapeake in June and August as well. These northern high risk regions are mostly developed areas where vulnerability to disease is particularly high (Figure 33). Across all months, the risk of transmission is especially high in the center of the city. Many of these high risk areas are reflective of the dasymetric map of vulnerability. By looking at the dasymetric map (Figure 33), it is clear that these high risk regions are areas classified as having a population with a high vulnerability to disease. Based on the ephemeral species abundance maps (Figure 27), one might expect the western side of Chesapeake to have a high risk of disease transmission. However, the low proportion of vulnerable people in western Chesapeake causes the risk index to be relatively low on that side of the city, with the exception of the northwestern corner of the

Western Branch. Overall, much of the rural area within the city was classified as having a low risk of disease infection from the ephemeral species from June to August.

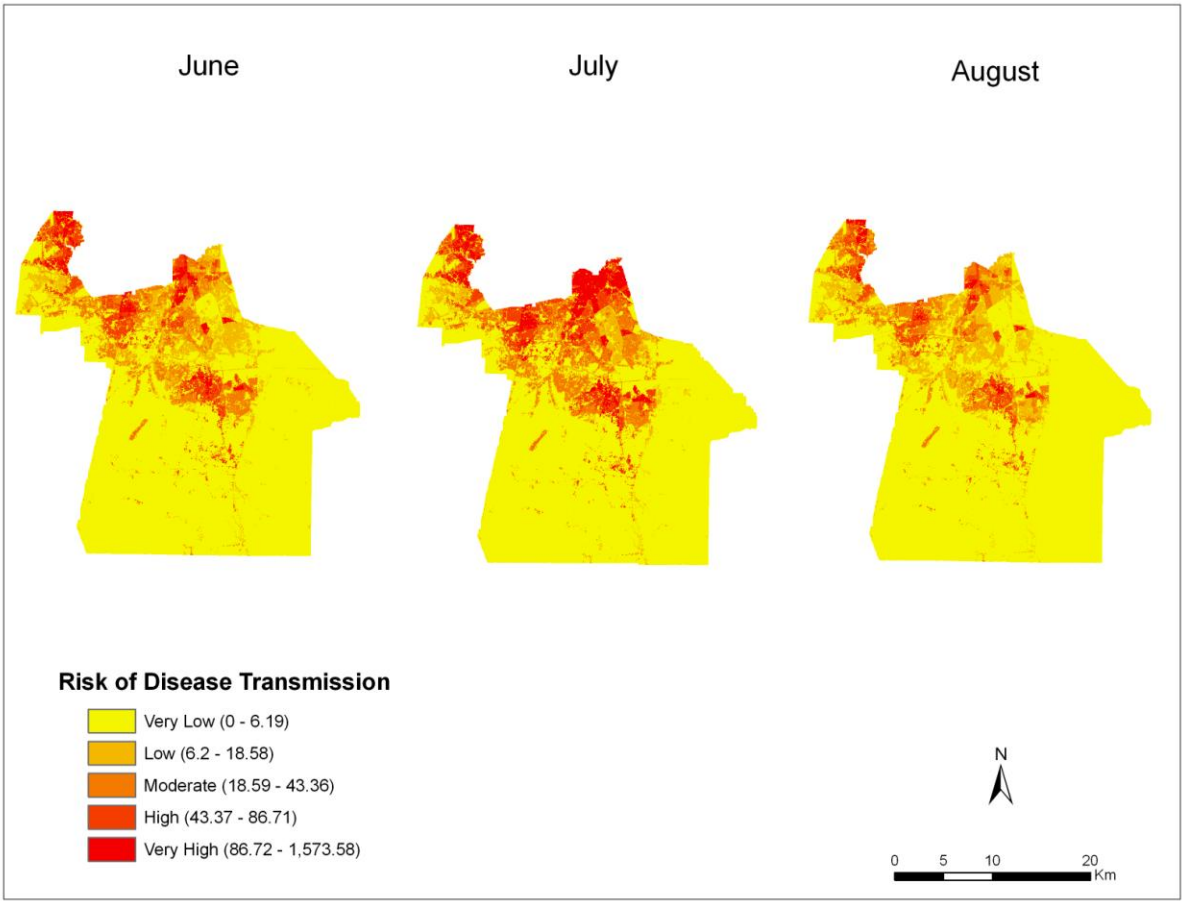

Figure 34: Risk of disease transmission from the ephemeral mosquito species. Map values were classified into quantiles.

Risk of Disease Infection from C. melanura

The risk of disease infection from *C. melanura* across Chesapeake is represented in Figure 35. The monthly risk indices were rendered on the same scale and were classified into quantiles. The risk patterns regarding *C. melanura* are similar to those for the ephemeral species. However, when viewed closely, it is apparent that each monthly risk index is distinctive. Across all months, the risk of disease transmission from *C. melanura* is particularly high in northern

Chesapeake. Central Chesapeake also exhibits a high risk of disease infection for all three months. In July, the highest risk areas are more widely distributed across northern Chesapeake. As mentioned with regard to the ephemeral species, these high risk areas are regions estimated to have a population that is highly vulnerable to disease. For all three months, a large portion of Chesapeake was predicted to have a very low risk of disease transmission from *C. melanura*.

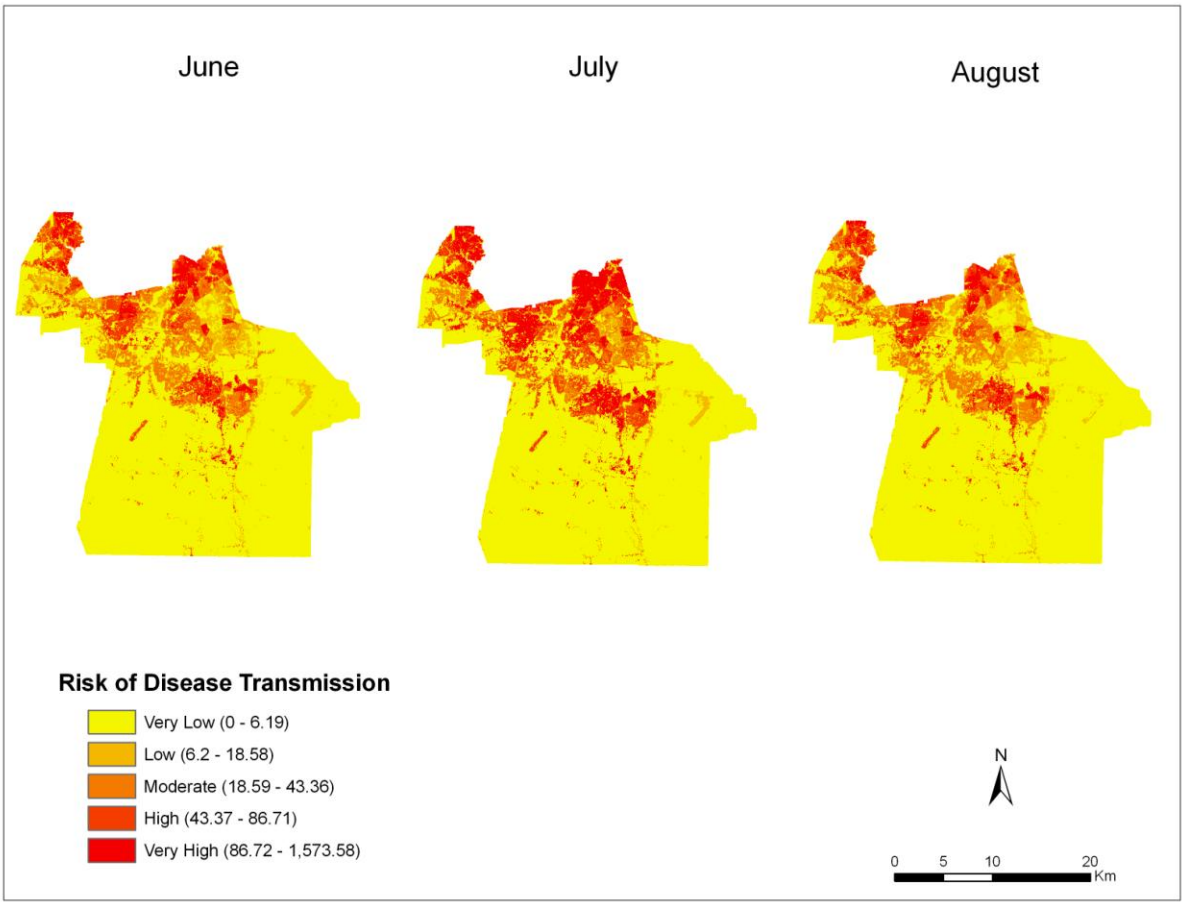

Figure 35: Risk of disease transmission from *C. melanura*. Values were classified into quantiles.

CHAPTER 5: DISCUSSION AND CONCLUSIONS

This chapter begins by discussing the patterns associated with the mosquito abundance and risk of disease transmission results. This chapter also describes the limitations associated with this study as well disease data that supports the model results. This chapter concludes with a summary of the significance of this research.

Mosquito Abundance Patterns

The linear regression results have provided valuable insight regarding the relationship between environmental variables and mosquito trap data in 2003. Based on the WSC linear regression model, we can conclude that temperature, rainfall, and TMI had the greatest impact on mosquito presence in western Chesapeake. Using these results as well as the HSI model, populations of *A. vexans, P. columbiae,* and *C. melanura* were predicted to be very high in western Chesapeake. This western region where abundance is especially high, surrounds the Great Dismal Swamp. It is no surprise that abundance is predicted to be high in this region, as the Great Dismal Swamp is known to be heavily populated with mosquitoes (Pettie, 1976). The wet conditions of the swamp provide an ideal habitat for mosquitoes to breed. These high abundance regions in the west are mostly covered by wetlands or cultivated croplands. Swamps and wetlands are known to be the prime breeding grounds for *C. melanura*. Cultivated croplands also have been proven to be ideal habitats for mosquitoes. According to Ward et al. (2009), agricultural runoff and irrigation from cultivated croplands can support mosquito presence. Ditches and temporary pools of water can also serve as breeding grounds for mosquitoes. In regard to the ephemeral species, the high numbers predicted to reside in rivers and open water was expected. According to Crans (2004), the largest numbers of these species are found in flood plains where rivers overflow their banks, but significant numbers can be produced from virtually any area where fresh ground water accumulates on an intermittent basis.

Comparatively, eastern Chesapeake is predicted to have a low monthly abundance of both types of mosquitoes. These predictions are partially based on the linear regression model which predicted that the environmental variables would have a limiting effect on mosquito presence in central and eastern Chesapeake. This prediction could be partly attributed to the limited number of mosquito captures in eastern Chesapeake. In general, the traps on the eastern side of the city have significantly less mosquitoes than the western side of the city (Figures 28 and 31). Eastern Chesapeake is covered by various types of land cover. Agricultural land such as cultivated croplands and pastures cover much of southeastern Chesapeake. Although irrigation and runoff from cultivated land can support mosquito populations, these regions are expected to be a poorer habitat for mosquitoes due to the high drainage potential. Although there are highly drained areas across eastern Chesapeake, the drainage potential varies across this side of the city (Figure 8). One pattern among the abundance results can be seen in northern Chesapeake, particularly on the northern tip of the city. This region was predicted to have a very low abundance of both mosquito types in July and August. The northern portion of Chesapeake is dominated by low and high intensity developed land. Because urban areas are not the primary habitat of the three mosquito species under consideration, these developed areas are not expected to have a large number of mosquitoes. Another obvious trend is the low number of mosquitoes predicted for August. The trap data shows that August had significantly less mosquito captures in August compared to the other months (Figures 27 and 30). The capture data is surprising since Hurricane Isabel struck Chesapeake in September of 2003. The average temperature across Chesapeake was higher in August compared to other months, which would potentially increase the number of mosquitoes.

The model results were considerably different than the surfaces interpolated from the mosquito captures. Overall, the interpolated surfaces show more spatial and temporal variation compared to the model results. However, using the interpolation method to estimate the distribution of mosquito counts can be limiting. For example, in eastern Chesapeake, ephemeral abundance was interpolated to be high in July and August based on only one trap site. The trap data symbology (Figure 28) illustrates that one trap site in eastern Chesapeake had a particularly high abundance of ephemeral species across all months. The high abundance of this particular trap caused a large portion of eastern Chesapeake to have a high abundance of ephemeral species. If the trap data set included more trap sites, the IDW approach could more accurately interpolate the number of mosquitoes across Chesapeake. Another limitation is that many of the trap sites were not counted during certain months. If the trap data included a more even distribution of trap sites and regular count intervals, these surfaces could be a more reliable source for estimating mosquito abundance. The abundance model on the other hand, may be more accurate due to the various determinant variables taken into account. Mosquito presence is influenced by many interacting factors, particularly climatic variables (Gage et al., 2008). By incorporating environmental variables into the abundance model, the results may be more accurate than relying on vector abundance alone.

Risk of Disease Transmission

In general, the risk of disease transmission from mosquitoes does not vary drastically between the two species groups. Because the risk values were influenced equally by the vulnerability and abundance values, the risk results represent the mean of the two variables. Regions with a high abundance of mosquitoes were not necessarily predicted to be at high risk of disease transmission. For instance, the western side of Chesapeake was expected to have a high

risk of infection based on the high number of mosquitoes predicted. However, because the number of vulnerable people in western Chesapeake is especially low, the risk of disease transmission is also low along western Chesapeake. Regions that were predicted to have a high risk of disease transmission were areas that coincided with a high vulnerability to disease infection.

Overall, areas at greatest risk of disease exposure are the more developed regions. Northern and central Chesapeake are predicted to be at very high risk of disease infection from both groups of mosquitoes. However, north Chesapeake is not predicted to have a high abundance of either mosquito type in June or August. Therefore, in July and August, the high risk prediction in northern Chesapeake is based solely on the highly vulnerable nature of the population. Central Chesapeake however, is predicted to have a large abundance of mosquitoes for most months. Because northern and central Chesapeake have a higher density of people compared to other regions, it seems reasonable that people in these areas are more likely to become infected with a mosquito-borne disease. Developed regions contain more points of vulnerability such as schools and nursing homes, increasing the vulnerable population in these areas. According to Sutherst (2004), higher human population densities can have profound effects on the transmission potential of diseases.

Study Limitations

Although this thesis has attempted to avoid the problems commonly involved with predicting the risk of disease transmission, this study also faces some limitations. One major constraint is the inconsistencies in the mosquito trap data. A major problem in the abundance model is the uneven distribution of trap sites across the city. Southeastern Chesapeake, in particular, has a limited number of mosquito traps compared to the rest of the city. With a

broader range of trap locations, the linear regression model could more accurately predict the effects that the environmental variables have on mosquito presence. Another issue with the trap data is the inconsistency in the frequency of trap counts. In other words, trap captures were not counted at consistent weekly intervals. Although the trap counts were normalized to take into account the number of trap nights, uniform trap counts could potentially have led to more sensitive model results. With a more complete data set, the relationship between the independent variables and the trap counts may have been more significant. Also, trap data may have not been the best variable for predicting the risk of disease infection. A more effective variable would have been the sites of human infection. However, disease cases are often underreported and this type of data would be extremely difficult to access. Nonetheless, Chesapeake has a much more comprehensive mosquito data set compared to surrounding jurisdictions.

Another limiting variable is the AWAT temperature dataset. Because the monthly temperature values are constant across the city, the spatial variation in temperature is lost. If the temperature values had been spatially-dependent, the relationship between temperature and the trap data may have been more significant. Other spatially-dependent variables may have been considered for this study. Wind speed or direction may have been useful variables for estimating vector abundance. Wind activity can interact with the flight activity of mosquitoes and help disperse them to new areas (Service, 1980).

Another limitation of this study was the lack of consideration for mosquito control efforts in Chesapeake. Due to discrepancies that may exist between vector abundance and risk, it is important to consider factors limiting mosquito populations. For instance, mosquito control efforts in Chesapeake could have limited the number of mosquitoes in areas predicted to have a high abundance. In Chesapeake, control efforts such as adulticiding, larviciding, and source

reduction are implemented as needed, making it difficult to analyze the patterns associated with mosquito control efforts. Ultimately, these disparities could affect the trap counts and risk estimation across Chesapeake. Although small-scale control efforts were applied across Chesapeake in 2003, no large-scale control efforts were employed. In 2003, aerial pesticide spraying was limited to cities such as Newport News, Hampton, and Pocuoson (Schnaars, 2003).

Model Validation

It is difficult to validate the models created in this thesis due to the lack of human disease data for Chesapeake, Virginia. In 2003, there were no human cases of WNV or EEE in Chesapeake (Virginia Department of Health, 2004). Therefore, the risk indices cannot be compared to actual disease cases. In 2003, 20 pools of mosquitoes were found to be positive for *C. melanura* infected with EEE, while 10 pools were infected with *C. melanura* positive for WNV (Virginia Department of Health, 2004). This data confirms that *C. melanura* mosquitoes were in fact a health threat to Chesapeake in 2003. However, bird, equine, and sentinel flock cases of WNV and EEE were reported for this year (Figures 36-37). These cases may not provide a validation of the model since the model estimates risk to humans, rather than animal hosts, but they do lend some credence to the model. Some studies however, have found that animal cases can be accurate indicators of human disease cases. Eidson et al. (2001) evaluated a system of dead bird surveillance as an early warning system for WNV in New York state. They found that dead bird reports preceded confirmation of viral activity in humans by at least three months. There are no obvious similarities between the disease cases and the risk predictions. Disease cases in animals however, are expected to be positively related to mosquito abundance. The high density of WNV cases in northeastern Chesapeake (Figure 36) does show a strong correlation with the mosquito abundance results. Across all months, abundance was predicted to

be high in northwestern Chesapeake for both groups of species. A more obvious relationship can be seen between EEE cases and *C. melanura* abundance. In 2003, the majority of EEE cases occurred in western Chesapeake, surrounding the Dismal Swamp. The abundance of the EEE vector, *C. melanura* was predicted to be high in western Chesapeake from June through August. The high number of disease cases in western Chesapeake lends support to the accuracy of the mosquito abundance model.

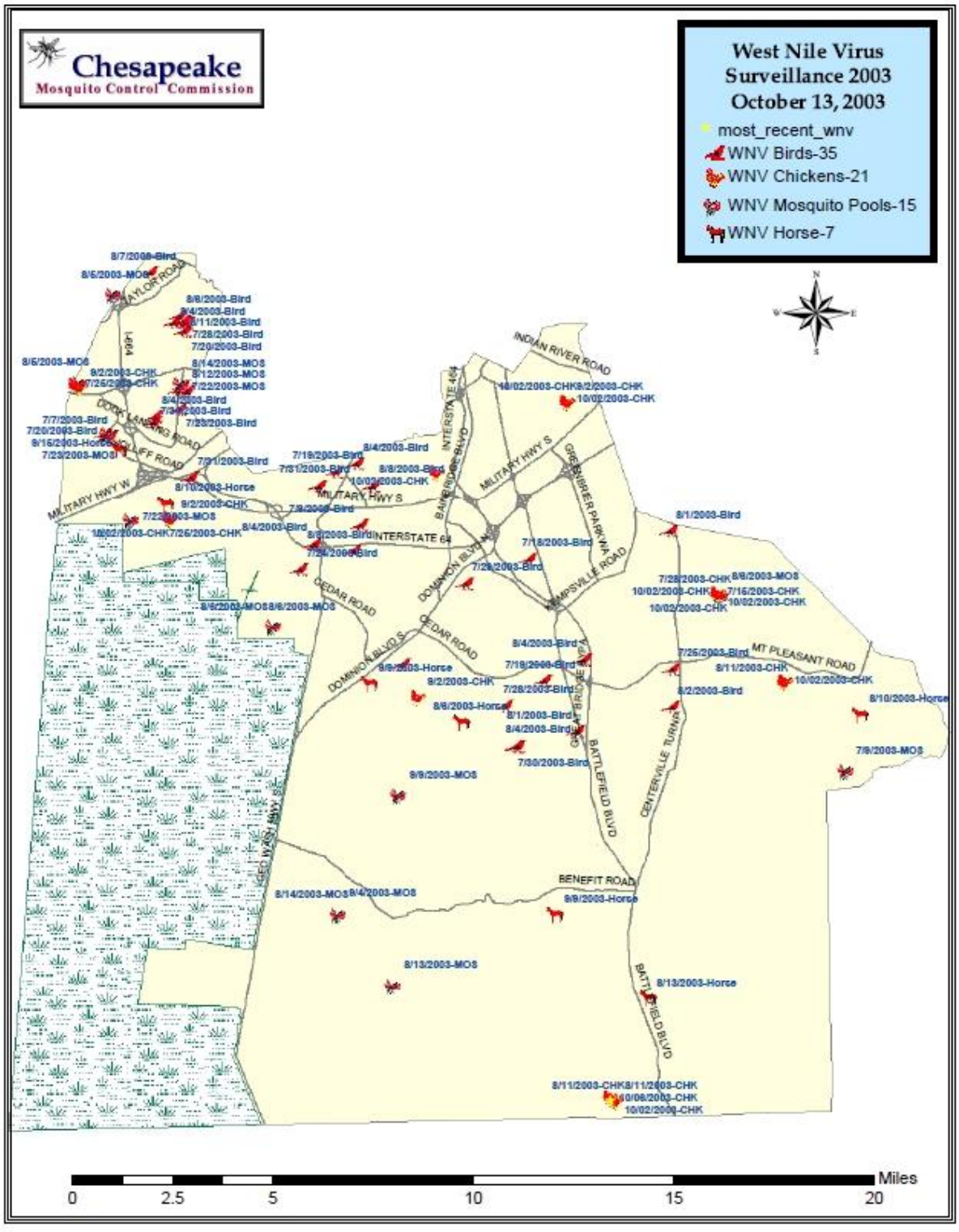

Figure 36: Cases of WNV in birds, chickens, and horses across Chesapeake Virginia in 2003. This map was created by Chesapeake Mosquito Control GIS.

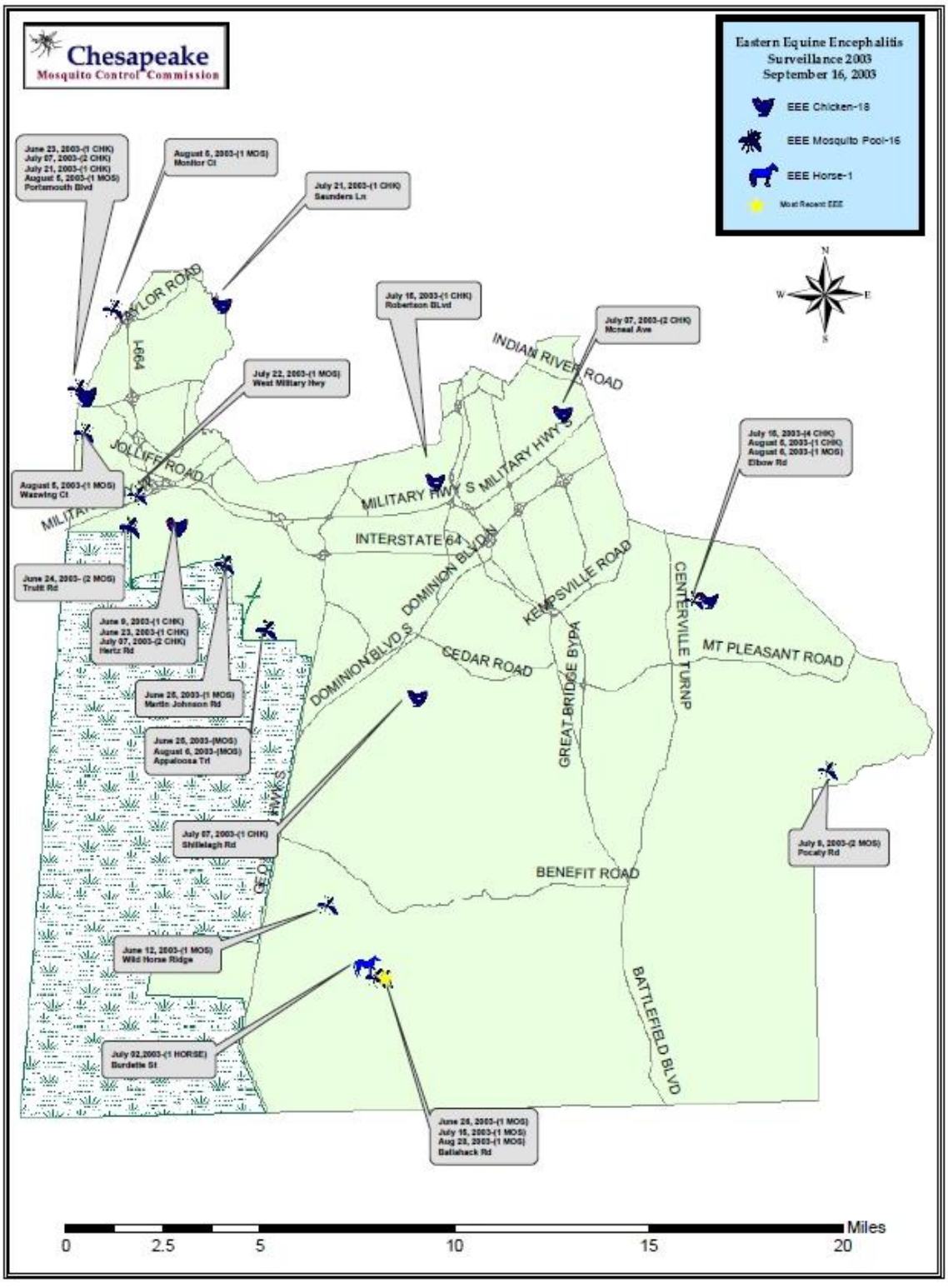

Figure 37: Cases of EEE in birds, chickens, and horses across Chesapeake Virginia in 2003. This map was created by Chesapeake Mosquito Control GIS.

Significance of Research

As vector-borne diseases continue to persist, many researchers and healthcare officials are concerned with estimating and mapping disease risk. Unfortunately, many of these attempts to estimate risk have been limited. Risk estimation studies are often not dynamic or predictive. According to Sutherst (2004), there have not yet been thorough quantitative studies addressing the many processes at work involved with infectious diseases. This thesis has attempted to address these and other shortcomings to accurately predict the risk of disease transmission from mosquitoes.

Many studies estimate the risk of disease exposure based on disease incidence. According to Ostfeld, Glass, and Keesing (2005), discrepancies between risk and incidence can pose a problem when estimating risk. For instance, the use of preventative measures such as mosquito bednets and water filtration can reduce incidence where risk of exposure is high. Inconsistent standards of disease reporting can also cause inaccuracies in risk estimation. Under-reporting as well as over-reporting of infectious diseases are a common problem. Discrepancies between locations where infections were obtained and where the diseases were reported is also a common issue. This study has avoided these issues by predicting the risk of disease transmission rather than simply mapping where disease cases have occurred.

Another way this study has attempted to improve upon risk modeling techniques, is to predict vector abundance rather than to simply map the presence of vectors. Many studies often use vector presence to estimate risk, rather than vector abundance. According to Ostfeld, Glass, and Keesling (2005), disease risk is more closely correlated with the abundance of vectors, rather than with the presence of the vector. Using vector presence to estimate risk can also be constraining because the direct causal relationship linking environmental conditions to vector

presence is often not established. This study has excluded this issue by using statistical methods to directly link environmental variables with mosquito presence.

Another shortcoming this study has addressed is the failure to incorporate human vulnerability into risk assessment studies. More studies are using predictive modeling to estimate risk of disease transmission, but few take into account human behavior or vulnerability. According to McCarthy et al. (2001), effective modeling of future risk for vector-borne disease outbreaks needs to take into account human behavior that increases exposure. Sutherst (2004) also explains that human vulnerability and socioeconomic changes have major significance in future disease patterns. Vector abundance can be an effective method for estimating areas at high risk of disease infection, however, without considering the nature of the population, it is difficult to accurately estimate risk. This thesis has attempted to fill this gap by predicting the risk of disease transmission using both environmental and human data.

According to Glass et al. (1995), there is a need to extend risk analysis to larger, less defined areas, while reducing the expenditure of time and resources. This study has addressed this issue by creating a time and cost efficient model that can assess risk over a large area. Although there were limitations to this study, the goal of this thesis was to create a portable and reproducible model that could predict the risk of disease transmission. In this regard, this study was successful. With the appropriate data, the models created for this thesis could be applied to another city to identify areas at high risk for disease infection. These techniques could be especially useful prior to an extreme weather event such as a hurricane. It is important to identify high-risk areas and communities in order to focus efforts toward adaptation of the existing disease management programs (Sutherst, 2004). By identifying high-risk areas in advance, healthcare officials can improve the efficacy of disease prevention measures. More

specifically, officials can target where to implement early-warning systems and educational programs. Knowing where infectious diseases are likely to emerge could aid healthcare managers in diagnosing and treating patients promptly. By predicting areas of high vector abundance, the mosquito abundance model can potentially help officials target where to implement mosquito control efforts. This could potentially reduce the high cost associated with mosquito control efforts. Hopefully, more studies will employ techniques such as the ones used in this study to help prevent the occurrence and the spread of infectious diseases.

REFERENCES

Ahern, M., R. S. Kovats, P. Wilkinson, R. Few and F. Matthies. 2005. Global Health Impacts of Floods: Epidemiologic Evidence. *Epidemiologic Reviews* 27: 36-46.

Albert, D. P., W. M. Gesler, B. Levergood. 2000. *Spatial Analysis, GIS, and Remote Sensing Applications in the Health Sciences*. Chelsea, MI: Ann Arbor Press.

Allen, T. R. and D.W. Wong. 2006. Exploring GIS, Spatial Statistics and Remote Sensing for Risk Assessment of Vector-borne Diseases: A West Nile Virus Example. *International Journal of Risk Assessment and Management* 64(4-6): 253-275.

American Mosquito Control Association. 2005. Mosquito-Borne Diseases. http://www.mosquito.org/mosquito-information/mosquito-borne.aspx. (last accessed 30 April 2010).

Beck, L. R., M. H. Rodriguez, S. W. Dister. A. D. Rodriguez, E. A. Rejmankova, A. Ulloa, R. A. Mexa, D. R. Roberts, J. F. Paris, M. A. Spanner, R. K. Washino, C. Hacker, and L. J. Legters. 1994. Remote Sensing as a Landscape Epidemiologic Tool to Identify Villages at High Risk of Transmission. *The American Journal of Tropical Medicine and* Hygiene 51(3): 271-280.

Becker, N. 2000. *Entomopathogenic Bacteria*. Netherlands, Kluwer Academic Publishing.

Bellows, A. S. 2007. Modeling Habitat and Environmental Factors Affecting Mosquito Abundance In Chesapeake,Virginia. Ph.D. Dissertation, Old Dominion University.

Beven, K. J. 1007. Topmodel: a critique. *Hydrologic Processes* 11: 1069-1085.

Brownstein, J. S., H. Rose, D. Purdy, J. R. Miller, M. Merlino, F. Mostashari, and D. Fish. 2002. Spatial Analysis of West Nile Virus: Rapid Risk Assessment of an Introduced Vector-borne Zoonosis. *Vector-borne and Zoonotic Diseases* 2(3): 157-164.

Brownstein, J. S., T. R. Holford, and D. Fish. 2003. A Climate-based Model Predicts the Spatial Distribution of the Lyme Disease Vector Ixodes scapularis in the United States. *Environmental Health Perspectives* 111(9): 1152-1157.

Bryan**,** J. H., D. H. Foley, and R.W. Sutherst. 1996. Malaria Transmission and Climate Change in Australia. *Medical Journal of Australia* 164: 345-347.

Caillouet, K.A., J.C. Carlson, D. Wesson, and F. Jordan. 2008. Colonization of Abandoned Swimming Pools by Larval Mosquitoes and Their Predators Following Hurricane Katrina. *Journal of Vector Ecology* 33(1): 166-172.

Cameron, D and I. G. Jones. 1983. John Snow, the Broad Street Pump and Modern Epidemiology. *International Journal of Epidemiology* 12(4): 393-396.

Ceccato, P., S. J. Connor, I. Jeanne, and M. C. Thomson. 2005. Application of Geographical Information Systems and Remote Sensing Technologies for Assessing and Monitoring Malaria Risk. *Parasitologia* 47: 81-96

Centers for Disease Control and Prevention (CDC). 2003. Epidemic/Epizootic West Nile Virus in the United States: Revised Guidelines for Surveillance, Prevention, and Control. *U.S. Department of Health and Human Services, Public Health Service Report* 3: 1-78.

Centers for Disease Control and Prevention (CDC). 2006. West Nile Virus: What You Need To Know. http://www.cdc.gov/ncidod/dvbid/westnile/wnv_factsheet.htm (last accessed 2 Februrary 2010).

Centers for Disease Control and Prevention (CDC). 2009. Eastern Equine Encephalitis. http://www.cdc.gov/EasternEquineEncephalitis/Epi.html (last accessed 29 October 2009).

Chesapeake Mosquito Control Commission. 2010. Mosquito Control. http://www.chesapeake.va.us/services/depart/mosquito/index.shtml (last accessed 27 March 2010).

Craig, M. H., R. W. Snow, and D. Le Sueur. 1999. A Climate-based Distribution Model of Malaria Transmission in Sub-Saharan Africa. *Parasitology Today* 15(3): 105-111.

Crans, W. G. 2004. A Classification System for Mosquito Life Cycles: Life Cycle Types for Mosquitoes of the Northeastern United States. *Journal of Vector Ecology* 29: 1-10.

Crist, E. P. and R. C. Cicone. 1984. Application of the Tasseled Cap Concept to Simulated Thematic Mapper Data. *Photogrammetric Engineering and Remote Sensing* 50(3): 343-352.

Cromley, E.K. and S.L. McLafferty. 2002. *GIS and Public Health*. New York: Guilford Press.

Eidson, M., N. Komar, F. Sorhage, R. Nelson, T. Talbot, F. Mostashari, R. Mclean, and the West Nile Virus Avian Surveillance Group. 2001. Crow Deaths as a Sentinel Surveillance System for West Nile Virus in the Northeastern United States, 1999. *Emerging Infectious Diseases* 7(4): 615-620.

Epstein, P.R. 2005. Climate Change and Human Health. *The New England Journal of Medicine* 353(14): 1433-1436.

Ford, T. E., R. R. Colwell, J. B. Rose, S. S. Morse, D. J. Rogers, and T. L. Yates. 2009. Using Satellite Images of Environmental Changes to Predict Infectious Disease Outbreaks. *Emerging Infectious Diseases* 15(9): 1341-1346.

Gage, K.L., T.R. Burkot, R.R. Eisen, and E.B. Hayes. 2008. Climate and Vectorborne Diseases. *American Journal of Preventitive Medicine* 35(5): 436-450.

Gatton, M.L. A. Kelly-Hope, B.H. Kay, and P. A. Ryan. 2004. Spatial-Temporal Analysis of Ross River Virus Disease patterns in Queensland, Australia. *The American Journal of Tropical Medicine and Hygiene* 71(5): 629-635.

Gatrell, A. and M. Loytonen. 1998. GIS and Health. Philadelphia, PA: Taylor & Francis.

Glass, G.E., B. S. Schwartz, J.M. Morgan, D.T. Johnson, P.M. Noy, and E. Israel. 1995. Environmental Risk Factors for Lyme Disease Identified with Geographic Information Systems. *American Journal of Public Health* 85(7): 944-948.

Glass, G.E., T.M. Shields, R.R. Parmenter, D. Goade, J.N. Mills, J. Cheek, J. Cook, and T.L. Yates. 2006. Predicted Hantavirus Risk in 2006 for the Southwestern U.S. *Occasional Papers, Museum of Texas Tech University* 255(1): 1-16.

Glass, R.I. and E.K. Noji. 1992. *Public health surveillance* New York: Van Nostrand Reinhold.

Gratz, N.G. 1999. Emerging and Resurging Vector-borne Diseases. *Annual Review of Entomology* 44: 51-75.

Guerra, M., E. Walker, C. Jones, S. Paskewitz, M.R. Cortinas, A. Stancil, L. Beck, M. Bobo, and U. Kitron. 2002. Predicting the Risk of Lyme Disease: Habitat Suitability for *Ixodes scapularis* in the North Central United States. *Emerging Infectious Diseases* 8(3): 289-297.

Hassan, A.N., M.A. Kenawy, H. Kamal, A.A. Abdel Sattar, and M.M. Sowilem. 2003 GIS-based Prediction of Malaria Risk in Egypt. *Eastern Mediterranean Health Journal* 9(4): 548-558.

Hayes, R.O. and A.D. Hess. 1964. Climatological Conditions Associated with Outbreaks of Eastern Encephalitis. *The American Society of Tropical Medicine and Hygiene* 13(6) 851-858.

Hoshen, M.B., A.P. Morse, E. Worrall, S.J. Connor, M.C. Thomson. 2005. The Modeling of Malaria Epidemics: Weather and prediction of Malaria Cases. *Geography and Health* 9: 103-123.

Hu, H., P. Singhasivanon, N.P. Salazar, K. Thimasarn, X. Li, Y. Wu, H. Yang, D. Zhu, S. Supavej, and S. Looarecsuwan. 1998. Factors Influencing Malaria Endemicity in Yunnan Province, PR China (analysis of spatial pattern by GIS). *Southeast Asian Journal of Tropical Medicine and Public Health* 29(2): 191–200.

Hunter, P.R. 2003. Climate Change and Waterborne and Vector-borne Diseases. *Journal of Applied Microbiology* 94: 37S-46S.

Kitron, U. 2000. Risk Maps: Transmission and Burden of Vector-borne Diseases. *Parasitology Today* 16 (8): 324-325.

Kitron, U., J. Michael, J. Swanson, and L. Haramis. 1997. Spatial Analysis of the Distribution of Lacrosse Encephalitis. *American Journal of Tropical Meteorology* 57(4): 469-475.

Lacey, L.A., C. M. Lacey. 1990. The Medical Importance of Riceland Mosquitoes and their Control Using Alternatives to Chemical Insecticides. *Journal of the American Mosquito Control* 6(2): 1-93.

Lawson, A.B. 2001. *Statistical Methods in Spatial Epidemiology*. West Sussex, England: Wiley.

Mahmood, F. and W.J. Crans. 1998. Effect of Temperature on the Development of Culiseta melanura (Diptera: Culicidae) and its Impact on the Amplification of Eastern Equine Encephalomelitis Virus in Birds. Journal of Medical Entomology 35 (6): 1007–1012.

Manuel, J. 2006. In Katrina's Wake. *Environmental Health Perspectives*. 114(1): A32-A39.

Martens, P., R.S. Kovats, S. Nijhof, P. de Vries, M. T. J. Livermore, D. J. Bradley, J. Cox, A. J. McMichael. 1999. Climate Change and Future Populations at Risk of Malaria- A Review of Recent Outbreaks. *Global Environmental Change* 9(1): 89-107.

Martens, W.J. M., T.H. Jetten, J. Rotmans, and L.W. Nielsen. 1995. Climate Change and Vector-borne Diseases: A Global Modelling Perspective. *Global Environmental Change* 5(3): 195-209.

Mather, F.J., L.E. White, E.C. Langlois, C.F. Shorter, C.M. Swalm, J.G. Shaffer, and W.R. Hartley. 2004. Statistical Methods for Linking Health, Exposure, and Hazards. *Environmental Health Perspectives* 112(14): 1440-1445.

McCarthy, J.J., Canziani, O.F., Leary, N.A., Dokken, D.J., White, K.S. (Eds.). 2001. Climate Change 2001: Impacts, Adaptation, and Vulnerability. Contribution of Working Group II to the Third Assessment Report of the Intergovernmental Panel on Climate Change. Cambridge: University Press, Cambridge.

Meade, M.S. and R.J. Earickson. 2005. *Medical Geography*. New York, NY: Guildford Press.

Mennis, J. and T. Hultgren. 2006. Intelligent Dasymetric Mapping and its Application to Areal Interpolation. *Cartography and Geographic Information Science* 33(3): 179-194.

Nasci, R .S. and C. G. Moore. 1998. Vector-borne Disease Surveillance and Natural Disasters. *Emerging Infectious Diseases* 4(2): 333-334.

Noji, E.K. 1997. *The Public Health Consequences of Disasters*. New York: Oxford University Press.

Ostfeld, R.S., G.E. Glass, and F. Keesing. 2005. Spatial Epidemiology: An Emerging (or Re-Emerging) Discipline. *Trends in Ecology and Evolution* 20(6): 328-336.

Panditrao, M., P. Jeevan, and T. Akbar. 2006. Use of Geographic Information Systems (GIS) to Predict Vector-borne Disease Outbreaks: A crucial step towards cost effective prevention of diseases. Proposal submitted to the “Bears Breaking Boundaries” Contest.

Peterson, R.K., P.A. Macedo, and R.S. Davis. 2006. A Human-Health Risk Assessment for West Nile Virus and Insecticides Used in Mosquito Management. *Environmental Health Perspectives* 114 (3): 366–372.

Pettie, S. T. 1976. Preserving the Great Dismal Swamp. *Journal of Forest History* 20(1): 28-33.

Rose, R.I. 2001. Pesticides and Public Health: Integrated Methods of Mosquito Management. *Emerging Infectious Diseases* 7(1): 17-23.

Schaeffer, B., B. Mondet, and S. Touzeau. 2008. Using a Climate-Dependent Model to Predict Mosquito Abundance: Application to *Aedes* (*Stegomyia*) *africanus* and *Aedes* (*Diceromyia*) *furcifer* (Diptera: Culicidae). *Infection Genetics and Evolution* 8(4): 422-432.

Service, M.W. 1980. Effects of Wind on the Behaviour and Distribution of Mosquitoes and Blackflies. *Interational Journal of Biometeorology* 24(4): 347-353.

Shaman, J., M. Stieglitz, C. Stark, S Le Blancq, and M. Cane. 2002. Using a Dynamic Hydrology model To Predict Mosquito Abundances in Flood and Swamp Water. *Emerging Infectious Diseases* 8(1): 6-13.

Shnaars, C. 2003. Localities Might Pay to Replace Spraying. *The Daily Press* 16 March.

Shone, S. M., P.N. Ferrao, C.R. Lesser, D.E. Norris, and G.E. Glass. 2001. Analysis of Mosquito Vector Species Abundances in Maryland using Geographic Information Systems. *Annals of the New York Academy of Sciences* 951: 364-368.

Sleeter, R. 2004. Dasymetric mapping techniques for the San Francisco Bay region, California: Urban and Regional Information Systems Association, Annual Conference, Proceedings, Reno, Nev., November 7–10, 2004.

Slocum, T.A., R.B. McMaster, F.C. Kessler, and H.H. Howard. 2009. Dasymetric Mapping. In *Thematic Cartography and Geovisualization*, Third edition, 271-280. Pearson/Prentice Hall.

Smith, C.M. and C.S. Graffeo. 2005. Regional Impact of Hurricane Isabel on Emergency Departments in Coastal Southeastern Virginia. *Academic Emergency Medicine* 12(12): 1201-1205.

Speilman, A. and M. D'Antonio. 2001. *Mosquito: A Natural History of Our Most Persistent and Deady Foe*. New York: Hyperion.

Sutherst, R.W. 1998. Implications of Global Change and Climate Variability for Vector-borne Diseases: Generic Approaches to Impact Assessments. *International Journal for Parasitology* 28: 935-945.

Sutherst, R.W. 2004. Global Change and Human Vulnerability to Vector-borne Diseases. *Clinical Microbiology Reviews* 17(1): 136-173.

Tanser, F.C., B. Sharp, D. le Sueur. 2003. Potential Effect of Climate Change on Malaria in Africa. *The Lancet* 362(9398): 1792-1798.

Thier, A. 2001. Balancing the Risks: Vector Control and Pesticide Use in Response to Emerging Illness. *Journal of Urban Health: Bulletin of the New York Academy of Medicine* 78(2): 372-381.

Thomson, M.C., S.J. Connor, P. Milligan, and S.P. Flasse. 1997. Mapping Malaria Risk in Africa: What Can Satellite Data Contribute? *Parasitology Today* 13(8): 313-318.

Turner, M.G. 1989. Landscape Ecology: The Effect of Pattern on Process. *Annual Review of Ecology and Systematics* 20: 171-197.

United States Geologic Society (USGS). 2009. Dasymetric Mapping Tools. http://geography.wr.usgs.gov/science/dasymetric/data.htm (last accessed 9 December 2009).

Virginia Department of Health. 2004. Arbovirus Data 2003. http://www.vdh.virginia.gov/epidemiology/DEE/Vectorborne/arboviral/documents/testresults/2003.html (last accessed 12 March 2010).

Ward, M.P., C.A. Wittich, G. Fosgate, and R. Srinivasan. 2009. Environmental Risk Factors for Equine West Nile Virus Disease Cases in Texas. *Veterinary Research Communications* 33(5): 461-471.

Waring, S., A. Zakos-Feliberti, R. Wood, M. Stone, P. Padgett, R. Arafat. 2005. The Utility of Geographic Information Systems (GIS) in Rapid Epidemiological Assessments Following Weather-related Disasters: Methodological Issues Based on the Tropical Storm Allison Experience. *International Journal of Hygiene and Environmental Health* 208: 109-116.

Washino, R.K. and B.L. Wood. 1994. Application of Remote Sensing to Vector Arthropod Surveillance and Control. *American Journal of Tropical Medicine and Hygiene* 50(6): 134-144.

Watson, J.T., M. Gayer, and M.A. Connolly. 2007. Epidemics After Natural Disasters. *Emerging Infectious Diseases* 13(1): 1-5.

Wilson, M.L. 2002. Emerging and Vector-borne Diseases: Role of High Spatial Resolution and Hyperspectral Images in Analyses and Forecasts. *Journal of Geographic Systems* 4: 31-42.

World Health Organization (WHO). 2004. Using Climate to Predict Disease Outbreaks: A Review. Communicable Diseases Surveillance and Response, Roll Back Malaria, Geneva, 2004.

APPENDIX A: 2003 *C. melanura* Trap Data

Location	**June**	**July**	**August**	**Total**	**Trap Nights**	**Normalized Total**
NW River Park	27	326	35	496	25	19.84
Timberwood	16	115	19	210	18	11.67
3110 Monitor Ct	71	350	109	692	21	32.95
5040 Portsmouth Blvd	45	1178	1133	3476	25	139.04
4704 Waxwing Ct	11	563	483	7163	20	358.15
4821 W Military HWY (past Econo Lodge)	175	3336	515	7279	23	316.48
Truitt Rd	577	8699	7783	25521	24	1063.38
Martin Johnson Rd	586	9277	2086	21921	23	953.09
Kentucky Trail	273	789	313	6977	21	332.24
Appaloosa Trail	220	2229	1337	10349	24	431.21
Shipyard Rd	2	694	55	1222	18	67.89
1943 Elbow Rd	112	2340	210	3567	25	142.68
Across from 2512 Pocaty RD	798	926	104	2138	23	92.96
2032 Johnstown Rd	69	214	4	717	16	44.81
472 Albemarle Dr	11	111	6	162	19	8.53
Fernwood Farms	20	206	84	582	24	24.25
3636 Ballahack Rd	156	596	221	1518	24	63.25
2520 Wild Horse Ridge	1155	1672	1133	5635	22	256.14
RRR (3531 Bunch Walnuts)	19	433	26	708	25	28.32
Rokeby Ave	15			16	2	8
1536 Bainbridge Blvd		64	7	77	10	7.7
Hanes St (Godwin Ave)	15	57	10	181	25	7.24
4210 Cornland Rd	1039	2972	359	9385	25	375.4
Raquet Club-Back Rd-Tunbridge	747	784	111	1821	17	107.12

S. Military Hwy (Ches. Fence)	2	152	5	186	15	12.4
2308 Silvertown	70	75	107	915	16	57.19
1341 Barbara Ct (Oakridge)	25	139	78	835	21	39.76
Hallmark Way (Shillelagh Farms)		857	252	3407	16	212.94
2333 Bugle dr		18		18	1	18
4712 White Owl Crescent		210		210	1	210
3933 Chadswyck RD		132	41	173	2	86.5
McNeal Ave.		0	3	6	13	0.46
Deep Creek Shop		32	1	33	2	16.5
BARN WAY		1257		1257	1	1257
2861 Meadow Wood Dr.		3		3	1	3
4736 Barn Swallow Dr.		191		191	1	191
Columbo/Coffman		360		360	1	360
AMES CIR		81		81	1	81
4421 Taylor Rd				17	1	17
2332 Pocaty Rd				32	1	32

APPENDIX B: 2003 Ephemeral Species Trap Data

Location	June	July	August	Total	Trap Nights	Normalized Total
NW River Park	5	134	12	331	25	13.24
Timberwood (3904 Savannah Dr)	6	62	6	91	18	5.06
3110 Monitor Ct	78	49	10	145	21	6.90
WB stables (5040 Portsmouth Blvd)	382	249	71	1112	25	44.48
4704 Waxwing Ct	130	35	10	341	20	17.05
West Military Hwy	284	177	38	546	23	23.74
Truitt Rd	149	47	18	368	24	15.33
Martin Johnson Rd	165	249	14	1097	23	47.70
Kentucky Trl	29	3	2	160	21	7.62
Appaloosa Trl	69	103	19	303	24	12.63
Shipyard Rd	2	49	9	200	18	11.11
1943 Elbow Rd	15	102	7	237	25	9.48
Pocaty Rd	8	14	5	60	23	2.61
2032 Johnstown Rd	27	9	1	48	16	3.00
472 Albemarle Dr	157	11	56	240	19	12.63
Fernwood Farms (Mapleshore Dr)	191	39	16	554	24	23.08
3636 Ballahack Rd	643	359	298	1722	24	71.75
2520 Wild Horse Ridge	2294	528	28	2944	22	133.82
RRR (3531 Bunch Walnuts)	30	40	13	213	25	8.52
Rokeby Ave	9			13	2	6.50
1536 Bainbridge Blvd		35	5	79	10	7.90
Haynes Ave	69	101	16	390	25	15.60
4210 Cornland Rd	194	169	8	494	25	19.76
Tunbridge Stn (Back Rd)	8	35	10	84	17	4.94

S. Military Hwy (Ches. Fence)	33	182	2	280	15	18.67
2308 Sivertown Ave	60	406	400	1257	16	78.56
Oakridge (1341 Barbara Ct)	61	91	7	207	21	9.86
Hallmark Way (Shillelagh Farms)		147	24	608	16	38.00
2333 Bugle dr		8		8	1	8.00
4712 White Owl Crescent		20		20	1	20.00
3933 Chadswyck RD		11	1	12	2	6.00
McNeal Ave.		14	3	24	13	1.85
Deep Creek Shop		2	0	2	2	1.00
Barn Way		2		2	1	2.00
2861 Meadow Wood Dr.		9		9	1	9.00
4736 Barn Swallow Dr.		8		8	1	8.00
Columbo/Coffman		10		10	1	10.00
AMES CIR		1		1	1	1.00
4221 Taylor Rd				8	1	8.00
2332 Pocaty Rd				5	1	5.00